A decision support system for the placement of radio transmitters in mobile communication networks

Thorsten Schmidt-Dumont

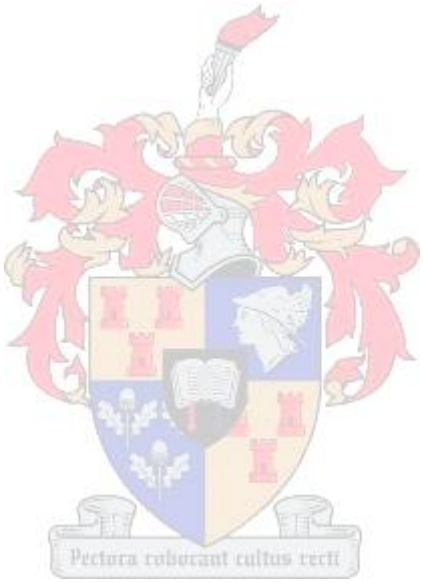

Year project presented in partial fulfilment of the requirements for the degree of
Bachelor of (Industrial) Engineering
in the Faculty of Engineering at Stellenbosch University

Supervisor: Prof JH van Vuuren

December 2015

Declaration

By submitting this project electronically, I declare that the entirety of the work contained therein is my own, original work, that I am the sole author thereof (save to the extent explicitly otherwise stated), that reproduction and publication thereof by Stellenbosch University will not infringe any third party rights and that I have not previously in its entirety or in part submitted it for obtaining any qualification.

Date: December 1, 2015

Abstract

Mobile telecommunication has become an essential communication channel in the modern world. Network providers are faced with the challenge of providing as many people in as many different areas as possible with communication network access. Multiple factors have to be taken into account when radio transmitter placement decisions are made. Generally, maximum area coverage and the average signal level provided to the demand region are of prime importance in these decisions. These criteria give rise to a bi-objective facility location problem with the goal of achieving an acceptable trade-off between maximising the total area coverage and maximising the average signal level provided to the demand region by a network of radio transmitters.

The so-called *network planning problem* for second generation networks can be decomposed into an offline *coverage subproblem* and an online *frequency assignment subproblem*. For third and fourth generation networks the frequency assignment and coverage subproblems cannot be addressed separately, due to the nature of radio interface. The focus of this project, however, is on the planning of the coverage subproblem which can be addressed independently of the frequency allocation subproblem in the context of second generation networks.

A thorough review is provided of the literature related to facility location with special emphasis on the placement of radio transmitters. This is followed by the establishment of a suitable bi-criterion framework for evaluating the effectiveness of a given set of placement locations for a network of radio transmitters. This framework is based on both area coverage and average signal level provided to the demand region, taking radio signal propagation loss, as well as the unobstruction of the line of sight and the first Fresnel ellipsoid between transmitters and potential receivers (which are required for effective radio transmission) into account. This framework is used to formulate a novel bi-objective facility location model which may form the basis for decision support with a view to identifying high-quality trade-offs between maximising total area coverage and maximising the average signal level provided. A decision support system capable of solving user-specified instances of this bi-objective radio transmitter location problem is also designed and implemented on a computer.

The decision support system is finally applied to a special case study involving an area around Stellenbosch so as to demonstrate its practical use and flexibility. The suitability of transmitter placement suggestions provided by the system is discussed in the context of this special case by comparing them to actual placements that have been made by network providers.

Uittreksel

Sellulêre telekommunikasie het 'n onmisbare kommunikasiekanaal in die moderne wêreld geword. Netwerkverskaffers staar die uitdaging in die gesig om soveel moontlik mense in soveel verskillende gebiede moontlik van netwerktoegang te voorsien. Verskeie faktore moet in ag geneem word wanneer plasingsbesluite vir radiosenders op selfoontrings geneem word. Oor die algemeen is maksimale area-oordekking en gemiddelde seinsterkte in die oordekte gebied van kardinale belang in sulke besluite. Hierdie kriteria gee aanleiding tot 'n twee-doelige fasiliteitliggingsprobleem waarin daar gesoek word na 'n aanvaarbare afruiling tussen die maksimering van area-oordekking en die maksimering van gemiddelde seinsterkte in die gebied wat deur 'n versameling radiosenders oordek word.

Die sogenaamde *netwerkbeplanningsprobleem* vir tweede generasie sellulêre telekommunikasienetwerke kan in 'n aflyn *oordekkingsdeelprobleem* en 'n aanlyn *frekwensie toekenningsdeelprobleem* onderverdeel word. Vir derde en vierde generasie netwerke kan hierdie frekwensie toekennings- en oordekkingsdeelprobleme vanweë die aard van radiosein interferensie nie apart aangespreek word nie. Die fokus val in hierdie projek egter op die oordekkingsdeelprobleem, wat wel in die konteks van tweede generasienetwerke onafhanklik van die frekwensie toekenningsdeelprobleem aangepak kan word.

'n Deeglike literatuurstudie word oor liggingsprobleme gedoen, met spesifieke verwysing na die plasing van radiosenders. Daarna word 'n dubbel-kriterium raamwerk vir die evaluering van die doeltreffendheid van 'n gegewe netwerk van radiosenders daargestel. Hierdie raamwerk berus op beide area-oordekking en gemiddelde seinstekte in die oordekte gebied, en neem ook radioseinverliese sowel as die onbelemmering van die lyn van sig en die eerste Fresnelellipsoïed tussen senders en potensiële ontvangers (wat vir doeltreffende radiokommunikasie vereis word) in ag. Hierdie raamwerk word gebruik om 'n nuwe, twee-doelige fasiliteitliggingsmodel daar te stel wat as basis kan dien vir die ontwikkeling van besluitsteun ten opsigte van die bepaling van hoë-kwaliteit afruilings tussen die maksimering van area-oordekking en die maksimering van gemiddelde seinsterkte in die gebied wat oordek word. 'n Besluitsteunstelsel wat gebruikersgespesifiseerde gevalle van hierdie twee-doelige fasiliteitliggingsmodel kan oplos, word ook ontwerp en rekenaarmatig geïmplementeer.

Die besluitsteunstelsel word laastens op 'n spesiale gevallestudie toegepas wat betrekking het op 'n gebied wat die dorp van Stellenbosch insluit om sodoende die buigsaamheid en praktiese bruikbaarheid daarvan te demonstreer. Die sinvolheid van die plasingsvoorstelle waarmee die stelsel vorendag kom, word met die werklike plasing van selfoontorings in die betrokke gebied vergelyk.

ECSA Exit Level Outcomes Reference

Outcome	Reference	
	Chapter	**Page**
1. Problem solving: Demonstrate competence to identify, assess, formulate and solve convergent and divergent engineering problems creatively and innovatively.	*All*	*All*
5. Engineering methods, skills and tools, including information technology: Demonstrate competence to use appropriate engineering methods, skills and tools, including those based on information technology.	*3,4,5 & 6*	*25–76*
6. Professional and technical communication: Demonstrate competence to communicate effectively, both orally and in writing, with engineering audiences and the community at large.	*All*	*All*
9. Independent learning ability: Demonstrate competence to engage in independent learning through well developed learning skills.	*2,3,4,5 & 6*	*9–76*
10. Engineering professionalism: Demonstrate critical awareness of the need to act professionally and ethically and to exercise judgement and take responsibility within own limits of competence.	*All*	*All*

Acknowledgements

The author wishes to acknowledge the following people and institutions for their various contributions towards the completion of this work:

- My supervisor, Prof JH van Vuuren, for sharing his broad knowledge, for his patience, guidance, relentless effort and his belief in me. I appreciate his time, dedication and hard work in ensuring that the work contained in this project is of a high standard.
- My parents, for the continuous support and unwavering belief in me throughout the duration of my studies.
- Finally, my friends, family and classmates for making the past four years an unforgettable time.

Table of Contents

List of Reserved Symbols

Symbols in this project conform to the following font conventions:		
$\boldsymbol{x}$	Symbol denoting a **vector**	(Lower case boldface)
$\boldsymbol{A}$	Symbol denoting a **matrix**	(Upper case boldface)
$\mathcal{A}$	Symbol denoting a **set**	(Upper case calligraphy)

Variables

Symbol	Meaning
A_{max}	The maximum number of epochs that may pass without acceptance of a move
A_{min}	The minimum number of accepted moves before an epoch completes
α	The parameter denoting the allowable first Fresnel ellipsoid obstruction
D	The distance between a transmitter and a receiver
f	The frequency of radio transmission
h_b	The base station antennae height above ground level
h_m	The receiver antennae height above ground level
I_{max}	The maximum number of iterations per epoch
k	The number of transmitters which are to be located
$L_{b(i,j)}$	The radio signal propagation loss between points i and j
λ	The wavelength of the radio waves
P_t, P_t'	The power transmitted at the base station (measured in different units)
S_{min}	The threshold minimum signal level required for effective radio transmission
T_c	The temperature during epoch c

Vectors

Symbol	Meaning
$\boldsymbol{x}$	The (binary) location decision vector
$\boldsymbol{c}$	The coverage importance vector

Matrices

Symbol	Meaning
$\boldsymbol{A}^{(\alpha)}$	The potential coverage matrix
$\boldsymbol{C}^{(\alpha)}$	The quality of demand satisfaction matrix
$\boldsymbol{S}^{(P_t,\alpha)}$	The potential signal strength matrix
$\boldsymbol{Q}^{(P_t,\alpha,S_{min})}$	The quality of signal strength matrix

Sets

Symbol	Meaning
$\mathcal{A}$	The archive containing the nondominated front
$\mathcal{I}$	The set of facility placement candidate locations

Performance measures

Symbol	Meaning
$\Gamma_c^{(\alpha)}(\boldsymbol{x})$	The coverage performance measure
$\Gamma_\ell^{(P_t,\alpha,S_{min})}(\boldsymbol{x})$	The average signal level performance measure

List of Acronyms

2G: Second Generation

3G: Third Generation

4G: Fourth Generation

ATM: Automatic Teller Machine

CDMA: Code Division Multiple Access

COST: European Cooperation in the Field of Scientific and Technical Research

DCA: Dynamic Channel Assignment

DFD: Data Flow Diagram

DNC: Demand Node Concept

DSS: Decision Support System

FCA: Fixed Channel Assignment

GDP: Gross Domestic Product

GIS: Geographic Information System

GUI: Graphical User Interface

LTE: Long Term Evolution

LOS: Line of Sight

MOP: Multiobjective Optimisation Problem

nLOS: Near Line of Sight

NLOS: Non Line of Sight

OFDM: Orthogonal Frequency-Division Multiplexing

SA: Simulated Annealing

SADC: Southern African Development Community

SIR: Signal Interference Ratio

SOP: Single-Objective Optimisation Problem

TDMA: Time Division Multiple Access

W-CDMA: Wideband — Code Division Multiple Access

List of Figures

List of Tables

List of Algorithms

CHAPTER 1

Introduction

Contents

1.1 Project Background and Origin

Mobile telecommunication has revolutionised the modern world. Smartphones and similar devices are used on a daily basis to communicate through many different types of electronic media. This has sparked a trend, especially among the younger generation, of always having to be connected and up-to-date on what is going on, not only in their own lives, but also in the lives of others. Similar trends may be seen among business people, who can now use their smartphones or tablets to complete almost any business transaction. It has, therefore, become an absolute priority for mobile telecommunication network providers to cover as much area as possible in their service provision. Currently, network providers have the choice of using a combination of second, third or fourth generation networks for their service provision.

Second Generation (2G) networks use the *Time Division Multiple Access* (TDMA) protocol according to which the bandwidth bought by the mobile provider is partitioned into frequency channels of a specific bandwidth, generally in the order of 200 kHz. These channels are then assigned to receivers, each call having one channel allocated to it. Should there be no available channels when a new call is made, the call is blocked until a channel opens to which the call can be assigned. The allowable time during which a call can be blocked is limited and depends on the policy adopted by the network provider. If a channel does not open up during the allowable blocking time, the call is terminated. Channel assignment to the receiver can be performed in one of two ways: *Fixed Channel Assignment* (FCA) or *Dynamic Channel Assignment* (DCA). In FCA, each base station only has a limited number of channels allocated to it over the available frequency band. These are then assigned to the receivers as calls are made. In DCA, however, the entire bandwidth is available for use by all transmitters and different assignment policies

are in place according to which new calls are treated. The general objective for any channel assignment policy is to minimise the number of blocked calls. The channel assignment is usually the final step of the network planning process, but is an operational task, as opposed to a strategic task, and hence repeated in an online fashion whereas other planning aspects, such as transmitter placement decisions, are strategic and are performed once-off in an off-line fashion [27].

In *Third Generation* (3G) networks, the *Code Division Multiple Access* (CDMA) protocol is used instead of channel assignment. The result is that the entire bandwidth available to the service provider is partitioned into 1.25 MHz wide channels for CDMA or 5 MHz wide channels for *Wideband — Code Division Multiple Access* (W-CDMA) networks. These wider channels can, however, be shared by several receivers. If only one receiver is using the channel, the entire bandwidth is allocated to that receiver, whereas the bandwidth is shared between users as soon as more than one receiver is allocated to a channel. The result is that broadband data speeds are now available on mobile devices due to the wider bandwidth. Since the bandwidth is shared by multiple users, no frequency assignment is required as in 2G networks. There are, however, other limitations on 3G networks. Due to increased complexity, the planning for 3G networks cannot be decomposed into an offline coverage problem and an online frequency allocation problem, but other factors, such as signal quality constraints and transmission power, have a greater influence and thus need to be taken into account [2].

Fourth Generation (4G) networks, also known as *long term evolution* (LTE) networks, are, as the name suggests, an evolution of 3G network technology. Once again, the focus in LTE networks is on higher data speeds. LTE networks use the protocol of *Orthogonal Frequency-Division Multiplexing* (OFDM) to partition the 5 MHz wideband frequency channels into smaller 180 kHz wide transmission channels instead of using them directly as in 3G networks. Each user is assigned a certain number of the smaller channels, called resource blocks which, when combined, result in higher download speeds. Each 5 MHz channel is (as in 3G networks) therefore shared between users, meaning that a high network load will result in decreased download speeds. This implies that an allocation of channels to users is again required, which is typically achieved by using advanced scheduling mechanisms in both the frequency and time domains [22].

The choice of the type of network and the resulting placement of radio transmitters forming the network is of primary importance to network providers, especially when taking into account the prospective growth of smartphone users in Africa. Reed *et al.* [31] state that "the number of smartphone connections will rise from about 79 million at the end of 2012 to 412 million by 2018, according to forecasts by Informa." It is, however, not only the number of new smartphone connections that is expected to achieve such impressive growth. 2G networks and feature phones

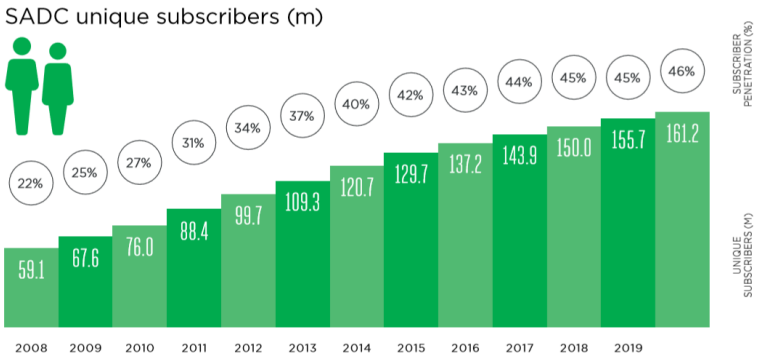

FIGURE 1.1: *The expected growth of SADC unique subscribers during the period 2008–2020 [4].*

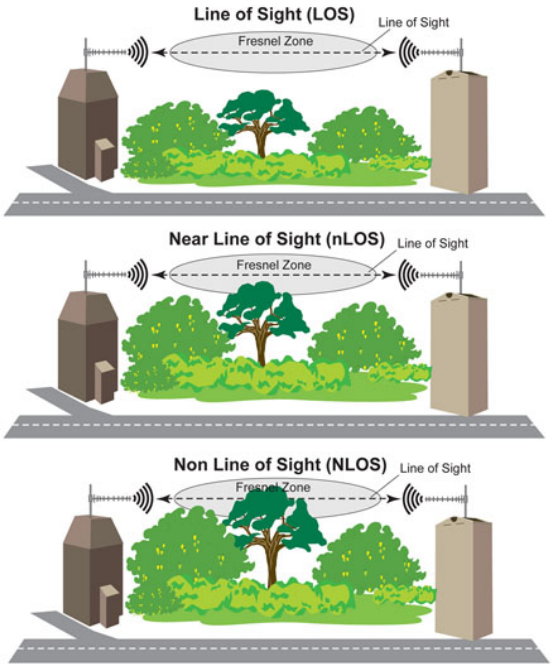

FIGURE 1.2: *Various notions related to line of sight between a radio transmitter and receiver [26].*

are expected to remain a key aspect of mobile networks in Sub-Saharan Africa where, due to the relatively low *Gross Domestic Product* (GDP), smartphones remain beyond reasonable levels of affordability for a large portion of the population. The expected growth in the number of unique mobile subscribers in the *Southern African Development Community* (SADC) countries during the period 2008–2020 is shown in Figure 1.1. This will especially be the case in semi-urban and rural areas, where new mobile networks are established [4].

In a country as large as South Africa then, the effective placement of radio transmitters aimed at high-quality mobile network service provision presents a major challenge. As a result, the placement of radio transmitters is under constant debate. Multiple factors have to be taken into account when new radio transmitter placement decisions are made. The focus in this project will be on the area that a network of radio transmitters is able to cover. Whereas the total area covered by the network is usually of prime importance, the average signal level provided to the covered areas is also of considerable interest, especially in densely populated urban areas, since this will maximise the quality of signal provided. These considerations naturally result in a bi-objective optimisation facility location problem with the goal of achieving an acceptable trade-off between maximising the total coverage as well as maximising the average signal level achieved by a network of radio transmitters. These objectives are conflicting in the sense that placing transmitters far apart tends to increase their coverage, while placing them closer together tends to increase the average signal level provided by them.

The area that can be covered by a transmitter depends upon three main factors, namely the power of the transmitter, the type and configuration (antenna height and beam direction) of the antenna installed at the transmitter, and the topography and land cover of the surrounding area [24].

For an area to be considered covered, an unobstructed line of visibility between the transmitter and receiver should at the very least be achieved. If this direct line of visibility is obstructed, then a situation of *Non Line Of Sight* (NLOS) is said to prevail. Radio wave transmission does, however, not only depend on a clear line of visibility between transmitter and receiver.

Radio transmission generates an infinite family of nested ellipsoids called *Fresnel ellipsoids*. For effective transmission, the innermost of this family of ellipsoids, called the *first Fresnel ellipsoid* (or sometimes the *Fresnel zone*), should also be unobstructed. If an unobstructed line of visibility exists between a transmitter and receiver, but the first Fresnel ellipsoid is partially obstructed, *Near Line Of Sight* (nLOS) is said to have been achieved, whereas if both the direct line of visibility and the first Fresnel ellipsoid between the transmitter and receiver are unobstructed, then (full) *Line Of Sight* (LOS) is said to have been achieved. These notions are illustrated graphically in Figure 1.2.

1.2 Problem Statement

The main aim in this project is to design and demonstrate the working of a flexible, computerised *decision support system* (DSS) capable of suggesting high-quality placement alternatives for a network of radio transmitters which achieve suitable trade-offs between the conflicting objectives of maximising network area coverage and maximising the average signal level provided to the covered areas. This DSS is based on a bi-objective combinatorial optimisation modelling approach and is applicable to cellular telephone transmission towers operating according to 2G technology.

1.3 Project Objectives

Nine objectives are pursued in this project, namely:

I To *conduct* a thorough survey of the literature related to:

(a) facility location problems in general,

(b) models for the placement of a network of radio transmitters in particular,

(c) the nature and appropriate ranges of parameters required for effective radio transmission, and

(d) terrain elevation and other data required to generate an instance of the bi-objective radio transmitter location problem described in the previous section.

II To *establish* a suitable framework for evaluating the effectiveness of a given set of placement locations for a network of radio transmitters in respect of its total area coverage and the average signal level provided.

III To *formulate* a bi-objective facility location model suitable for use as the basis for decision support in respect of the location of a network of radio transmitters with a view to identify high-quality trade-offs between maximising total coverage area and maximising average signal level. The model should take as input the parameters and data identified in Objectives I(c)–(d) and function within the context of the framework of Objective II.

IV To *design* a generic *decision support system* (DSS) capable of suggesting high-quality trade-off locations for user-specified instances of the bi-objective radio transmitter location problem described in the previous section. The DSS should incorporate the location model of Objective III.

V To *implement* a concept demonstrator of the DSS of Objective IV in an applicable software platform. This concept demonstrator should be flexible in the sense of being able to take as input an instance of the bi-objective radio transmitter location problem described in the previous section via user-specification of the parameters and data of Objectives I(c)–(d) and it should produce as output a set of high-quality trade-off transmitter locations for that instance.

VI To *verify* and *validate* the DSS implementation of Objective V according to generally accepted modelling guidelines.

VII To *apply* the concept demonstrator of Objective V to a special case study involving realistic radio transmission parameters and real elevation data for a specified portion of terrain.

VIII To *evaluate* the effectiveness of the DSS and associated concept demonstrator of Objectives IV–VI in terms of its capability to identify high-quality trade-off solutions in the context of the case study of Objective VII.

IX To *recommend* sensible follow-up work related to the work in this project which may be pursued in future.

1.4 Methodological Approach

This project is executed in four stages. The first stage consists of a thorough literature review, specifically of the literature mentioned in Objective I of §1.3. Research related to facility location problems in general, as well as their specific application to the placement of radio transmitters forming part of a communication network, are studied in fulfilment of Objectives I (a) and (b). This approach is followed in order to understand the different types of facility location problems available in the literature and possible ways of finding high-quality feasible solutions to such problems using suitable models and algorithms. In pursuit of Objective I (c), the study also includes a review of the various factors which influence effective radio transmission specifically. These factors need to be taken into account in decision support related to the placement of radio transmitters. This part of the literature study also includes an investigation into suitable approaches toward modelling radio wave propagation, which is required to establish a realistic framework for evaluating the effectiveness of a set of given placement locations, as stated in Objective II. Finally, the literature study concludes with a description of the geographic and other data required to generate a specific instance of the above-mentioned bi-objective radio transmitter location problem, in fulfilment of Objective I (d).

The second stage of the project is the development stage. During this stage, Objectives II, III and IV of §1.3 are pursued. The pre-optimisation framework for evaluating the effectiveness of a given set of placement locations for radio transmitters is established. This is achieved by using a suitable software package to determine the area coverage of a given set of radio transmitter locations, taking into account obstruction of the line of visibility and of the first Fresnel ellipsoid between the transmitter and receiver, as well as signal propagation loss, in order to determine the areas receiving adequate coverage. This stage also includes the development of the mathematical model used to solve specific instances of the bi-objective optimisation problem described in Objective III. Due to the complexity of the combinatorial optimisation task, a suitable metaheuristic is employed to solve the mathematical model. The implementation of the metaheuristic also forms part of this stage. The design of the DSS described in Objective IV also commences during this stage of the project. This design provides an indication of the data flows through the system, clearly depicting all the required input data, as well as the output

the user receives, and also explaining how the mathematical model and the pre-optimisation framework are incorporated into the DSS.

The next stage of the project is the implementation stage. Objective V of §1.3 is pursued during this stage, which entails an implementation of the DSS as a concept demonstrator in a suitable software environment. This demonstrator is capable of aiding network planners in making radio transmitter location decisions. The system allows an operator to specify feasible placement areas, as well as expected call demand data, which is weighed in the coverage objective, and yield as output a set of high-quality trade-off transmitter placement suggestions measured according to both the total coverage and average signal level objectives.

The fourth and final stage is the verification and evaluation stage. During this stage, Objectives VI to IX are pursued. The first step is to research the appropriate, generally accepted modelling guidelines mentioned in Objective VI, in order to be able to conduct a meaningful verification and validation of the DSS described above. Thereafter, as mentioned in Objective VII, a case study of a specific instance of the radio transmitter facility location problem is conducted. For the case study, a real-life instance of the bi-objective facility location problem mentioned above is solved using the DSS concept demonstrator of Objective V. The results of the case study, measured according to the total coverage and the average signal level objectives, are used to verify the effectiveness of the DSS in terms of its capability to suggest a set of high-quality trade-off solutions for a network of radio transmitter locations, as described in Objective VIII. Finally, after a critical evaluation of the results of the case study, a summary of what has been achieved, together with suitable follow-up work and possible improvements which may be pursued in future, is put forward in fulfilment of Objective IX.

1.5 Project Scope

Due to the complexity of the facility location problem considered, the scope of this project is limited by the following assumptions:

Clutter. The geographic data required to solve an instance of the radio transmitter location problem (such as terrain elevation data) typically do not contain information on trees or buildings which may obstruct the first Fresnel ellipsoid during radio communication. Such information is ignored in this project. In urban areas, buildings generally have such a major influence on radio transmissions that indoor solutions often have to be implemented. In large forests, on the other hand, surrounding trees often also affect the level of coverage, usually resulting in significant signal level fluctuations. Due to the increased network load in urban areas, mobile providers will, however, generally set up more transmitters at coverage-restricted locations in order to improve network quality.

Network loading. Poor transmission quality is often a result of high network load. This is typically the case in densely populated urban areas. Studies are normally undertaken by network providers in order to assess network quality. Such studies are usually based on a statistical analysis and are applicable to existing networks. The focus of this project is, however, on suggesting locations so as to maximise coverage in areas that have previously not been covered. Areas which are currently densely populated or which exhibit high expected population growth may, in any case be weighted in the coverage objective. Quality considerations due to network loading nonetheless fall outside of the scope of this project.

Base station configuration. As stated above, the area a transmitter is able to cover depends upon the power of the signal emitted by the transmitter as well as the type and config-

uration of the antenna and the topographical information of the surrounding area. In this project, the focus is on suggesting suitable placement locations for a network of radio transmitters based on topographical information only. The antenna configuration is not considered. Instead, approximations of maximum coverage radii for radio transmitters, based on propagation power loss functions, are employed.

2G Networks. Second generation networks form the basis of most Sub-Saharan African mobile networks. Although trends in urban areas, where the demand for improved data speeds is ever-growing, are expected to move towards third and fourth generation networks, second generation networks are still of primary importance in semi-urban and rural areas. This may be attributed to the fact that people living in these areas are typically not in a financially strong enough position to afford smartphones (whose performance benefits from the improved download speeds in 3G and 4G networks). Due to the exponentially increasing complexity in modelling third and fourth generation networks, only 2G networks are considered in this project.

Channel assignment. As stated in the introduction, every receiver in a 2G network is assigned a frequency channel once a call is made to or from the receiver. The two methods for frequency allocation briefly explained in §1.1 form part of a complex online allocation problem in its own right. This is especially the case in areas with overlapping coverage, because signal interference has to be considered. Since the focus in this project is, however, on the placement of a network of radio transmitters, the associated frequency allocation problem falls outside the scope of this project.

1.6 Project Time-line

A Gantt chart representation, providing the reader with an indication of the amount of time spent completing the various stages of the methodological approach described in §1.4, may be found in Appendix A.

1.7 Report Organisation

Apart from this introductory chapter, this report consists of a further six chapters. Chapter 2 contains a literature review of material which is of relevance to this project. Chapter 3 is devoted to the establishment of the framework according to which the effectiveness of a given set of placement locations for a network of radio transmitters can be evaluated. The focus in Chapter 4 falls on the formulation of the bi-objective facility location model which will form the basis of the DSS. The design of the DSS, which yields as output suggestions in respect of high-quality trade-off locations for the placement of radio transmitters for user-specified instances, is documented in Chapter 5. The effectiveness of the DSS is assessed in Chapter 6 according to its capability to uncover a set of high-quality trade-off locations for the placement of radio transmitters when applied to a special case study (which involves realistic radio transmission parameters and real elevation data for a specified portion of terrain). Finally, the project closes in Chapter 7 with a summary and appraisal of what has been achieved together with recommendations for related follow-up work which may be pursued in future.

CHAPTER 2

Literature Study

Contents

As stated in the previous chapter, the planning of radio transmission networks provides decision makers in the telecommunications industry with a significant challenge. This chapter is devoted to a thorough review of the literature related to facility location problems in §2.1, with specific focus on facility location models which have been used previously in the planning of radio transmission networks in §2.2. The focus shifts in §2.3 to wave propagation and various parameters which have an influence on radio communication over different types of surfaces. The chapter closes in §2.4 with a discussion of those data required to generate an instance of the bi-objective radio transmitter location problem described in the previous chapter, and a brief summary in §2.5 of the material included in this chapter.

2.1 Facility Location Models in General

Facility location decisions form a key element of the strategic planning of firms in both the private and public sectors, since these decisions are generally long term, often with profound influences on corresponding operational and even logistical decisions. Farahami and Hekmatfar [14] define facility location problems as problems which are formulated in order to locate a set of facilities (resources) with the aim of minimising the cost of satisfying a given set of demands (of customers) subject to a certain set of constraints.

According to Daskin [11], mathematical location models have been designed in order to address four key questions:

(a) How many facilities are required?

(b) Where should each of the facilities be located?

(c) What should the capacity/size of each facility be?

(d) How should the demand for the services provided by the facilities be allocated to each of the facilities?

Daskin [11] also states that the answers to these questions depend sensitively on the context in which the problem is solved as well as the underlying objectives of the location problem. The number of facilities to be placed and the capacity/size of these facilities are usually functions of a service/cost trade-off. Generally, the quality of the service provision increases as the number of facilities increases. The cost naturally also increases as the number of facilities increases, but it is often possible to take advantage of economies of scale, in the sense that fewer facilities with large capacities may be favourable. Finally, Daskin [11] reiterates that facility location models are also concerned with the allocation of demand to facilities and will thus often have to take certain demand allocation policies into account in order to comply with business rules.

Four basic types of facility location problems are described briefly in this section, namely *covering problems, centre problems, median problems* and *fixed-charge facility location problems.*

2.1.1 Covering Problems

In many facility location problems, the service received by a customer depends on the distance between the customer and the facility to which the customer has been assigned. Denote the set of customers by $\mathcal{J}$ and the set of facility candidate sites by $\mathcal{I}$. Fallah *et al.* [13] assume that in a covering problem, a customer can receive service from a facility as long as the distance that separates the customer from the facility does not exceed some predefined threshold, called the *coverage distance* or *coverage radius.* Daskin [11] goes on to explain that every demand node or customer $j \in \mathcal{J}$ usually has an associated subset, $\mathcal{N}_j \subseteq \mathcal{I}$ (say), of candidate facility nodes which can cover the demand node. Generally, this subset is specified in terms of binary coefficients a_{ij} which take the value 1 if the facility at candidate site $i \in \mathcal{I}$ is able to cover demand point $j \in \mathcal{J}$, or 0 otherwise. In order to determine the area that a facility can cover, a single coverage radius may be used for all demand nodes or, alternatively, the coverage distance may vary according to either the demand node receiving coverage or the candidate site in question (or both) [11]. Covering problems can further be broken down into two basic types of covering problems, namely *set covering problems* and *maximum covering problems.*

Daskin [11] describes the set covering problem as a problem in which the objective is to find a subset of facilities in $\mathcal{I}$ such that each demand point in $\mathcal{J}$ is covered by at least one facility while minimum cost is incurred.

Denote the cost of locating a facility at candidate site $i \in \mathcal{I}$ by f_i and define the decision variables

$$X_i = \begin{cases} 1 & \text{if a facility is located at candidate site } i, \\ 0 & \text{otherwise.} \end{cases} \tag{2.1}$$

Then the objective in the set covering problem is to

$$\text{minimise } z = \sum_{i \in \mathcal{I}} f_i X_i \tag{2.2}$$

subject to the constraints

$$\sum_{i \in \mathcal{I}} a_{ij} X_i \geq 1, \qquad j \in \mathcal{J}, \tag{2.3}$$

$$X_i \in \{0,1\}, \qquad i \in \mathcal{I}. \tag{2.4}$$

In the above formulation, the objective function (2.2) seeks to minimise the total cost of the facilities that are located. Constraint set (2.3) ensures that each demand node $j \in \mathcal{J}$ is covered by at least one facility, while constraint set (2.4) ensures the binary nature of the decision variables X_i for all $i \in \mathcal{I}$.

A key deficiency of the set covering problem is that it requires all demand points in $\mathcal{J}$ to be served [11]. The number of facilities required to serve all of the demand points will, however, often exceed the number of facilities that can actually be built (due to budgetary or other constraints), resulting in solutions which are not feasible from a practical point of view. Daskin [11] furthermore explains that the set covering problem treats all demand points equally, not taking variable demand levels at different demand nodes into account. This implies that in the set covering model, a demand node with an associated demand of 10 calls for service per year is equally as important as a demand node with an associated demand of 1 000 calls for service per year. These concerns have led to the practice of fixing the number of facilities which can be located instead of requiring that all demand is met. This relaxation of the total coverage constraint has led to the formulation of the maximumm demand covering problem, whose objective is maximising the demand that can be met with the added restriction on the number of facilities which can be built.

Denote the demand exhibited at customer $j \in \mathcal{J}$ by h_j and suppose a total of P facilities are to be located at sites in $\mathcal{I}$. Upon defining the auxiliary variables

$$Z_j = \begin{cases} 1 & \text{if node } j \in \mathcal{J} \text{ is covered,} \\ 0 & \text{otherwise} \end{cases}$$

in addition to the decision variables in (2.1), the objective in the maximum demand set covering problem is to

$$\text{maximise } z = \sum_{j \in \mathcal{J}} h_j Z_j \tag{2.5}$$

subject to the constraints

$$\sum_{i \in \mathcal{I}} a_{ij} X_i \geq Z_j \qquad j \in \mathcal{J} \tag{2.6}$$

$$\sum_{i \in \mathcal{I}} X_i \leq P, \tag{2.7}$$

$$X_i, Z_j \in \{0,1\}, \qquad i \in \mathcal{I},\ j \in \mathcal{J}. \tag{2.8}$$

In this formulation, the objective function (2.5) maximises the amount of demand that can be covered by P facilities. Constraint set (2.6) states that the demand at node $j \in \mathcal{J}$ cannot be

covered unless at least one facility which is able to cover node j has been selected. Constraint (2.7) ensures that no more than P facilities are located at sites in $\mathcal{I}$. Unless fewer than P facilities are able to cover the total demand, constraint (2.7) will be a binding constraint in any optimal solution. Finally, constraint set (2.8) ensures the binary nature of the decision and auxiliary variables.

Various other adaptations have been proposed for covering problems in order to accommodate certain problem-specific constraints [11].

2.1.2 Centre Problems

In the covering problems discussed in the previous section, the objective was to determine the location of the minimum number of facilities required to cover all demand nodes. In these problems, the coverage distance between the facility locations and the demand nodes was specified exogenously. Two major shortcomings of the set covering problem were, however, pointed out. These led to the development of the maximum demand covering problem, in which the constraint that all demand has to be met is relaxed.

Centre covering problems follow a different approach to overcome the shortcomings of the set covering problem. The constraint that all demand has to be met is still applicable. Instead of using the exogenously specified covering distances to determine the minimum number of facilities required in order to cover all demand nodes, however, the model seeks to determine the minimum coverage distance required to cover all the demand nodes. The resulting model is known as the *P-centre problem*, which can be described as a *minimax* problem, since the maximum distance between a demand point and its nearest facility has to be minimised [11]. This is achieved by a relaxation of the notion of coverage distance. The relationship between the set covering problem and the maximum demand problem, as well as the centre problem, is summarised in Figure 2.1.

Daskin [11] emphasises that the distinction between problems in which facilites can be placed anywhere within an area of interest, and those where facilities may only be placed at specified points or nodes is necessary. Those where facilities can be placed at arbitrary locations are known as *absolute centre problems*, whereas problems in which facilities can only be placed on specified nodes are classified as *vertex centre problems*.

Biazaran and SeyediNezhad [6] present the vertex P-centre problem as follows. Denote the length of a shortest path between candidate site $i \in \mathcal{I}$ and demand node $j \in \mathcal{J}$ by d_{ij}, the maximum distance between any demand node and its nearest facility by z and suppose that at most P facilities are to be located at sites in $\mathcal{I}$.

Upon defining the auxiliary variables

$$Y_{ij} = \begin{cases} 1 & \text{if demand node } j \in \mathcal{J} \text{ is assigned to a facility located at candidate site } i \in \mathcal{I}, \\ 0 & \text{otherwise} \end{cases}$$

in addition to the decision variables in (2.1), the objective in the P-centre problem is to

$$\text{minimise } z \tag{2.9}$$

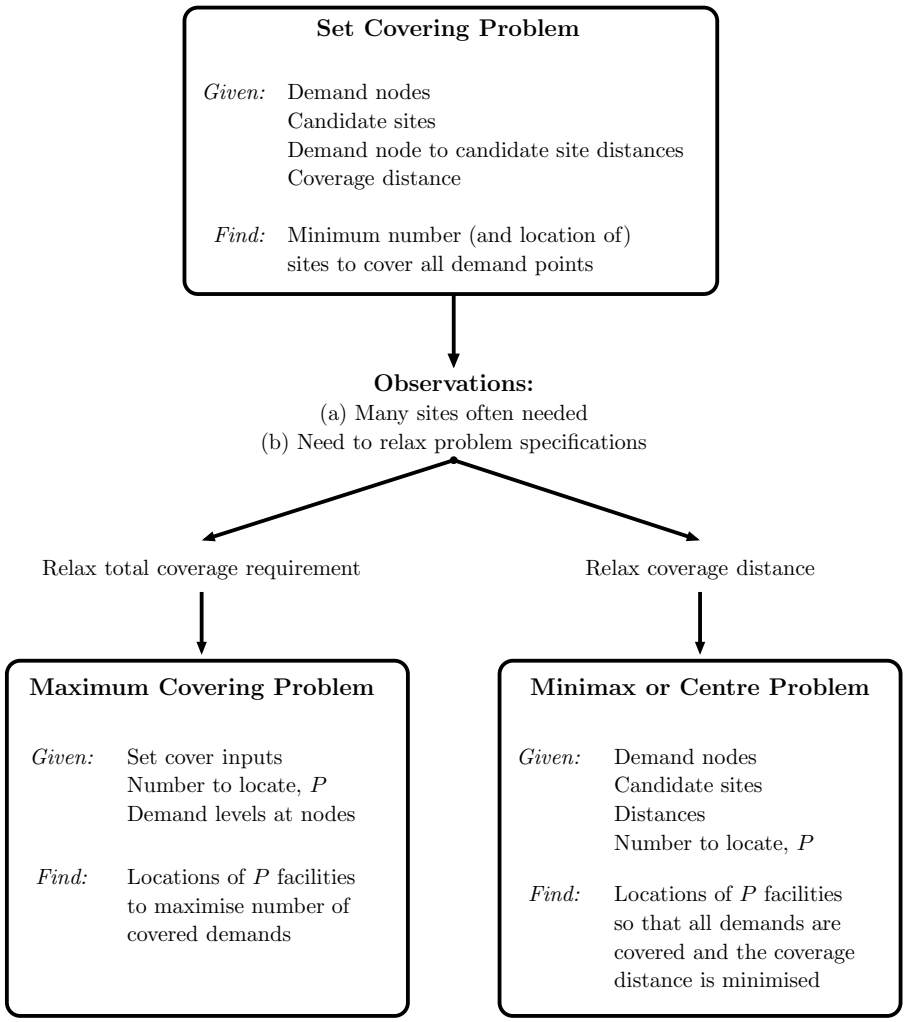

FIGURE 2.1: *The relationship between set covering, maximum covering and centre problems. Adapted from Daskin [11].*

subject to the constraints

$$\sum_{i\in\mathcal{I}} Y_{ij} \leq 1, \qquad j \in \mathcal{J} \tag{2.10}$$

$$\sum_{i\in\mathcal{I}} X_i \leq P, \tag{2.11}$$

$$Y_{ij} \leq X_i, \qquad i \in \mathcal{I},\ j \in \mathcal{J} \tag{2.12}$$

$$\sum_{i\in\mathcal{I}} d_{ij} Y_{ij} \geq z, \qquad j \in \mathcal{J}, \tag{2.13}$$

$$X_i, Y_{ij} \in \{0,1\}, \qquad i \in \mathcal{I},\ j \in \mathcal{J}. \tag{2.14}$$

The objective function (2.9) together with constraint set (2.13) minimises the maximum distance between a demand node $j \in \mathcal{J}$ and its nearest facility located at candidate site $i \in \mathcal{I}$. Constraint set (2.10) requires that all demand at a node $j \in \mathcal{J}$ must be allocated to exactly one facility at a candidate site $i \in \mathcal{I}$, for all demand nodes j. Constraint (2.11) ensures that at most P facilities are located, while constraint set (2.12) ensures that demand assignments can only be

made to open facilities. Constraint set (2.14) finally enforces the binary nature of the decision and auxiliary variables.

In order to solve the vertex P-centre problem on a general graph, Daskin [11] proposes an algorithm which employs a binary search mechanism to find an optimal solution by searching over the entire range of coverage distances for the smallest coverage distance such that all nodes can be covered. The algorithm adopts the following approach. Initial upper and lower bounds for the coverage distance are selected. Then, a set covering problem (see §2.1.1) is solved using the average of the upper and lower bound distances as the coverage distance in the objective function. If the number of facilities required to cover all nodes is smaller than or equal to P, the upper bound of the P-centre problem is taken as the coverage distance used in the set covering problem. If, however, the number of facilities required, as determined by solving the set covering problem, is greater than P, the lower bound of the P-centre problem is taken as the coverage distance used in the set covering problem, incremented by 1. If the upper and lower bounds are equal, the procedure is terminated. Otherwise, a new set covering problem is solved using the updated values for the upper and lower bounds. A pseudo-code description of this procedure is given in Algorithm 2.1.

In Step 1 of Algorithm 2.1, the assignment $D_c^H \leftarrow (n-1)\max_{ij}\{d_{ij}\}$ is made, where n represents the number of nodes in the demand graph and where d_{ij} represents the length of the link between nodes i and j. By defining D_c^H in this manner it is ensured that the upper bound for the coverage distance is sufficiently large. This is the case since a path between any two nodes will consist of at most $n-1$ links and $\max_{ij}\{d_{ij}\}$ is the length of the longest link. As a result, $(n-1)\max_{ij}\{d_{ij}\}$ is, in fact, an upper bound on the distance between any pair of nodes in the network. In Step 5, $P^*(x)$ represents the minimum number of facilities required in an optimal solution to the set covering problem when the coverage distance is x. Finally, D_c^H and D_c^L represent upper and lower bounds on the objective function of the P-centre problem.

Once the algorithm has terminated, D_c^L represents the optimal value of the objective function (2.9) and the corresponding placement locations for the P-centre problem on a general graph are those given by the locations as suggested by the corresponding solution to the set covering problem.

Algorithm 2.1: Algorithm to find the solution to a P-centre problem on a general graph.

```
1 D_c^H ← sufficiently large number;
2 D_c^L ← 0;
3 while D_c^L ≠ D_c^H do
4 |   D_c ← largest integer ≤ (D_c^L + D_c^H)/2;
5 |   P*(D_c) ← solution to the set covering problem with coverage distance D_c;
6 |   if P*(D_c) ≤ P then
7 |   |   D_c^H ← D_c;
8 |   else
9 |   |   D_c^L ← D_c + 1;
```

Various alternative techniques for solving other instances of P-centre problems are also described in some detail by Daskin [11].

2.1.3 Median Problems

It is often the case in the real world that there is a direct relationship between the benefit yielded from associating a facility/demand node pair and the distance that separates the facility from the demand node. For example, the cost of serving a retail outlet from a centralised distribution centre may depend on the distance the goods have to travel from the distribution centre to the retail outlet. Median problems take this relationship between the reduced benefit with an increase in distance into account [11]. Often this distance/benefit relationship is modelled linearly, as it would typically be in the example of the distribution centre and the retail outlet mentioned above. Other, non-linear relationships are, however, also a possibility. Daskin [11] defines the P-median problem as "the problem to find the location of P facilities on a network so that the total cost is minimised." In this problem, the cost of serving the demand at node $j \in \mathcal{J}$ is determined as the product of the demand at node j and the distance between node j and the facility which serves it.

Denote the demand at node $j \in \mathcal{J}$ by h_j, the distance between facility candidate site $i \in \mathcal{I}$ and demand node $j \in \mathcal{J}$ by d_{ij}, and suppose that no more than P facilities are to be located at sites in $\mathcal{I}$. Upon defining the auxiliary variables

$$Y'_{ij} = \begin{cases} 1 & \text{if a facility placed at node } i \in \mathcal{I} \text{ is assigned to satisfy the demand at node } j \in \mathcal{J}, \\ 0 & \text{otherwise} \end{cases}$$

in addition to the decision variables in (2.1), the objective in the P-median problem is to

$$\text{minimise } z = \sum_{j=1}^{n} \sum_{i=1}^{n} h_j d_{ij} Y'_{ij} \tag{2.15}$$

subject to the constraints

$$\sum_{i \in \mathcal{I}} a_{ij} Y'_{ij} \geq 1, \qquad j \in \mathcal{J}, \tag{2.16}$$

$$\sum_{i \in \mathcal{I}} X_i \leq P, \tag{2.17}$$

$$Y'_{ij} \leq X_i, \qquad i \in \mathcal{I},\ j \in \mathcal{J}, \tag{2.18}$$

$$X_i, Y'_{ij} \in \{0, 1\}, \qquad i \in \mathcal{I},\ j \in \mathcal{J}. \tag{2.19}$$

The objective function (2.15) minimises the total demand-weighted distance between each demand node and the facility to which it has been assigned. Constraint set (2.16) ensures that each demand node $j \in \mathcal{J}$ is assigned to exactly one facility at site $i \in \mathcal{I}$, while constraint (2.17) ensures that at most P facilities are located. Constraint set (2.18) links the decision variables and the auxiliary variables, ensuring that the demand at node $j \in \mathcal{J}$ may only be served by a facility located at node $i \in \mathcal{I}$ if there is, in fact, a facility located at node i. Constraint set (2.19) finally ensures the binary nature of the decision and auxiliary variables.

2.1.4 Fixed-charge Facility Location Problems

In the models discussed above, it was assumed that the cost of locating a facility at a given candidate site is the same for all candidate sites. In practice, this is rarely the case, however. Alizadeh [1] describes the fixed-charge facility location problem as a classical location problem

which often forms the basis of complex location models implemented in the design of supply chains. The fixed-charge facility location problem addresses the shortcoming of not taking into account the fixed cost of locating a facility at a candidate site. The problem may be summarised as follows. As input, a set of demand nodes with known demand and a set of candidate location sites are specified. If a facility is located at a candidate site, a known fixed cost is incurred. Furthermore, the unit shipment cost from each candidate site to each demand point is also assumed to be known. The objective is then to find a set of facility locations such that the total fixed cost due to facility placement, together with the shipping cost resulting from the facilities serving demand nodes, is minimised [14].

Again denote the demand at node $j \in \mathcal{J}$ by h_j and the distance between facility candidate location $i \in \mathcal{I}$ and demand node $j \in \mathcal{J}$ by d_{ij}. Furthermore, let f_i be the fixed cost associated with locating a facility at candidate location $i \in \mathcal{I}$ and denote the cost per unit distance of satisfying one unit of demand by δ. Finally, define, in addition to the decision variables in (2.1), the auxiliary variable $\tilde{Y}_{ij}$ as the fraction of demand at node $j \in \mathcal{J}$ satisfied by a facility located at candidate site $i \in \mathcal{I}$.

Then the objective in the fixed-charge facility location problem is to

$$\text{minimise } z = \sum_{i \in \mathcal{I}} f_i X_i + \delta \sum_{j \in \mathcal{J}} \sum_{i \in \mathcal{I}} h_j d_{ij} \tilde{Y}_{ij} \tag{2.20}$$

subject to the constraints

$$\sum_{i \in \mathcal{I}} \tilde{Y}_{ij} = 1, \qquad j \in \mathcal{J}, \tag{2.21}$$

$$\tilde{Y}_{ij} \leq X_i, \qquad i \in \mathcal{I},\ j \in \mathcal{J}, \tag{2.22}$$

$$X_i \in \{0, 1\}, \qquad i \in \mathcal{I}, \tag{2.23}$$

$$\tilde{Y}_{ij} \geq 0, \qquad i \in \mathcal{I},\ j \in \mathcal{J}. \tag{2.24}$$

The objective function (2.20) minimises the total cost, which is the sum of the fixed facility location costs and the total demand-weighted distance between the facility and its corresponding demand nodes multiplied by the cost per unit distance per unit demand. Constraint set (2.21) requires that each demand node $j \in \mathcal{J}$ is served, while constraint set (2.22) ensures that the demand at node $j \in \mathcal{J}$ cannot be allocated to a facility located at candidate site $i \in \mathcal{I}$ unless a facility is, in fact, located at candidate site $i \in \mathcal{I}$. Constraint sets (2.23) and (2.24) again ensure the binary and non-negative nature of respectively the decision variables and the auxiliary variables, respectively. Since the facilities are uncapacitated, all the demand at node $j \in \mathcal{J}$ will be allocated to the nearest open facility located at candidate site $i \in \mathcal{I}$. As a result, the demand assignment variables $\tilde{Y}_{ij}$ will assume integer values.

Naturally, it is typically not the case that facilities have unlimited capacity to satisfy demand in real-world applications. As Daskin [11] points out, capacities are important in many facility location problems. An automotive assembly plant may, for example, be able to assemble 500 vehicles during a regular eight-hour shift. Even if the plant were to operate for 24 hours per day, the maximum capacity would still be restricted to 1 500 vehicles per day. Thus Alizadeh [1] proposes an extension of the uncapacitated fixed-charge facility location problem in which capacitated facilities are considered. This is easily done by including the additional constraint set

$$\sum_{j \in \mathcal{J}} h_j \tilde{y}_{ij} \leq k_i X_i, \qquad i \in \mathcal{I} \tag{2.25}$$

in the problem formulation (2.20)–(2.24), where k_i represents the capacity of a facility located at candidate site $i \in \mathcal{I}$.

2.1.5 Extensions of Location Models

The covering, centre, median and fixed-charge location problems discussed above form the basis of most facility location models used in practice. In most cases, however, these basic models need to be extended in various ways, in order to accommodate a variety of real-life implications [11]. Two of the more common extensions of the basic models described above are briefly recounted in this section.

Multiobjective Models

Due to the fact that facility location decisions are usually long-term and thus strategic in nature, it is likely that several conflicting objectives need to be considered when facility placement decisions are made [11]. An example of this is encapsulated in the conflicting objectives of simultaneously maximising total area coverage and maximising average signal level in the radio transmission facility location problem described in §1.1. Hekmatfar and SteadiSeifi [18] describe how, due to the presence of conflicting objectives, no single optimal solution usually exists, as often the improvement of one objective will result in the reduction of the benefit gained measured according to another objective. As a result, Hekmatfar and SteadiSeifi [18] introduce the notion of a nondominated or efficient solution. Daskin [11] explains this notion as follows: "In general, a solution ϕ is inferior if there exists some solution θ that is as good as ϕ in terms of all the objectives and θ is strictly better than ϕ in terms of at least one objective. In that case, solution θ dominates solution ϕ which is inferior to or dominated by solution θ."

A number of different models exist for finding a suitable trade-off between conflicting objectives in order to find a non-dominated solution which will best suit the decision maker. A number of these models are discussed by Hekmatfar and SteadiSeifi [18].

Hierarchical Models

In the basic models discussed above it was assumed that only one type of facility had to be located. According to Bastani and Kazemzadeh [5], however, many facilities are hierarchical in nature, usually in terms of the services they provide. Daskin [11] elucidates the hierarchical nature of the interaction between facilities in the context of the banking industry. *Automatic teller machines* (ATMs) are at the lowest hierarchical level and offer only basic services, such as the withdrawal of money or account balance enquiries. Branch offices provide customers with the same services, as well as a variety of other services, such as the application for a residential loan or the purchasing of government bonds. Finally, main branches provide all services available at lower levels as well as others. Large corporate loans might, for example, only be handled at the main branch of a bank [11].

It is often useful to classify distributed facility networks according to the services offered by their constituent facilities as well as the regions over which these facilities can provide services. For a facilitation of the discussion Daskin [11] numbers the possible services from 1 to m. In the same manner he numbers the levels (or types of facilities) in the hierarchy from 1 to m, where level 1 represents the lowest order of facility (*e.g.* the ATM) and level m represents the highest order of facility. He then continues to classify five types of hierarchical systems.

A *successively inclusive facility hierarchy* is one in which a level m facility will provide all services. More generally, in such a hierarchy, a level b facility will provide all levels of service offered by a facility at level $b-1$, together with at least one additional service. Those services offered by a level b facility which are not offered by a level $b-1$ facility may be grouped together and called *level b services*. In a *successively exclusive facility hierarchy*, a level b facility only offers services of level b. In other words, in a *successively exclusive facility hierarchy* the set of services offered by a level b facility has no intersection with the set of services offered by a facility at level j, where $j \neq b$. In a successively inclusive hierarchy, a *locally inclusive service hierarchy* is one in which a level b facility located at node i offers services of type 1 through b to node i, but surrounding nodes $j \neq i$ only receive services of type b. More simply stated, only services of type b are exported to other nodes. In contrast, a *globally inclusive service hierarchy* is a hierarchy in which a level b facility located at node i provides services of all levels 1 through b to customers at all nodes. A *successively exclusive service hierarchy* exists when a level b facility located at node i can only provide services of level b to customers at all nodes [11].

Several models have been formulated in order to solve instances of the above types of hierarchical facility location problems. Daskin [11] discusses a number of these models.

2.2 Models for Radio Transmitter Placement in Particular

In second generation mobile telecommunication networks, the network planning problem may be decomposed into two distinct phases: *coverage planning*, which involves antennae placement in order to achieve maximum service coverage, and *capacity planning* which involves frequency assignment planning [3]. The coverage planning problem has generally been modelled using variations on the celebrated set covering problem described in §2.1.1. Amaldi *et al.* [3] describe this problem, known in the context of radio transmitter network planning as the *coverage problem*, as follows: Given an area where service provision has to be guaranteed, determine those locations where radio transmitters should be placed and specify their configurations such that each point (or user) in the service area receives an adequate signal level. Two main modelling approaches have been adopted in the literature to solve instances of the coverage problem [3].

2.2.1 Continuous Optimisation Models

In continuous optimisation models, a specified number, k (say), of base stations are to be located at any site within the given space which is to be covered, where the antennae co-ordinates are the continuous variables of the problem. This space may exclude certain forbidden areas in which no transmitter placements are allowed. In certain cases, other parameters, such as the antennae orientations and/or the transmission power, may also be considered as variables. Amaldi *et al.* [3] claim that the most important element of this type of optimisation model is the propagation prediction model used to estimate the signal intensity at each point in the coverage area. Various functions have been developed over the years for signal estimation, ranging from simple empirical models, such as those developed by Hata [17], to more sophisticated ray tracing methods, such as that proposed by Iskander and Yun [20]. The objective function of the coverage problem is usually determined by some measure of the quality of service, such as the largest minimum signal intensity at any location [3]. Due to the high complexity of propagation loss functions, global optimisation techniques are usually employed to tackle these problems, as illustrated by Sherali *et al.* [36] who employ a convex combination (weighted average) of two objective functions as defined below.

Minisum Objective Function. This function seeks to minimise the sum of all the weighted path loss predictions in the design space along with a penalty term which represents a path loss greater than a specified threshold value for a specific demand point. The penalty term serves to ensure that the maximum acceptable path loss is not exceeded. The optimisation of this function with respect to transmitter location aims to improve the overall coverage in the design space. A drawback of this function is that it might ignore several remote receiver points while still returning a high quality overall weighted average.

Minimax Objective Function. In order to ensure that even the most remote receiver location receives adequate coverage, this function seeks to minimise the maximum of all the weighted path loss predictions, including a penalty for exceeding the maximum acceptable path loss. The problem with this function is that it focuses on the worst-case scenario at the expense of the overall weighted coverage.

A convex combination of the above-mentioned objective functions is often used in order to take advantage of the respective merits of each of the objective functions while minimising their drawbacks. The resulting model accommodates two types of design constraints. The first constraint is treated as a "soft" constraint and ensures that each receiver location in the design space receives an adequate signal level. This constraint is incorporated in the model using a penalty term in the minisum objective function. The second constraint type restricts the transmitter placement location to specified acceptable subsets of the design space.

Using a three-dimensional design space X, Sherali *et al.* [36] denote the hyperrectangle representing the feasible transmitter location space as $Q \equiv \{(x, y, z) \in \mathbb{R}^3 : 0 \leq x \leq h_1, 0 \leq y \leq h_2, 0 \leq z \leq h_3\}$. Furthermore $j \in \{1, \ldots, m\}$ represents indices for the given receiver locations, w_j represents the relative priority weight ascribed to the j-th receiver location, $g_j(x, y, z)$ represents the path loss at the j-th receiver location for a given transmitter location, s_j represents the maximum tolerated path loss threshold at the j-th receiver location, μ_j represents a suitable penalty factor for violating the prescribed path loss threshold at receiver location j and $\psi \in [0, 1]$ is the convex combination weight used to compose the minisum and minimax objective functions.

The aim of the single transmitter facility location problem is to

$$\text{minimise } f(x, y, z) = \psi f_1(x, y, z) + (1 - \psi) f_2(x, y, z) \tag{2.26}$$

subject to the constraints

$$0 \leq x \leq h_1, \quad 0 \leq y \leq h_2, \quad \text{and} \quad 0 \leq z \leq h_3, \tag{2.27}$$

where $f_1(x, y, z)$ represents the minisum objective function

$$f_1(x, y, z) = \frac{1}{m} \sum_{j=1}^{m} w_j [g_j(x, y, z) + \mu_j \max\{0, g_j(x, y, z) - s_j\}] \tag{2.28}$$

and

$$f_2(x, y, z) = \max\, w_j [g_j(x, y, z) + \mu_j \max\{0, g_j(x, y, z) - s_j\}] \tag{2.29}$$

is the minimax objective function.

As demonstrated by Sherali *et al.* [36], this model can easily be adapted for problems in which multiple transmitter placements are to be made.

2.2.2 Discrete Optimisation Models

The second coverage problem modelling approach involves the use of discrete mathematical models. In discrete optimisation models, a number of test sites or demand nodes representing users of the network have to be identified from a predetermined set within the service area. Instead of allowing base stations to be placed at any location in the coverage area, discrete mathematical models therefore restrict the positioning of these base stations to a set of so-called candidate sites. In these models, the area covered by each base station is determined *a priori*, generally using a radio wave propagation predictor and taking the surrounding topology and morphology of the terrain into account [27]. The area covered by a base station located at a candidate site is therefore assumed to be known in such an optimisation model.

Krzanowski and Raper [24] explain that in both the continuous and discrete modelling paradigms, *total cover problems* require the determination of the minimum number of facilities in order to meet all the demand. In contrast, *partial cover problems* arise when the number of facilities to be placed is fixed and the locations have to be chosen so as to maximise the demand that can be covered using the limited number of facilities. A further extension of the partial cover problem is the so-called *general cover problem*, in which the objective is to minimise the maximum distance between a facility and the demand points it covers. Mathar and Niessen [27] demonstrate how the coverage problem is an extension of the classical minimum cost set covering problem discussed in §2.1.1.

In order to formulate the coverage problem as a minimum cost set covering problem, Amaldi *et al.* [3] introduce the following variables. Let $\mathcal{S} = \{1, \ldots, m\}$ represent the set of all the possible candidate sites for radio transmitter placement. Then, for each $i \in \mathcal{S}$, let the set $\mathcal{D}_i$ represent all the different base station configurations which can be installed at candidate site i. Since the installation cost of a base station at a candidate site can vary, not only due to environmental factors, but also as a function of the base station configuration, let c_{id} represent the installation cost of a base station with configuration $d \in \mathcal{D}_i$ at candidate site $i \in \mathcal{S}$. Finally, let the set $\mathcal{J} = \{1, \ldots, n\}$ denote all the demand nodes or test points. Using the information from the propagation predictor, the binary parameter

$$a_{ijd} = \begin{cases} 1 & \text{if the signal from a base station installed at candidate site } i \text{ with} \\ & \text{configuration } d \text{ is sufficient to cover demand node } j, \\ 0 & \text{otherwise} \end{cases}$$

can be derived *a priori*. Amaldi *et al.* [3] further define the decision variable

$$\hat{Y}_{id} = \begin{cases} 1 & \text{if a base station with configuration } d \in \mathcal{D}_i \text{ is installed at candidate site } i \in \mathcal{S}, \\ 0 & \text{otherwise.} \end{cases}$$

The objective of the minimum cost set covering problem is then to

$$\text{minimise } z = \sum_{i \in \mathcal{S}} \sum_{d \in \mathcal{D}_i} c_{id} \hat{Y}_{id} \tag{2.30}$$

subject to the constraints

$$\sum_{i \in \mathcal{S}} \sum_{d \in \mathcal{D}_i} a_{ijd} \hat{Y}_{id} \geq 1, \qquad j \in \mathcal{J}, \tag{2.31}$$

$$\sum_{d \in \mathcal{D}_i} a_{ijd} \hat{Y}_{id} \leq 1, \qquad i \in \mathcal{S}, \tag{2.32}$$

$$\hat{Y}_{id} \in \{0, 1\}, \qquad i \in \mathcal{S},\ d \in \mathcal{D}_i. \tag{2.33}$$

Constraint set (2.31) ensures that all demand nodes are covered by at least one base station, while constraint set (2.32) ensures that for each base station only one configuration is selected. Constraint set (2.33) finally ensures the binary nature of the decision variables.

It is often the case, however, that due to limitations on the installation cost, the covering requirement is treated as a "soft constraint" and as a result the problem requires a trade-off between maximising coverage and containing installation cost. In order to uncover such a trade-off, Amaldi *et al.* [3] introduce a further explicit variable

$$\hat{Z}_j = \begin{cases} 1 & \text{if demand node } j \in \mathcal{J} \text{ is covered,} \\ 0 & \text{otherwise.} \end{cases}$$

The objective of the resulting maximum coverage problem is then to

$$\text{maximise } z = \nu \sum_{j \in \mathcal{J}} \hat{Z}_j - \sum_{i \in \mathcal{S}} \sum_{d \in \mathcal{D}_i} c_{id} \hat{Y}_{id} \tag{2.34}$$

subject to the constraints

$$\sum_{i \in \mathcal{S}} \sum_{d \in \mathcal{D}_i} a_{ijd} \hat{Y}_{id} \geq \hat{Z}_j, \qquad j \in \mathcal{J}, \tag{2.35}$$

$$\sum_{d \in \mathcal{D}_i} a_{ijd} \hat{Y}_{id} \leq 1, \qquad i \in \mathcal{S}, \tag{2.36}$$

$$\hat{Y}_{id} \in \{0,1\}, \qquad i \in S,\ d \in \mathcal{D}_i, \tag{2.37}$$

$$\hat{Z}_j \in \{0,1\}, \qquad j \in \mathcal{J}, \tag{2.38}$$

where $\nu > 0$ is a suitable trade-off parameter allowing both objectives to be expressed in economic terms. The introduction of the variable $\hat{Z}_j$ results in the modification of constraint set (2.31) to constraint set (2.35), which ensures that all the demand accounted for in the objective function is, in fact, covered by a base station. Constraint set (2.36) again ensures that at most one configuration is selected for a given base station, while constraint sets (2.37) and (2.38) ensure the binary nature of the decision variables.

As Amaldi *et al.* [3] point out, one problem in both the above models is that they do not take overlaps between cells (the area covered by a specific base station) into account. This becomes very important later during the frequency allocation phase of capacity planning when dealing with handover (*i.e.* the possibility of a user remaining connected while moving from one cell to another). To overcome this shortcoming, cell boundaries can be set up during the network planning phase by introducing variables which explicitly assign demand nodes to base stations. An example of this is given by Amaldi *et al.* [3].

Due to the large dimensions of the optimisation problems typically involved in radio transmitter facility location planning problems, metaheuristics are often employed as approximate optimisation techniques. Simulated annealing has, for example, been used by Mathar and Niessen [27] in an instance where the complexity of the optimisation problem places an optimal solution out of reach of current computing technology. Krzanowski and Raper [24] instead used a hybrid genetic algorithm designed to take the surrounding geography into account during the site selection process.

2.3 Effective Transmission Requirements

As stated in §1.1, for an area to be considered covered, an unobstructed line of visibility between the transmitter and receiver should at the very least be achieved. If this direct line of visibility is obstructed, then a situation of *Non Line Of Sight* (NLOS) is said to prevail. Radio wave transmission does, however, not only depend on a clear line of visibility between transmitter and receiver. Radio transmission generates an infinite family of nested radio waves in the form of ellipsoids, called *Fresnel ellipsoids*. These ellipsoids all have both the transmitter and receiver at their foci. Ideally, the innermost member of this family of ellipsoids, called the *first Fresnel ellipsoid*, should also be unobstructed. If an unobstructed line of visibility exists between a transmitter and receiver, but the first Fresnel ellipsoid is partially obstructed, *Near Line Of Sight* (nLOS) is said to have been achieved, whereas if both the direct line of visibility and the first Fresnel ellipsoid between the transmitter and receiver are unobstructed, then (full) *Line Of Sight* (LOS) is said to have been achieved. Studies conducted in the San Francisco Bay area by Feuerstein *et al.* [15] have shown an increased radio wave propagation loss when nLOS conditions exist.

Radio wave propagation loss is perhaps the most important factor influencing effective radio transmission. Iskander and Yun [20] define propagation loss at a point r as "the ratio of transmitted power at r_0, $P_t(r_0)$, over the received power at r, $P_t(r)$." In free space, the propagation loss, in dB, can simply be expressed as

$$L(r_0, r) = 10 \log \frac{P_t(r_0)}{P_r(r)} = -10 \log \frac{G_t G_r \lambda^2}{(4\pi)^2 D^2}, \tag{2.39}$$

where G_t and G_r are the gains of the transmitting antennae and the receiving antennae, respectively, D is the distance between the transmitter at r_0 and the receiver at r, and λ is the wavelength in free space [20]. In order to ensure effective radio wave transmission, this propagation loss must remain below a specified threshold value in order to provide a signal of the required intensity [36].

Various models and techniques have been developed in order to determine the propagation loss between two points in obstructed space. These propagation loss prediction models may be divided into three different types, namely empirical, theoretical and site-specific models. Empirical models are developed by taking extensive field measurements from which the equations are then derived. Due to variations in the surrounding environment, however, the empirical models may lack in accuracy when applied to an area which is different to the one where the measurements on which the formulas are based, were made. Empirical models are generally used for propagation predictions in macrocells which have radii ranging from 1 km to 30 km [25]. The advantage of using empirical models is that they are simple and efficient to use [20].

Site-specific models, such as the ray-tracing model introduced by Seidel and Rappaport [35], are based on very detailed numerical methods, and as a result require detailed and accurate input parameters, including data on the specific locations of buildings, their heights and the distances between the walls of these buildings. These models are generally used when propagation predictions are made for microcells with radii up to 1 km or picocells which have radii up to 500 m [25], and as a result are generally used in urban areas. The disadvantage of using the site-specific propagation models is the large computational overhead which may even be beyond the computational capability of present computers [20].

Theoretical models are derived from the underlying physics, but are based on the assumption of ideal conditions. As a result they typically achieve a middle ground between the accuracy of the site-specific models and the computational efficiency of the empirical models [20].

In Europe, research efforts in respect of propagation prediction models is promoted by the *European Cooperation in the Field of Scientific and Technical Research* (COST) which is "an open, flexible framework for research and development cooperation between universities, industry and research institutions" [16]. One aim of the so-called *COST 231 action* has been to elaborate on powerful prediction models, many of which have now become widely accepted. These include extensions to Hata's empirical model [17], which address several shortcomings of the original model proposed by Hata, such as the so-called COST 231-Hata Model and the COST-231-Walfisch-Ikegami Model [16]. For example, the COST 231-Hata Model takes the frequency f, the distance between the antennae D, the base station antenna height h_b and the mobile antenna height h_m into account. Then, as outlined in [25], the COST 231-Hata Model yields the basic propagation loss

$$L_b = 46.3 + 33.9 \log f - 13.82 \log h_b - a(h_m) + (44.9 - 6.55 \log h_b) \log d + C_m \tag{2.40}$$

(in dB), where

$$a(h_m) = (1.1 \log f - 0.7)h_m - (1.56 \log f - 0.8) \tag{2.41}$$

and

$$C_m = \begin{cases} 0 \text{ dB} & \text{for suburban areas with medium tree density,} \\ 3 \text{ dB} & \text{for metropolitan centres.} \end{cases}$$

The COST 231-Hata Model is restricted to the following range of parameters:

$$\begin{aligned} f &\in [1500, 2000] \text{ MHz,} \\ h_b &\in [30, 200] \text{ m,} \\ h_m &\in [1, 10] \text{ m, and} \\ D &\in [1, 20] \text{ km.} \end{aligned}$$

The model is further restricted to use in macrocells. Also, the base station antennae heights must be above the roof-top levels of the buildings adjacent to the base station for the model to yield accurate results. As stated above, more sophisticated models (often based on numerical methods) are used for radio signal propagation loss predictions in microcells.

2.4 Data Required for Radio Transmitter Placement Decisions

When placing radio transmitters, the complex distribution of expected demand patterns for the service to be provided, the presence of area-specific geographic features, such as topography, morphology and the type of land cover, as well as the technological aspects and capabilities of the network, have to be taken into account simultaneously [24]. In addition, the service area for the network and information on possible locations for the placement of the transmitters have to be known. Krzanowski and Raper [24] propose the use of *geographic information systems* (GISs) to obtain the required information related to the topography, morphology and the land cover for the area under consideration. GIS is a technology designed specifically to handle environmental and spatial information with great accuracy.

In the models discussed in §2.2, the demand plays a crucial role in the facility location process. It is, however, not as easy to obtain expected demand values as it is to acquire environmental information. Demand has become increasingly important due to the transition of mobile radio communication into a mass communication technology. As a result, demand coverage may be converted to monetary terms and viewed as revenue coverage [43]. This led to the development of the *demand node concept* (DNC) by Tutschku and Tran-Gia [44], which is a discrete population

model for expected mobile traffic description. The DNC represents the spatial distribution of the expected demand at discrete points, known as *demand nodes*. Each demand node represents a fixed quantum of demand, usually accounted for by a fixed number of call requests per unit time. Based on the land use of an area, the spatial traffic distribution may be derived using complex estimation methods and stored in a traffic matrix. From this traffic matrix, the demand nodes may then be generated using a partitional clustering method [43].

Kzanowski and Raper [24] present a similar method for estimating expected demand, which is calculated as the weighted sum of vehicular traffic, the population and the business counts in the area of interest. Each of these factors contribute to the resulting traffic layer, which is a direct input to their hybrid genetic algorithm for transmitter location in wireless networks.

2.5 Chapter Summary

A thorough review of the different types of facility location models was given in this chapter. This review included the well-known covering problem, the centre problem, the median problem and the fixed-charge facility location problem, as well as common extensions which may be applied to these basic models so as to improve their accuracy when dealing with real-life situations. This was followed by an investigation of models which have specifically been used for the placement of radio transmitters in mobile telecommunication networks. It was found that generally two main approaches have been followed in the literature to solve the radio transmitter facility location problem: A continuous optimisation approach and a discrete optimisation approach. Various factors that have an influence on the effectiveness of radio transmission were discussed in order to gain insight into the factors which significantly influence the quality of the transmission provided by the transmitters located in a mobile telecommunication network. It was found that the line of sight between a transmitter, the first Fresnel ellipsoid and radio signal propagation loss are the most important factors to be considered in the development of a decision support framework for the location of transmitters in a mobile telecommunication network. Finally, an investigation was conducted into which data are required in order to generate an instance of the bi-objective optimisation problem described in §1.1.

CHAPTER 3

Transmitter Location Quality Evaluation

Contents

This chapter is devoted to the establishment of a suitable framework for evaluating the effectiveness of a given set of placement locations for a network of radio transmitters. The focus in §3.1 is on the line of sight between a transmitter and a receiver, as well as the first Fresnel ellipsoid generated by the electromagnetic waves of the radio communication. In §3.2, the focus then shifts to the propagation prediction model used to ensure that the potential receiver demand points receive an adequate signal level in order to be considered covered. Section 3.3 is devoted to an explanation of two performance measures according to which the quality of a network of transmitter placement locations may be evaluated. The chapter closes in §3.4 with a brief summary of the material included in this chapter.

3.1 Line of Visibility and First Fresnel Ellipsoid Obstruction

The decision support framework developed in this project for radio transmission tower placement is based on a discrete facility location modelling approach, as discussed in §2.2. The input to the process of determining radio transmission coverage of an area by a given set of transmitters is a matrix of entries corresponding to a rectangular grid of placement candidate sites (which are also the coverage demand points) containing terrain elevations above sea level for some specified area of interest. For a demand point in this area to be considered covered by a potential transmitter, an unobstructed LOS (*i.e.* an unobstructed line of visibility as well as, to some extent, an unobstructed first Fresnel ellipsoid) should exist between the transmitter and the demand point, as discussed in §1.1. Bresenham's well-known line drawing algorithm [29], which is widely used in computer graphics to determine which pixels need to be coloured when drawing straight lines on screen displays, may be used to determine those entries in the matrix which form the line of communication between the transmitter and receiver locations under investigation. A complete description of Bresenham's line drawing algorithm, as outlined by McKinney and Agarwal [29], is given in pseudo-code form Algorithm 3.1.

In Step 1 of Algorithm 3.1, the endpoints of the line segment under consideration are swapped, if necessary, to ensure that the change in the x values as one moves along the line segment remains positive. By doing this, two further scenarios for the algorithm are eliminated. The values $\mathrm{d}x$ and $\mathrm{d}y$ determined in Step 2 represent the difference in the x and y coordinates spanned by the line segment, respectively, and are required to determine which one of two scenarios of Bresenham's line drawing algorithm is applicable to the line segment under consideration. The value of a variable s, which is an indicator for the gradient of the line segment under consideration, is determined in the if-statement spanning Steps 3–6. If this gradient is positive, s is assigned the value 1, whereas for a negative gradient, s is assigned the value -1. The first scenario of Bresenham's line drawing algorithm, which is applicable when the value $\mathrm{d}x$ is larger than the value $\mathrm{d}y$, is described in Steps 8–17. In this scenario, the x value is incremented during every iteration. The value p first calculated in Step 9 is an error term used to determine whether the y value should also be incremented. At the beginning of each iteration of the while-loop, the pixel corresponding to the current x and y values is coloured, thus forming a part of the straight line on the screen display. The while-loop spanning Steps 20–33 follows a similar pattern as the one spanning Steps 8–17, with the exception that in this scenario, the value $\mathrm{d}y$ is greater than the value $\mathrm{d}x$ and, as a result, the y value will be incremented by s during every iteration, while the value p is used to determine whether the x value should also be incremented.

Example 3.1 (**Bresenham's line drawing algorithm**). *Suppose Bresenham's line drawing algorithm has to be used to determine which points of a* 20×20 *grid of integer coordinates lie on a line drawn from the coordinates* $(x_1', y_1') = (15, 2)$ *to* $(x_2', y_2') = (10, 19)$. *Since the coordinates are not arranged in such a manner that* $x_1' \leq x_2'$, *meaning that the coordinate set* (x_2', y_2') *represents the "left endpoint" of the line, the two points are interchanged in Step 1 of Algorithm 3.1 such that* $(x_1, y_1) = (10, 19)$ *and* $(x_2, y_2) = (15, 2)$. *Next,* $\mathrm{d}x = 5$ *and* $\mathrm{d}y = 17$ *are calculated in Step 2. Since* $\mathrm{d}y \leq 0$, s *is assigned a value of* -1 *in Step 6. The variables* x *and* y *are initialised to* 10 *and* 19, *respectively in Step 7, while* p *is initialised to* 7 *in Step 9. The results of each iteration of the while-loop spanning Steps 20–33 of Algorithm 3.1 are summarised in Table 3.1. The while-loop terminates after* 17 *iterations when* $y = y_2$. *The pixels approximating the straight line from* $(10, 19)$ *to* $(15, 2)$ *are shown graphically in Figure 3.1.* □

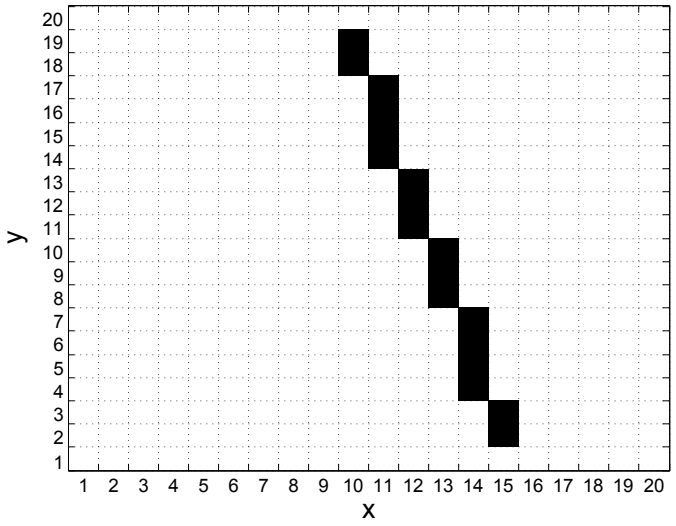

FIGURE 3.1: *The output of Bresenham's line drawing algorithm when used to draw a line from the coordinates* $(10, 19)$ *to* $(15, 2)$.

At each of the demand points along the line determined by Bresenham's line drawing algorithm, the difference in elevation between the lower boundary of the first Fresnel ellipsoid and the

Algorithm 3.1: Bresenham's line drawing algorithm [29]

Input : The endpoints (x_1, y_1) and (x_2, y_2) for the line segment.
Output: A set of pixels approximating the line segment from (x_1, y_1) to (x_2, y_2).

```
1  Arrange the coordinates such that x_1 < x_2, that is, (x_1, y_1) is the left endpoint;
2  dx ← x_2 − x_1 and dy ← y_2 − y_1;
3  if dy ≤ 0 then
4      s ← 1;
5  else
6      s ← −1;
7  x ← x_1 and y ← y_1;
8  if |dy| ≤ |dx| then
9      p ← 2s dy − dx;
10     while x ≤ x_2 do
11         Set pixel(x, y);
12         if p < 0 then
13             p ← p + 2s dy;
14         else
15             y ← y + s;
16             p ← p + 2(s dy − dx);
17         x ← x + 1;
18 else
19     p ← 2s dx − dy;
20     while y ≠ y_2 do
21         Set pixel(x, y);
22         if dy ≥ 0 then
23             if p ≤ 0 then
24                 p ← p + 2s dx;
25             else
26                 x ← x + 1;
27                 p ← p + 2(s dx − dy);
28         else if p ≤ 0 then
29             x ← x + 1;
30             p ← p + 2(s dx − dy);
31             else
32                 p ← p + 2s dx;
33         y ← y + s;
34 Output pixel (x_2, y_2)
```

Iteration	1	2	3	4	5	6	7	8	9
Set Pixel	$(10, 19)$	$(10, 18)$	$(11, 17)$	$(11, 16)$	$(11, 15)$	$(11, 14)$	$(12, 13)$	$(12, 12)$	$(12, 11)$
p	-3	21	11	1	-9	15	5	-5	19
x	10	11	11	11	11	12	12	12	13
y	18	17	16	15	14	13	12	11	10
Iteration	10	11	12	13	14	15	16	17	
Set Pixel	$(13, 10)$	$(13, 9)$	$(13, 8)$	$(14, 7)$	$(14, 6)$	$(14, 5)$	$(14, 4)$	$(15, 3)$	
p	9	-1	23	13	3	-7	17	7	
x	13	13	14	14	14	14	15	15	
y	9	8	7 s	6	5	4	3	2	

TABLE 3.1: *The results of the* 17 *iterations of the while-loop in Bresenham's line drawing algorithm when used to draw a line from* $(10, 19)$ *to* $(15, 2)$.

demand point's elevation above sea level may be compared in order to determine whether or not a LOS exists between the demand points. The radius of revolution around the line segment connecting the foci of the first Fresnel ellipsoid (hereafter called the *axial radius*) at any point p on the surface of the ellipsoid between the transmitter and receiver is given by

$$r = \sqrt{\frac{\lambda d_1 d_2}{D}}, \tag{3.1}$$

where d_1 represents the distance along the line of visibility between p and the transmitter, d_2 represents the distance along the line of visibility between p and the receiver, $D = d_1 + d_2$ is the total distance between the transmitter and receiver, and λ represents the wavelength of the transmitted signal. The distances d_1, d_2 and D in (3.1) may be approximated using the theorem of Pythagoras in cases where the elevations of the transmitter and receiver differ. These parameters are illustrated graphically in Figure 3.2.

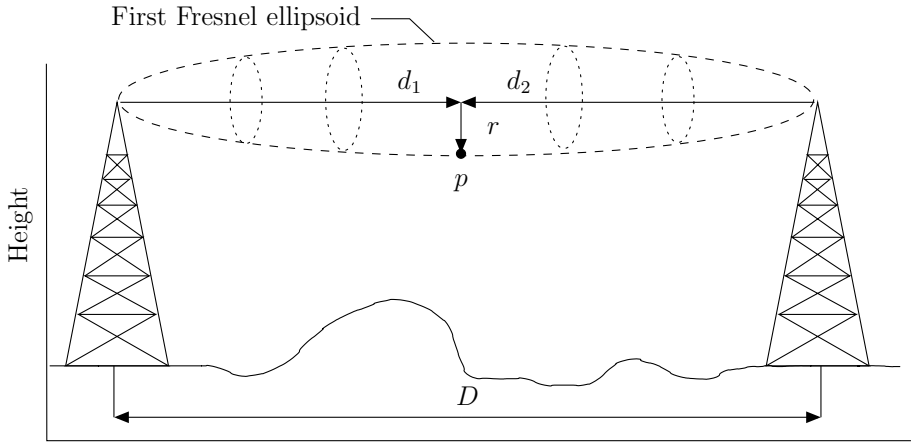

FIGURE 3.2: *The parameters of the first Fresnel ellipsoid.*

In order to illustrate how the framework for evaluating the effectiveness of a given set of placement locations in this project works, a real data set containing elevation data for an area in the South African Western Cape is used in all the remaining examples in this chapter. The set contains elevation data for $n = 400$ points forming a 20×20 grid. The latitude distance between two successive points in the grid is approximately 308.1 metres, while the longitude distance between two successive points is approximately 256.6 metres. A surface plot of these elevation data is shown in Figure 3.3.

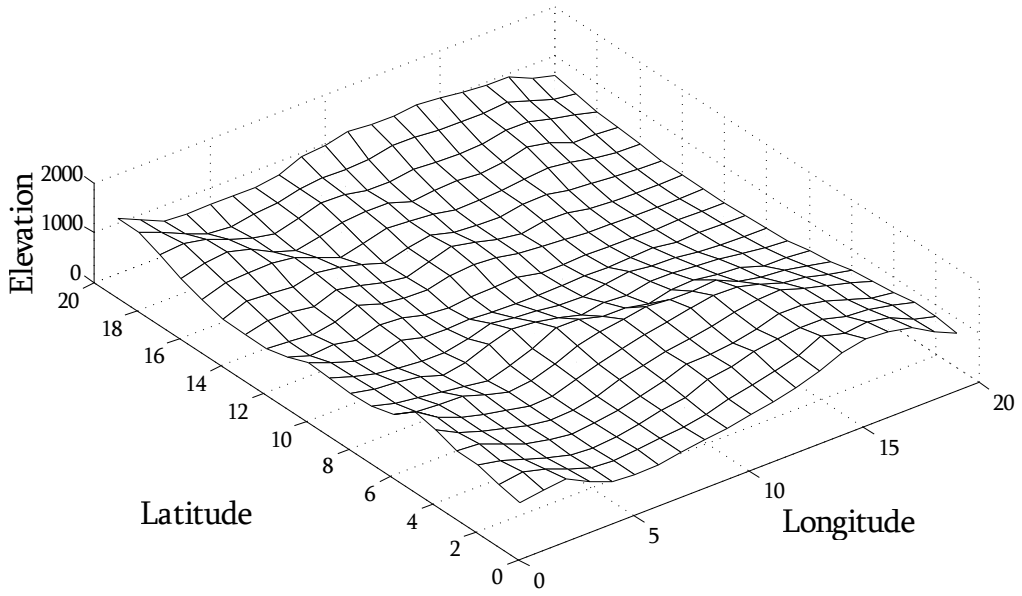

FIGURE 3.3: *Surface plot of the elevation data used for the examples in this chapter.*

Example 3.2 (**The axial radius of the first Fresnel zone**). *Suppose the axial radii of the first Fresnel ellipsoid generated between a transmitter placed at point* $(15, 2)$ *and a receiver located at point* $(10, 19)$ *of the grid considered in Example 3.1 has to be determined at the points* $(14, 7)$ *and* $(12, 12)$. *The frequency used to determine the wavelength required for the calculation of the axial radii of the first Fresnel ellipsoid is 1 800 MHz, which is commonly used in 2G cellular telephone networks [33]. At this frequency, the wavelength* λ *is 0.167 metres. As stated above, the longitude distance (taken here to be in the x-direction) between two successive grid points is* 308.1 *metres, while the latitude distance (i.e. in the y-direction) between two successive grid points is* 256.6 *metres. The angle* τ *between the line of visibility and a horizontal line may be calculated as*

$$\tau = \tan^{-1} \frac{\mathrm{d}z}{\sqrt{(308.1\mathrm{d}x)^2 + (256.6\mathrm{d}y)^2}},$$

as illustrated in Figure 3.4. For the line in question, τ *is calculated to be* $5.801°$. *Using the theorem of Pythagoras, the distance* D *may be calculated as*

$$D = \frac{\sqrt{(308.1\mathrm{d}x)^2 + (256.6\mathrm{d}y)^2}}{\cos\tau}.$$

Furthermore, $\mathrm{d}x = 5$ *and* $\mathrm{d}y = 17$, *where* $\mathrm{d}x$ *and* $\mathrm{d}y$ *have the same meaning as in Algorithm 3.1, while the difference in altitude of the transmitter and receiver is* $\mathrm{d}z = 470$ *metres. As a result,* D *is calculated to be* $4\,650.03$ *metres. At the point* $(14, 7)$, $x = 14$ *and* $y = 7$. *The distance* d_1 *may therefore be calculated as*

$$d_1 = \frac{\sqrt{(308.1(x - x_1))^2 + (256.6(y - y_1))^2}}{\cos\tau} = 1\,326.27 \text{ metres.}$$

It follows that

$$d_2 = D - d_1 = 3\,323.76 \text{ metres.}$$

Now that all the parameters are known, the axial radius of the first Fresnel ellipsoid between a transmitter placed at $(15, 2)$ *and a receiver located at* $(10, 19)$ *may be calculated as*

$$r = \sqrt{\frac{\lambda d_1 d_2}{D}} = \sqrt{\frac{0.167 \times 1\,326.27 \times 3\,323.76}{4\,650.03}} = 12.57 \text{ metres}$$

at grid point $(14, 7)$. *Using the same formulae as above,* $d_1 = 2\,652.53$ *metres and* $d_2 = 1\,997.50$ *metres at grid point* $(12, 12)$. *In this case, therefore, the axial radius of the first Fresnel ellipsoid is* $r = 13.79$ *metres.* □

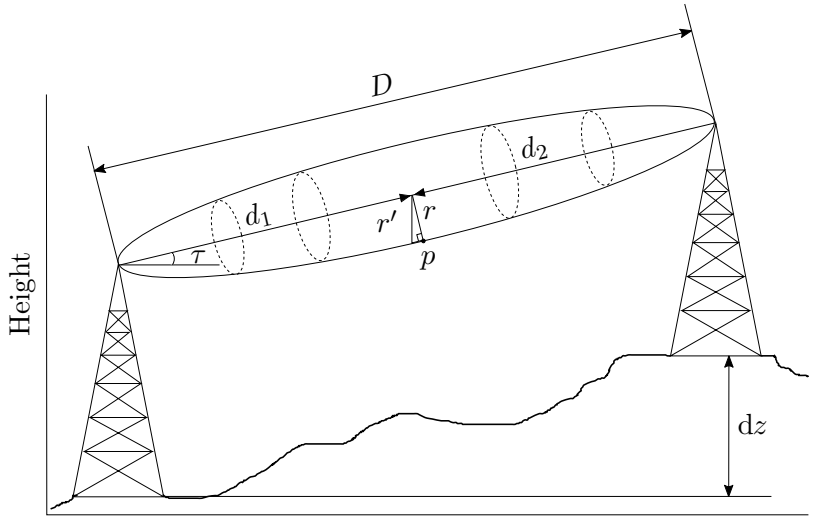

FIGURE 3.4: *The adjusted parameters of the first Fresnel ellipsoid, taking a difference in elevation between the transmitter and receiver into account.*

The test for unobstruction of the first Fresnel ellipsoid is performed by considering the equation of the straight line of visibility between the transmitter and the demand point, and comparing the lowest point of the first Fresnel ellipsoid and the height of the line of visibility. A parameter $\alpha \in [0, 1]$ is, however, introduced as a user-scalable measure of the required extent to which the first Fresnel ellipsoid should be unobstructed. Only if the elevation of the lowest point on the first Fresnel ellipsoid, multiplicatively scaled by the parameter α, between transmitter candidate site i and demand point j is higher than the elevation above sea level for all points along all surface points above the line determined by the Bresenham line drawing algorithm between i and j, the demand point may be considered covered in terms of communication *feasibility* by the transmitter candidate site. In this case, the next step will be to test whether the signal propagation loss between the transmitter and receiver is below a user-specified threshold, using a propagation prediction model, in order to determine whether the demand point may be considered covered in terms of communication *quality*. The procedure of testing for unobstruction of the first Fresnel ellipsoid is outlined in pseudo-code form in Algorithm 3.2.

In Step 1 of the algorithm, the difference in elevation $\mathrm{d}z$ between the endpoints of the line segment under consideration, taking into account the antennae heights of the transmitter h_b and the receiver h_m, is determined. The variable τ calculated in Step 2 represents the angle between the line of visibility and the horizontal plane. In Step 3, the length of the line of visibility D between the transmitter and the receiver is then computed. The for-loop spanning Steps 4–10 is used to test whether the nLOS condition holds for the given value of α at each of the points along the line determined by Bresenham's line drawing algorithm. For each point, the parameters d_1, d_2 and r in Figure 3.2 are computed according to (3.1). The value r is adjusted using trigonometry in order to find the vertical component of the axial radius displacement r', as illustrated in Figure 3.4. The variable ϕ computed in Step 8 is used to determine the elevation of the line of visibility at the point under consideration. The if-statement spanning Steps 9–10 tests whether the visibility condition holds at the point under consideration. The if-else statement spanning Steps 11–13 ensures, before the algorithm returns "true" for $LOS_{i,j,\alpha}$, that $LOS_{i,j,\alpha}$ has been incremented at each point along the line and as a result does, in fact, exist.

Algorithm 3.2: Determining whether LOS for a specified α exists.

Input : A grid of elevation data, a set of points along the line joining two points i and j as determined by Bresenham's line drawing algorithm, distances x_{dist} and y_{dist} between two consecutive points on the x and y axes respectively, antennae heights h_b and h_m, and the required level of first Fresnel ellipsoid unobstruction α.

Output: A binary variable $LOS_{i,j,\alpha}$ indicating whether the first Fresnel ellipsoid between candidate site i and demand point j is sufficiently unobstructed.

$\mathrm{d}z \leftarrow grid(x_1, y_1) + h_b - grid(x_2, y_2) + h_m$;
$\tau \leftarrow \tan^{-1} \frac{\mathrm{d}z}{\sqrt{(x_{dist}\mathrm{d}x)^2+(y_{dist}\mathrm{d}y)^2}}$;
$D \leftarrow \frac{\sqrt{(x_{dist}\mathrm{d}x)^2+(y_{dist}\mathrm{d}y)^2}}{\cos\tau}$;
for $k = 2$ *to (number of points* -1*)* **do**
    $d_1 \leftarrow \frac{\sqrt{((x_k-x_1)\times x_{dist})^2+((y_k-y_1)\times y_{dist})^2}}{\cos\tau}$;
    $d_2 \leftarrow D - d_1$;
    $r' \leftarrow \frac{\sqrt{\lambda d_1 d_2/D}}{\cos\tau}$;
    $\phi \leftarrow \frac{d_1}{D}$;
    if $(grid(x_1, y_1) + h_b - \mathrm{d}z \times \phi - \alpha r') \geq grid(x_k, y_k)$ **then**
        $LOS_{i,j,\alpha} \leftarrow nLOS + 1$
if $LOS_{i,j,\alpha}/(number\ of\ points - 2) = 1$ **then**
    $LOS_{i,j,\alpha} \leftarrow 1$ **else**
        $LOS_{i,j,\alpha} \leftarrow 0$
Return $LOS_{i,j,\alpha}$;

Example 3.3 (**Obstruction of the first Fresnel ellipsoid**). *Suppose a transmitter with antenna height $h_b = 10$ metres is located at $(15, 2)$ and a receiver with antenna height $h_m = 2$ metres is located at $(10, 19)$. Since the coordinates $(15, 2)$ and $(10, 19)$ lie on the line computed in Example 3.1, the points are already known at which the comparisons (required to determine whether the first Fresnel ellipsoid is sufficiently unobstructed) should be performed. For each of the points along this line, the axial radius r of the first Fresnel ellipsoid was calculated and subtracted from the height of the line of sight between the transmitter and receiver. These values may be found in Table 3.2. The first Fresnel ellipsoid with the transmitter and receiver at its foci is sufficiently unobstructed for the values $\alpha = 0$ or $\alpha = 0.5$, for example. When $\alpha = 1$, however, the first Fresnel ellipsoid may no longer be considered unobstructed. This situation is illustrated in Figure 3.5. As a result, it may be concluded that the first Fresnel ellipsoid is sufficiently unobstructed if, in order to provide high-quality coverage, a value of $\alpha = 0.5$ is required. If, however, the coverage quality requirement is increased to $\alpha = 1$, the first Fresnel ellipsoid may no longer be considered unobstructed.* □

Now that the area of demand points covered by a transmitter placed at a given location can be determined, a so-called view shed plot may be associated with the transmitter placement. A *view shed* is a graphical representation distinguishing between the areas for which the first Fresnel ellipsoids with one focus at a transmitter are sufficiently unobstructed (*i.e.* the areas which can be covered by the transmitter), and the areas that the transmitter is unable to cover.

The quality of a transmitter placement may be evaluated according to the percentage of the demand it is able to cover, as well as the average signal level provided to the demand region. Let $\mathcal{I} = \{1, \ldots, n\}$ denote the set of transmitter candidate locations and receiver (demand) locations. A *coverage importance* value c_j is associated with each demand node $j \in \mathcal{I}$. The

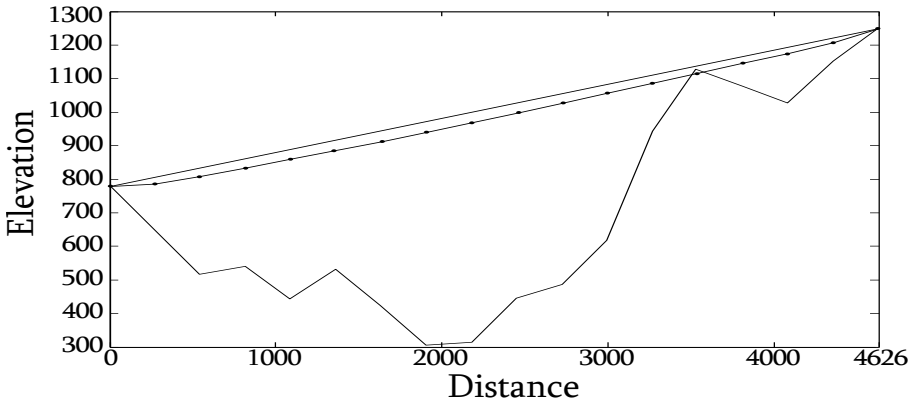

FIGURE 3.5: *The line of visibility and first Fresnel ellipsoid lower boundary for the data in Example 3.3.*

percentage of the demand covered by a transmitter location is simply calculated as the sum of the coverage importance values c_j of the demand nodes covered by a transmitter, divided by the sum of the coverage importance weightings c_j for all $j \in \mathcal{I}$.

Example 3.4 (**The view shed and coverage of a single transmitter placement**). *Suppose a transmitter is to be placed at the surface point* $(10, 7)$ *in Figure 3.3 and that the view shed representing the areas that the transmitter will be able to cover must be plotted. Suppose, furthermore, that the percentage of the binary demand data, shown in Figure 3.6 (a), which the transmitter is able to meet, should be determined. As input, the values* $f = 1\,800$ *MHz,* $h_b = 50$ *metres,* $h_m = 2$ *metres and* $\alpha = 1$ *are used. The points on the terrain surface that the transmitter is able to cover can be determined by repeated use of Algorithm 3.2. The view shed plot for a transmitter located at the point* $(10, 7)$ *is shown in Figure 3.6 (b). The corresponding percentage of the demand covered may be determined as* 58.41%. □

	Grid Point	$(10,19)$	$(10,18)$	$(11,17)$	$(11,16)$	$(11,15)$	$(11,14)$	$(12,13)$	$(12,12)$	$(12,11)$
	Elevation	779	649	516	541	443	532	423	305	314
$\alpha = 0$	Fresnel radius	0	0	0	0	0	0	0	0	0
	Lowest Fresnel	779.0	791.2	853.6	867.7	881.9	896.1	958.5	972.6	986.8
	LOS-Status	✓	✓	✓	✓	✓	✓	✓	✓	✓
$\alpha = 0.5$	Fresnel radius	0	3.1	4.6	5.3	5.9	6.3	6.7	6.8	6.9
	Lowest Fresnel	779.0	788.1	848.9	862.4	876.0	890.0	951.8	965.8	979.9
	LOS-Status	✓	✓	✓	✓	✓	✓	✓	✓	✓
$\alpha = 1$	Fresnel radius	0	6.4	9.3	10.7	11.7	12.6	13.3	13.7	13.9
	Lowest Fresnel	779.0	785.0	844.3	857.1	870.2	883.6	945.1	959.0	973.0
	LOS-Status	✓	✓	✓	✓	✓	✓	✓	✓	✓
	Grid Point	$(13,10)$	$(13,9)$	$(13,8)$	$(14,7)$	$(14,6)$	$(14,15)$	$(14,4)$	$(15,3)$	$(15,2)$
	Elevation	446	487	618	943	1148	1078	1027	1153	1249
$\alpha = 0$	Fresnel radius	0	0	0	0	0	0	0	0	0
	Lowest Fresnel	1049.2	1063.4	1077.5	1134.0	1154.1	1168.3	1182.4	1244.8	1249.0
	LOS-Status	✓	✓	✓	✓	✓	✓	✓	✓	✓
$\alpha = 0.5$	Fresnel radius	6.9	6.8	6.7	6.3	5.9	5.3	4.7	3.2	0
	Lowest Fresnel	1042.3	1056.5	1070.9	1133.6	1148.8	1162.9	1177.8	1241.6	1249.0
	LOS-Status	✓	✓	✓	✓	✓	✓	✓	✓	✓
$\alpha = 1$	Fresnel radius	13.9	13.7	13.3	12.5	11.7	10.7	9.2	6.2	0
	Lowest Fresnel	1035.3	1050.0	1064.2	1127.4	1142.4	1157.6	1171.3	1239.0	1249.0
	LOS-Status	✓	✓	✓	✓	×	✓	✓	✓	✓

TABLE 3.2: *The elevations above sea level, the axial radii of the first Fresnel ellipsoid and the elevations of the lower boundary of the first Fresnel ellipsoid for* $\alpha = 0$, $\alpha = 0.5$ *and* $\alpha = 1$ *along the Bresenham line from a transmitter placed at* $(15, 2)$ *to a receiver located at* $(10, 19)$.

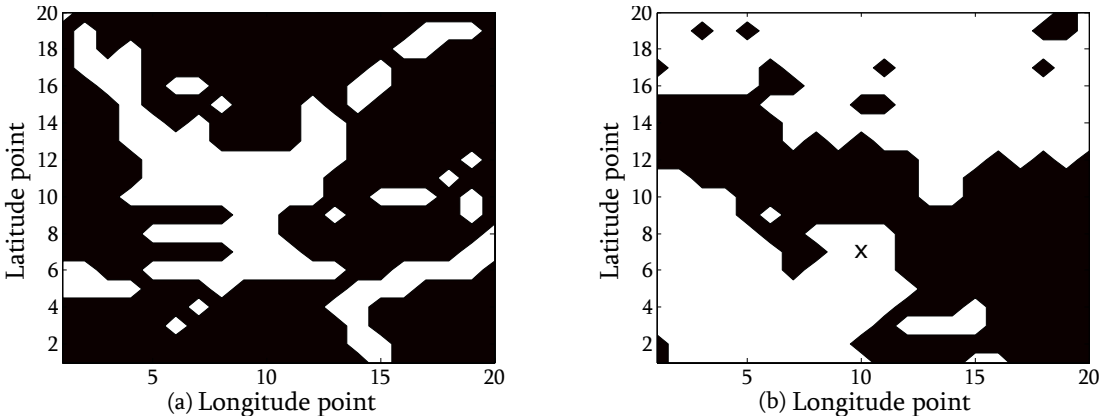

FIGURE 3.6: *Demand data for use in Example 3.4 in (a), and a view shed plot for a transmitter placed at candidate site* $(10, 7)$ *in (b). The white areas indicate the points which require coverage in (a) and the points that are covered in (b), whereas the black areas indicate that no coverage is required at those points in (a) and that no coverage is received at those points in (b).*

3.2 Signal Propagation Loss

Amaldi *et al.* [3] claim that the propagation prediction model used to estimate the signal level at each of the demand points in the coverage area of a cellular telephone communication network is a crucial element of the network planning process. An empirical approach to signal propagation prediction is adopted in this project since the focus here is on macrocells, in which the type of land cover is only roughly known. More specifically, the propagation loss model selected for use in this project is the COST 231-Hata Model (2.40)–(2.41), described in §2.3.

The frequency f and antennae height parameters h_b and h_m are specified by the user and are thus input parameters to the model. The distance D between the transmitter at candidate site i and receiver at demand point j is the same as that used for the calculation of the axial radius of the first Fresnel ellipsoid in §3.1, as illustrated in Figure 3.2. Since all the parameters are known, the resulting predicted radio signal propagation loss can be determined according to (2.40)–(2.41). The predicted propagation loss $L_{b(i,j)}$ at a receiver located at demand point j may therefore be subtracted from the transmitted signal strength at a transmitter located at candidate site i in order to measure the actual signal level at the receiver. The transmitted power P_t' may be converted to units of dBm, a decibel representation of Milliwatts, according to the transformation

$$P_t = 10 \log(1\,000 P_t'), \tag{3.2}$$

as described in [46]. A minimal threshold signal level S_{min} required to guarantee a sufficient quality of radio communication also has to be specified by the user and is usually also given in dBm.

Since the signal level at each of the locations of the grid may now be calculated, the average signal level provided to the demand points may simply be calculated as the sum of the signal levels at each of the covered demand points (*i.e.* those demand points with an importance rating $c_j > 0$ which receive an adequate signal level), divided by the number of covered demand points.

Example 3.5 (**Signal propagation loss over a specified area**). *Suppose the radio signal propagation loss has to be determined for the area considered in Examples 3.2, 3.3 and 3.4 when a radio transmitter is located at grid point* $(10, 7)$. *If* $f = 1\,800$ *MHz,* $h_b = 50$ *metres,* $h_m = 2$ *metres,* $P_t' = 20$ *W and* $S_{min} = -95$ *dBm, then the transmitted power can be calculated as*

$$P_t = 10\log(1\,000P_t) = 10\log(20\,000) = 43.01 \text{ dBm}.$$

When it is assumed that the first Fresnel ellipsoid is sufficiently unobstructed, the signal level provided to each point in the area may be calculated according to (2.40). The resulting signal level is shown graphically in Figure 3.7. If, however, the signal level is only calculated for those demand points in the grid for which the first Fresnel ellipsoid is sufficiently unobstructed, as determined using Algorithm 3.2 with a value of $\alpha = 1$, *the signal level in Figure 3.8 results. In this figure, any grid point for which the first Fresnel ellipsoid is not sufficiently unobstructed has been assigned a signal level of* -95 *dBm. The normalised average signal level provided to those locations with an importance value* $c_j > 0$ *is then calculated as* 55.46%. □

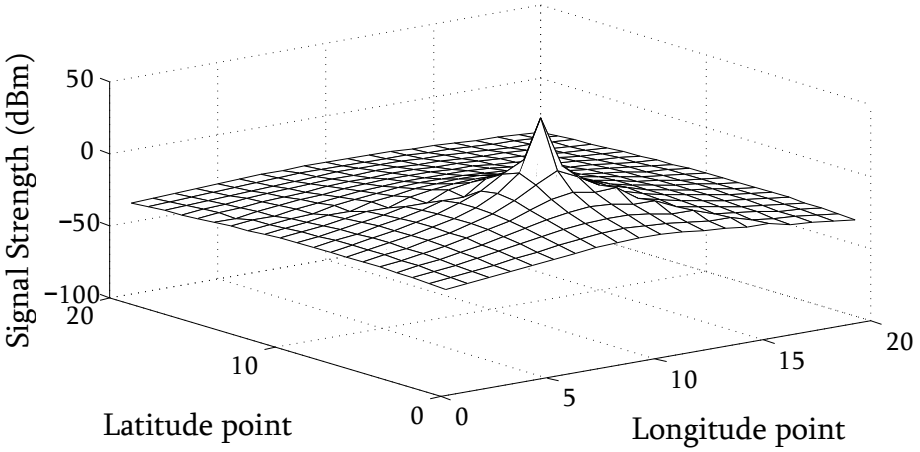

FIGURE 3.7: *Signal strength from a transmitter placed at* $(10, 7)$, *assuming that the first Fresnel ellipsoid is sufficiently unobstructed for all points in the grid.*

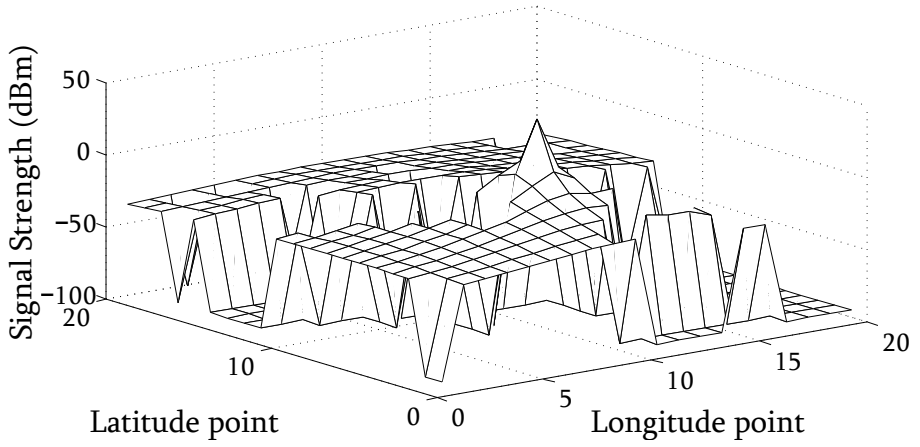

FIGURE 3.8: *Signal strength from a transmitter placed at* $(10, 7)$, *taking obstructions of the first Fresnel ellipsoid into account.*

3.3 Measuring the Placement Quality of a Transmitter Network

In the previous sections of this chapter it was explained how the quality of the placement location of a *single* transmitter may be measured in terms of two performance metrics: the portion of demand met by the transmitter (§3.1) and the average signal level emitted by the transmitter over the area in which it satisfies demand (§3.2). The purpose of this section is to elucidate how these performance metrics may be extended to the situation where a network of *more than one* transmitter is placed within the region of demand.

Let $\mathcal{I} = \{1, \ldots, n\}$ again denote the set of transmitter candidate locations and potential receiver locations. Then an $n \times n$ binary matrix measuring the degree to which coverage is achievable from each of the transmitter candidate locations may be populated by repeated use of Algorithm 3.2. This matrix is called the *potential coverage matrix* and is denoted by $\boldsymbol{A}^{(\alpha)}$, where α is the coverage requirement parameter introduced in §3.1. The rows of the potential coverage matrix represent the transmitter location candidate sites (*i.e.* potential signal supply points) while its columns represent the signal receiver sites (*i.e.* signal demand points) in $\mathcal{I}$. The entry in row i and column j of the potential coverage matrix is given by

$$A_{ij}^{(\alpha)} = \begin{cases} 1 & \text{if } LOS_{i,j,\alpha} = 1 \text{ (according to Algorithm 3.2),} \\ 0 & \text{otherwise.} \end{cases} \tag{3.3}$$

Since it is acknowledged that not all demand points are equally important in terms of demand satisfaction, a further $n \times n$, real-valued matrix called the *quality of demand satisfaction matrix* is introduced. The rows and columns of this matrix again represent the transmitter location candidate sites and the demand points, respectively. The entry in row i and column j of the quality of demand satisfaction matrix is given by

$$C_{ij}^{(\alpha)} = \begin{cases} c_j & \text{if } A_{ij}^{(\alpha)} = 1, \\ 0 & \text{otherwise,} \end{cases} \tag{3.4}$$

where c_j denotes the importance value associated with satisfying demand at demand point $j \in \mathcal{I}$, as introduced in §3.1.

Example 3.6 (**Potential quality of demand coverage**). *Consider again the grid of $n = 400$ potential transmitter candidate sites and demand locations of Examples 3.2–3.5. If these locations are numbered as illustrated in Figure 3.9, then $\mathcal{I} = \{1, \ldots, 400\}$. The potential coverage matrix and quality of demand satisfaction matrix are too large to present in numerical form. The potential coverage matrix is, however, presented graphically in Figure 3.10. Note that row 130 of the potential coverage matrix corresponds to the view shed information contained in Figure 3.6.*

□

Suppose the locations of a collection of transmitters in a radio communication network are captured by a binary decision vector $\boldsymbol{x} = [x_1, \ldots, x_n]^T$, where

$$x_i = \begin{cases} 1 & \text{if a transmitter is located at candidate site } i \in \mathcal{I}, \\ 0 & \text{otherwise.} \end{cases} \tag{3.5}$$

Then the degree to which transmission demand is actually satisfied by the transmitter placement decision embodied in the vector $\boldsymbol{x}$ above, weighted by the importance values associated with demand satisfaction at the various receiver locations, is given by

$$\Gamma_c^{(\alpha)}(\boldsymbol{x}) = \frac{\sum_{j=1}^{n} \max_i \{C_{ij}^{(\alpha)} x_i\}}{\sum_{j=1}^{n} c_j}. \tag{3.6}$$

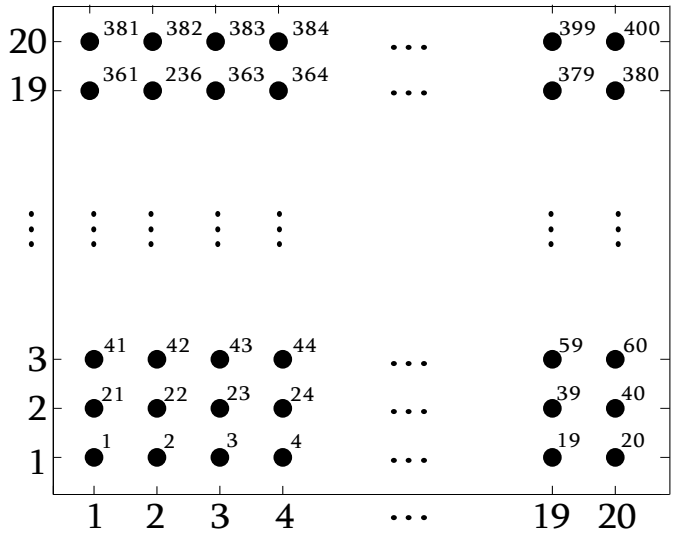

FIGURE 3.9: *Labelling of the transmitter candidate sites and demand points in the* 20×20 *grid of interest considered in Examples 3.2–3.6.*

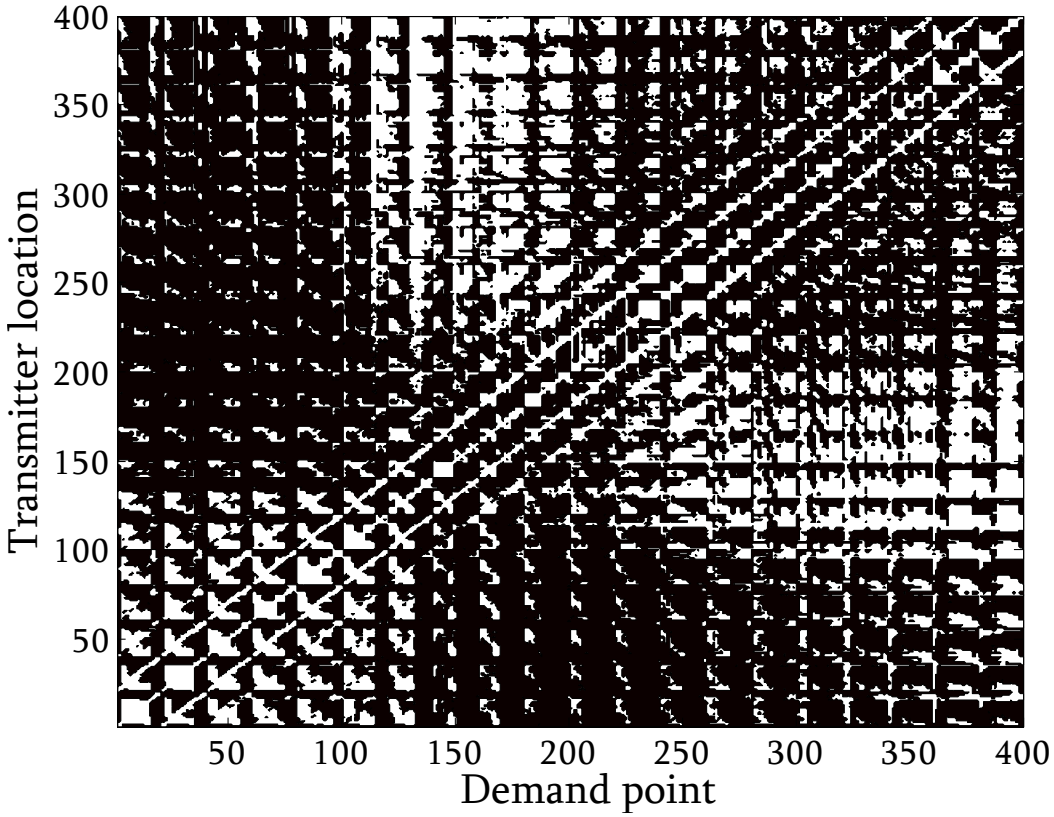

FIGURE 3.10: *The potential coverage matrix generated for Example 3.6, where a white cell denotes the potential coverage by a transmitter, and a black cell denotes that the transmitter is not able to cover the demand point.*

Note that double-counting of demand satisfaction importance values is prevented by the maximum operator in (3.6). This operator is included in (3.6) to ensure that if demand point $j \in \mathcal{I}$ is covered by k transmitters, then the importance value c_j of §3.1 will not be accounted for k times in $\Gamma_c^{(\alpha)}(\boldsymbol{x})$. This prevention of double-counting is desirable, because it is envisaged that

if the performance metric $\Gamma_c^{(\alpha)}(\boldsymbol{x})$ is used as a maximisation objective when seeking a good placement decision vector $\boldsymbol{x}$, a large value of $\Gamma_c^{(\alpha)}(\boldsymbol{x})$ should be achieved by covering as many different demand points as possible instead of focusing on coverage of a cluster of points with high coverage importance values, which may be covered multiple times so as to achieve a large value for the performance metric $\Gamma_c^{(\alpha)}(\boldsymbol{x})$.

Example 3.7 (**The quality of demand coverage associated with a placement decision**). *Suppose that a network of two transmitters located at* $(9, 7)$ *and* $(12, 12)$*, as well as a network consisting of three transmitters located at* $(13, 6)$*,* $(8, 9)$ *and* $(17, 19)$ *have to be evaluated in terms of their total coverage ability* $\Gamma_c^{(\alpha)}(\boldsymbol{x})$*. Using the potential coverage matrix and the quality of demand coverage matrix as calculated in Example 3.6, together with (3.6), a performance metric value* $\Gamma_c^{(\alpha)}(\boldsymbol{x}) = 82.30\%$ *is achieved for the network of two transmitters located at* $(9, 6)$ *and* $(12, 11)$*. For the network of three transmitters located at* $(13, 6)$*,* $(8, 9)$ *and* $(17, 19)$*, this performance metric is calculated to be* 81.42%*.* □

An $n \times n$ real-valued matrix measuring the degree to which signal strength is potentially achievable at demand points may also be populated by repeated application of the calculations described in §3.2. This matrix is called the *potential signal strength matrix* and is denoted by $\boldsymbol{S}^{(P_t,\alpha)}$. Its rows and columns again represent respectively the transmitter location candidate sites and receiver demand points. The entry in row i and column j of this matrix is given by

$$S_{ij}^{(P_t,\alpha)} = \begin{cases} P_t - L_{b(i,j)} & \text{if } A_{ij}^{(\alpha)} = 1 \text{ and } P_t - L_{b(i,j)} \geq S_{min}, \\ -\infty & \text{otherwise.} \end{cases} \tag{3.7}$$

In order to incorporate a minimum requirement in terms of acceptable signal strength as a guarantee for effective radio communication, a further $n \times n$ real-valued matrix, called the *quality of signal strength matrix* is introduced. This matrix is denoted by $\boldsymbol{Q}^{(P_t,\alpha,S_{min})}$, and its rows and columns again represent transmitter candidate location sites and receiver demand points, respectively. The entry in row i and column j of this matrix is given by

$$Q_{ij}^{(P_t,\alpha,S_{min})} = \begin{cases} S_{ij}^{(P_t,\alpha)} + |S_{min}| & \text{if } S_{ij}^{(P_t,\alpha)} \geq S_{min}, \\ 0 & \text{otherwise.} \end{cases} \tag{3.8}$$

Note that the minimum requirement value S_{min} is added to the signal level in (3.8) so as to ensure that the matrix does not contain any negative entries. The non-negative nature of the matrix is desirable when the performance measure of the average signal level in a covered demand region is computed, as it results in a simplification of the calculation of an appropriate average signal level performance metric. The addition of S_{min} will not negatively influence the value of the performance metric, since the performance metric is merely normalised in this way.

Example 3.8 (**Potential quality of signal transmission**). *Consider again the grid of* $n = 400$ *potential transmitter candidate sites and demand locations of Examples 3.2–3.5. If these locations are numbered as illustrated in Figure 3.9, then* $\mathcal{I} = \{1, \ldots, 400\}$*. The potential signal strength matrix and quality of signal strength matrix are too large to present in numerical form, but the former is presented graphically in Figure 3.11. Note that row 130 of the potential coverage matrix again corresponds to the signal strength values plotted three-dimensionally in Figure 3.8.*

□

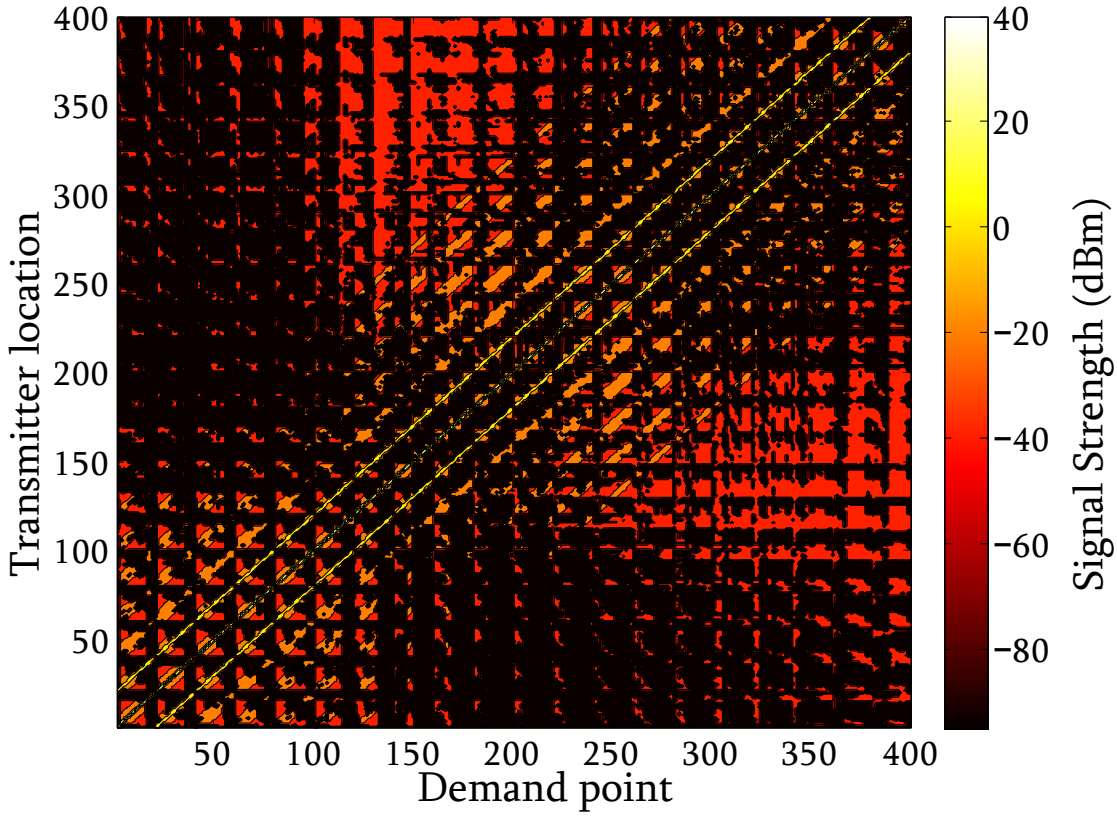

FIGURE 3.11: *The potential signal strength matrix generated in Example 3.8.*

The degree to which transmission signal quality is actually achieved by the transmitter placement decision embodied in the vector $\boldsymbol{x}$ in (3.5) is given by

$$\Gamma_{\ell}^{(P_t,\alpha,S_{min})}(\boldsymbol{x}) = \frac{\sum_{j=1}^{n} \max_i\{Q_{ij}^{(P_t,\alpha,S_{min})} x_i\} c_j}{\sum_{j=1}^{n} \max_i\{C_{ij}^{(\alpha)} x_i\} \times (P_t - S_{min})}. \tag{3.9}$$

The reason for taking the maximum over i in (3.9) is that the strongest signal level achieved from any transmitter i at demand point j should be incorporated into the performance metric $\Gamma_{\ell}^{(P_t,\alpha,S_{min})}(\boldsymbol{x})$. Note that, as in the performance metric $\Gamma_{c}^{(\alpha)}(\boldsymbol{x})$ in (3.6), no double-counting occurs in the summation of (3.9).

Example 3.9 (**Quality of signal strength associated with a placement decision**). *Suppose that the same networks as in Example 3.7, consisting of two transmitters located at* $(9, 7)$ *and* $(12, 12)$*, and of three transmitters located at* $(13, 6)$*,* $(8, 9)$ *and* $(17, 19)$*, have to be evaluated in terms of the average signal level they provide to the covered demand points. Using the potential signal strength matrix and the quality of signal strength matrix as calculated in Example 3.8, together with (3.9), a performance metric value* $\Gamma_{\ell}^{(P_t,\alpha,S_{min})}(\boldsymbol{x}) = 58.63\%$ *is achieved for the network of two transmitters located at* $(9, 6)$ *and* $(12, 11)$*. For the network of three transmitters located at* $(13, 6)$*,* $(8, 9)$ *and* $(17, 19)$*, this performance metric value is calculated to be* 55.86%*.*

□

Note that, for both performance metrics $\Gamma_{c}^{(\alpha)}(\boldsymbol{x})$ and $\Gamma_{\ell}^{(P_t,\alpha,S_{min})}(\boldsymbol{x})$ calculated in Examples 3.7 and 3.9, the network of two radio transmitters achieved higher values. This serves to illustrate how important the consideration of good transmitter placement locations is.

3.4 Chapter Summary

This chapter was devoted to the establishment of a framework for evaluating the effectiveness of a given set of placement locations for a network of radio transmitters. The initial focus in §3.1 was to determine the area over which, for a given single transmitter location, line of sight between the transmitter and potential receiver demand points would exist. As explained, this LOS depends on a sufficiently unobstructed first Fresnel ellipsoid which has its foci at the transmitter and receiver. Then the focus shifted in §3.2 to the signal propagation prediction model used to determine whether a potential receiver location would receive an adequate signal level should the transmitter, in fact, be located at the given position. Finally, the chapter closed in §3.3 with a discussion on how the quality of a network of multiple transmitter placements may be measured. This quality is quantified by two unitless performance measures: the percentage of the demand that can be met by the set of transmitter placement locations and the normalised average signal level provided by the transmitters in the demand region.

CHAPTER 4

Mathematical Model

Contents

This chapter is devoted to the formulation of a bi-objective facility location model suitable for use as a basis for decision support in respect of the location of a network of radio transmitters with a view to identify high-quality trade-offs between maximising total coverage area and maximising the average signal level in the covered demand region. The chapter opens in §4.1 with the definition of a number of key concepts in multiobjective optimisation that are used throughout the chapter. The focus in §4.2 shifts to the formulation of the mathematical facility location model proposed in this project. In §4.3, the method of simulated annealing is then proposed as a suitable metaheuristic for solving the model of §4.2. The chapter finally closes with a brief summary in §4.4.

4.1 Basic Concepts in Multiobjective Optimisation

According to Winston [48], the scientific approach to decision making typically involves the use of mathematical models. These models traditionally consist of the following components: objective function(s), decision variables, and constraints. The objectives of an optimisation problem are chosen in line with the goals of the decision maker and represent the specific aims the decision maker wants to achieve [32]. The decision variables are those variables forming part of the optimisation problem which are under control of the decision maker. These variables influence the performance of the model in terms of the objective function(s) which have been

adopted. In most cases, however, the possible values (or combinations of values) of the decision variables are restricted by constraints present in the optimisation problem [48].

A problem in which a single objective function is to be optimised over some decision space is called a *single-objective optimisation problem* (SOP), whereas a problem in which multiple objectives are to be optimised simultaneously is called a *multiobjective optimisation problem* (MOP) [8]. The general form of an MOP with q objective functions $f_1(\boldsymbol{x}), \ldots, f_q(\boldsymbol{x})$ may then be written as

$$\text{maximise } \boldsymbol{f}(\boldsymbol{x}) = [f_1(\boldsymbol{x}), \ldots, f_q(\boldsymbol{x})], \tag{4.1}$$

subject to the constraints

$$g_i(\boldsymbol{x}) \geq 0, \qquad i = 1, \ldots, r, \tag{4.2}$$
$$h_j(\boldsymbol{x}) = 0, \qquad j = 1, \ldots, s, \tag{4.3}$$
$$\boldsymbol{x} \in \mathbb{R}^n, \tag{4.4}$$

where $\boldsymbol{x} = [x_1, \ldots, x_n]$ denotes the vector of decision variables [32]. The *inequality constraint functions* are represented by $g_1(\boldsymbol{x}), \ldots, g_r(\boldsymbol{x})$ in (4.2), while $h_1(\boldsymbol{x}), \ldots, h_s(\boldsymbol{x})$ in (4.3) are *equality constraint functions*. A real-valued decision vector $\boldsymbol{x}$ is called *feasible* if it satisfies all the constraints in (4.2) and (4.3). The set of all feasible decision vectors of (4.2)–(4.3) form the so-called *decision space* of the problem, denoted here by $\mathcal{X}$.

For an SOP, a unique solution $\boldsymbol{x}^*$ which maximises the objective function may often be found. This is, however, typically not the case when solving an MOP. In this case, the solution process will generally yield a set of trade-off solutions, which leads naturally to the notion of Pareto optimality [8]. Two important concepts relating to Pareto optimality are the notions of a dominating (feasible) solution and of a nondominated (feasible) solution. A feasible solution $\boldsymbol{x} \in \mathcal{X}$ *dominates* another feasible solution $\boldsymbol{x}' \in \mathcal{X}$ if $f_i(\boldsymbol{x}) \geq f_i(\boldsymbol{x}')$ for all $i = 1, \ldots, q$ and $f_j(\boldsymbol{x}) > f_j(\boldsymbol{x}')$ for at least one $j \in \{1, \ldots, q\}$. A feasible decision vector $\boldsymbol{x}$ in some subset $\mathcal{S} \subseteq \mathcal{X}$ is *nondominated* in $\mathcal{S}$ if there exists no feasible decision vector $\boldsymbol{x}' \in \mathcal{S}$ that dominates $\boldsymbol{x}$. Winston [48] defines a feasible solution $\boldsymbol{x} \in \mathcal{X}$ to be *Pareto optimal* if it is nondominated in $\mathcal{X}$. The set containing all the Pareto optimal feasible solutions of (4.1)–(4.4) is the so-called *Pareto set* of the problem and is denoted by $\mathcal{P}_S$. The *Pareto front*, denoted by $\mathcal{P}_F$ is the set of all the objective function vectors corresponding to the Pareto set, *i.e.* $\mathcal{P}_F = \{\boldsymbol{f}(\boldsymbol{x}) | \boldsymbol{x} \in \mathcal{P}_S\}$. These notions are illustrated graphically in Figure 4.1.

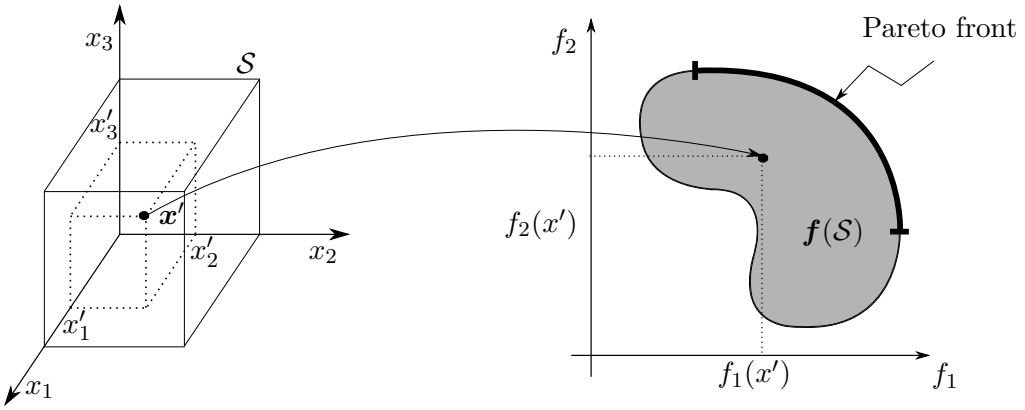

(a) Decision Space (b) Objective function space

FIGURE 4.1: *The decision space and corresponding objective space of an MOP.*

4.2 Bi-objective Radio Transmitter Location Model

Suppose that k transmission towers are to be located at some subset of n transmitter candidate sites. A coverage importance value c_j is associated with candidate site $j \in \{1, \ldots, n\}$, as stated in §3.1. The aim of the model is to achieve an acceptable trade-off between maximising the normalised accumulated coverage importance value $\Gamma_c^{(\alpha)}(\boldsymbol{x})$ of candidate sites actually covered by the k transmission towers, and maximising the normalised average signal level $\Gamma_\ell^{(P_t,\alpha,S_{min})}(\boldsymbol{x})$ of those candidate sites actually covered by the k transmission towers. The functions $\Gamma_c^{(\alpha)}(\boldsymbol{x})$ and $\Gamma_\ell^{(P_t,\alpha,S_{min})}(\boldsymbol{x})$ were defined in detail in §3.3.

The decision variables

$$x_i = \begin{cases} 1 & \text{if a radio transmission tower is placed at site } i, \\ 0 & \text{otherwise} \end{cases}$$

were also introduced in §3.3 for all $i = 1, \ldots, n$ and are employed in the model. The model objectives are therefore to

$$\text{maximise } f_1(\boldsymbol{x}) = \Gamma_c^{(\alpha)}(\boldsymbol{x}) \tag{4.5}$$

and to

$$\text{maximise } f_2(\boldsymbol{x}) = \Gamma_\ell^{(P_t,\alpha,S_{min})}(\boldsymbol{x}) \tag{4.6}$$

subject to the constraints

$$\sum_{i=1}^{n} x_i \leq k, \tag{4.7}$$

$$x_i \in \{0, 1\}, \qquad i = 1, \ldots, n. \tag{4.8}$$

In the above formulation, the objectives in (4.5) and (4.6) are conflicting in the sense that increasing $\Gamma_c^{(\alpha)}(\boldsymbol{x})$ (which is typically achieved by spacing the transmission towers far apart) usually decreases $\Gamma_\ell^{(P_t,\alpha,S_{min})}(\boldsymbol{x})$ which is, in turn, maximised by placing transmission towers not too far apart. Constraint (4.7) restricts the number of transmission towers placed to at most k, while constraint set (4.8) enforces the binary nature of the decision variable vector $\boldsymbol{x} = [x_1, \ldots, x_n]$. The model is therefore a special case of (4.1)–(4.4), where $r = 1$, $s = 0$ and $q = 2$. Note that no signal requirement constraint is included in the model, because of the minimum acceptable signal quality S_{min} which is already incorporated in the objective function $\Gamma_\ell^{(P_t,\alpha,S_{min})}(\boldsymbol{x})$.

Example 4.1 (**Determining the true Pareto fronts for a model instance**). *Suppose the Pareto fronts have to be determined for an instance of the model (4.5)–(4.8), using the same surface elevation data and coverage importance values as in Examples 3.2–3.8 for the placement of $k = 2$ and $k = 3$ transmitters, respectively. The Pareto-optimal solutions may be computed by brute force (i.e. by considering all $\binom{400}{2} = 79\,800$ and all $\binom{400}{3} = 10\,568\,800$ location combinations, respectively). The resulting Pareto-fronts are shown in Figure 4.2. Three solutions on these fronts, denoted by A, B and C, are also illustrated in decision space in the figure. The solution marked A achieves the largest average signal level for both the placements of $k = 2$ or $k = 3$ transmitters, while the solutions marked B and C achieve the largest coverage for the placements of $k = 2$ and $k = 3$ transmitters, respectively. The total times required on an Intel(R) Core(TM) i7-4700MQ 2.40 GHz processor with 4.00 GB RAM running in Matlab R2012b [28] within a Windows 8.1 64-bit operating system were 22.44 seconds and 3 543.35 seconds for the cases of placing $k = 2$ and $k = 3$ transmitters, respectively.* □

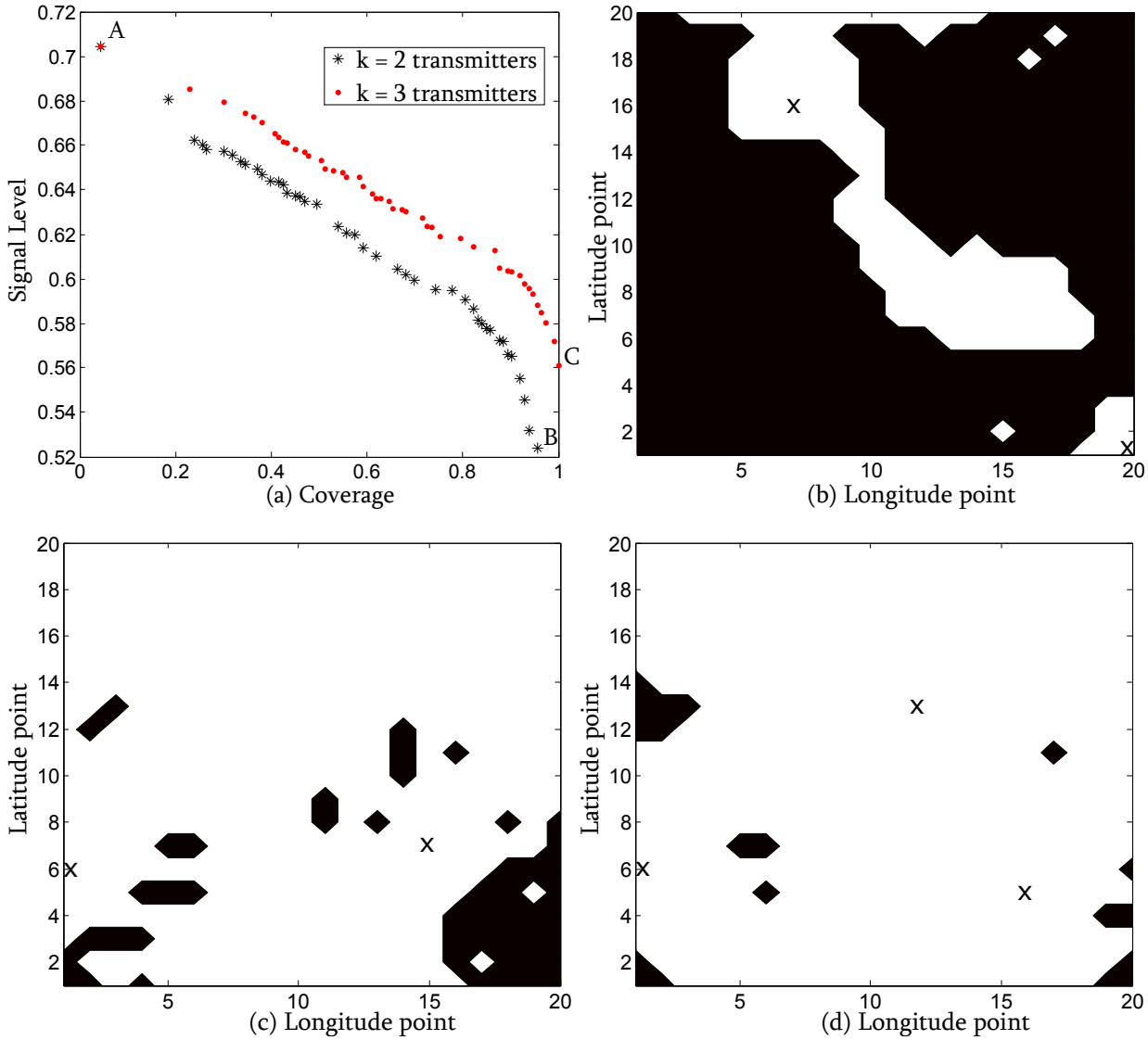

FIGURE 4.2: *Pareto optimal solutions for an instance of the radio transmitter facility location problem (4.5)–(4.8) with $k = 2$ and $k = 3$, respectively, using the same elevation and demand data as in Examples 3.2–3.9. The true Pareto fronts are shown in (a), while the extremal solutions denoted by A, B and C, in (a) are shown in (b), (c) and (d), respectively.*

4.3 The Method of Simulated Annealing

The high computational complexity associated with solving the model (4.5)–(4.8), as well as the non-linearity of the objective functions (4.5) and (4.6), places a brute-force model solution out of reach of current computation technology for realistically sized problem instances, as may be seen in the long brute-force computation times required to solve the small problem instances of Example 4.1. A more intelligent exact solution approach than the brute-force approach of Example 4.1 may involve the pre-computation of the quality of demand satisfaction and the quality of signal strength matrices used in the computation of the objective functions (4.5) and (4.6), followed by a binary programming model solution approach employing, for example, the standard branch-and-bound method [48]. In such an approach the bi-objective model nature may be accommodated by constraining one of the objective functions to at most some level $a \in (0, 1)$

and solving the single-objective problem with the remaining objective function maximised. This process may be repeated for various values of a to trace out the Pareto front in objective space. Anticipated disadvantages of this approach are two-fold: it may take long to solve a single-objective iteration by the branch-and-bound method, and the number of iterations required to trace out a Pareto front of suitable resolution may be large. These disadvantages may be alleviated to some extent by employing an advanced solution technique from the realm of combinatorial optimisation, such as Benders decomposition [10], but even such a sophisticated solution approach is expected to require long computation times for realistically sized problem instances.

An approximate solution methodology is therefore employed in this project instead to solve the model (4.5)–(4.8). Various (meta)heuristics (such as a local search heuristic, the method of tabu search and the method of simulated annealing) were considered for this purpose. Of these, the method of *Simulated Annealing* (SA) was selected due to its flexibility, its small set of parameters requiring user-specification and its ease of implementation. The general working of SA is described in this section, starting with the simplest incarnation of the method in the context of single-objective maximisation and then describing the necessary extensions required for multiobjective maximisation.

4.3.1 Single-objective Simulated Annealing Optimisation

The method of SA was first proposed by Kirkpatrick *et al.* [23] in 1983. Suppapitnarm *et al.* [40] explain how single-objective optimisation by SA is based the statistical mechanics of annealing in solids. The aim in the most basic form of the method of SA is to maximise a specified objective function $f(\boldsymbol{x})$ by the iterative application of a small, random change to a current decision vector $\boldsymbol{x}$ in order to obtain a neighbouring solution $\boldsymbol{x}'$ and then considering the resulting change $\triangle f(\boldsymbol{x}, \boldsymbol{x}') = f(\boldsymbol{x}) - f(\boldsymbol{x}')$ in the objective function value $f(\boldsymbol{x})$ relative to $f(\boldsymbol{x}')$, called the *difference in energy* associated with the solutions $\boldsymbol{x}$ and $\boldsymbol{x}'$. A solution $\boldsymbol{x}'$ resulting in an increase of the objective function value relative to the value $f(\boldsymbol{x})$ is immediately accepted and becomes the new current solution. If, however, the new solution $\boldsymbol{x}'$ results in a decrease in objective function value relative to the value $f(\boldsymbol{x})$, the probability of acceptance of $\boldsymbol{x}'$ as the new current solution is given by the well-known Metropolis rule [23]

$$\exp\left(-\frac{\triangle f(\boldsymbol{x}, \boldsymbol{x}')}{T}\right),$$

where T is a control parameter referred to as the *temperature* of the system. For large values of T, most new solutions are accepted. The intention is to provide a mechanism whereby the search is able to escape from local optima in the objective space. For small values of T, however, only new worsening solutions resulting in small decreases of the objective function value are accepted, if they are accepted at all. As a result, the search is typically initiated using a large value of T, allowing for as much exploration of the decision space as possible during the early stages of the search. The temperature T is then typically reduced in a regulated fashion, at the end of every one of a set of successive collections of iterations, called *epochs*, so that the search converges to a locally maximum solution. The first current solution, used to initialise the search is typically generated randomly.

4.3.2 Multiobjective Simulated Annealing Optimisation

In §4.3.1 above, the working of the method of SA was described for the simple case of SOPs. The purpose of this section is to describe how the method may be extended so as to be applicable to MOPs, as proposed by Smith *et al.* [37, 38].

The notion of archiving

Due to the fact that only a single solution is generated during each iteration of the SA search process, an external set, called an *archive* and denoted here by $\mathcal{A}$, is maintained in which all nondominated solutions found during the search process are recorded in the case of an MOP. All solutions generated during the search process are candidates for archiving, and are tested for dominance with respect to each of the solutions already in the archive. The archiving process for a bi-objective maximisation problem is illustrated graphically in Figure 4.3.

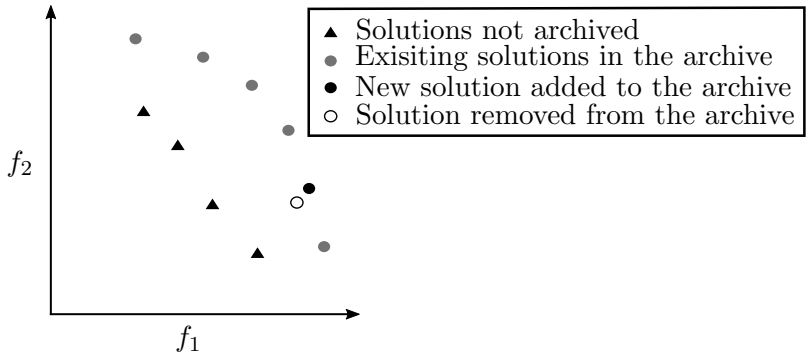

FIGURE 4.3: *The archiving process for a bi-objective maximisation process with objective functions f_1 and f_2.*

In single-objective maximisation problems, the sign of the difference in energy $\triangle f(\boldsymbol{x}', \boldsymbol{x})$ provides information as to whether the neighbouring solution $\boldsymbol{x}'$ performs better or worse than the current solution $\boldsymbol{x}$, or (very rarely) performs equally well. If the true Pareto front $\mathcal{P}_F$ were available *a priori*, it would be possible to define the energy (*i.e.* the performance of a solution in objective space in the context of SA) of a solution $\boldsymbol{x}$ as a measure of the portion of the Pareto front that dominates $\boldsymbol{x}$. Let $\mathcal{P}_F(\boldsymbol{x})$ represent the portion of $\mathcal{P}_F$ that dominates $\boldsymbol{x}$, that is

$$\mathcal{P}_F(\boldsymbol{x}) = \{\boldsymbol{y} \in \mathcal{P} \mid \boldsymbol{y} \prec \boldsymbol{x}\},$$

where $\boldsymbol{y} \prec \boldsymbol{x}$ indicates that $\boldsymbol{y}$ dominates $\boldsymbol{x}$. Then, the energy of $\boldsymbol{x}$ may be defined as

$$E(\boldsymbol{x}) = \mu(\mathcal{P}_F(\boldsymbol{x})),$$

where μ represents a measure defined on $\mathcal{P}_F$. In the case where $\mathcal{P}_F$ is continuous, μ may be taken as a Lebesgue measure (*i.e.* the length, area or volume for two, three or four objectives, respectively). In the case where $\mathcal{P}_F$ is discrete, however, $\mu(\mathcal{P}_F(\boldsymbol{x}))$ may simply be taken to be the cardinality of $\mathcal{P}_F(\boldsymbol{x})$ (*i.e.* the number of solutions forming part of $\mathcal{P}_F$ which dominate $\boldsymbol{x}$). Of course, if $\boldsymbol{x} \in \mathcal{P}_F$, then $E(\boldsymbol{x}) = 0$.

Due to the fact that the true Pareto front is typically unavailable during the course of the optimisation process, Smith *et al.* [38] instead proposed the use of an energy function defined in terms of the current estimate of the Pareto front, that is, the set of mutually nondominated solutions found thus far during the search process (*i.e.* the solutions in the archive $\mathcal{A}$). The energy

difference may then be calculated as the difference in their respective energies, normalised by the size of the archive. According to Smith *et al.* [38], use of such an energy measure encourages both coverage of and convergence to the true Pareto front.

Algorithm outline

To initialise the algorithm, a random feasible solution is placed in the archive $\mathcal{A}$. For each iteration of the algorithm, define $\tilde{\mathcal{A}} = \mathcal{A} \cup \{\boldsymbol{x}\} \cup \{\boldsymbol{x}'\}$, where $\boldsymbol{x}'$ represents a neighbouring solution generated from the current solution $\boldsymbol{x}$, and define $\tilde{\mathcal{A}}_{\boldsymbol{x}} = \{\boldsymbol{y} \in \tilde{\mathcal{A}} \mid \boldsymbol{y} \prec \boldsymbol{x}\}$, where $\mu(\tilde{\mathcal{A}}_{\boldsymbol{x}}) = |\tilde{\mathcal{A}}_{\boldsymbol{x}}| + 1$. An estimated energy difference between the solutions $\boldsymbol{x}$ and $\boldsymbol{x}'$ may then be calculated as

$$\triangle_E(\boldsymbol{x}', \boldsymbol{x}) = \frac{|\tilde{\mathcal{A}}_{\boldsymbol{x}'}| - |\tilde{\mathcal{A}}_{\boldsymbol{x}}|}{|\tilde{\mathcal{A}}|}. \tag{4.9}$$

Division by $|\tilde{\mathcal{A}}|$ in (4.9) ensures that the value $\triangle_E(\boldsymbol{x}', \boldsymbol{x})$ remains below unity, which provides a certain degree of robustness against fluctuations in the number of solutions in $\mathcal{A}$ over the course of the search. Whenever $\tilde{\mathcal{A}}$ is a nondominated set, the energy difference between any two of its elements is zero. The reason for the inclusion of the current solution $\boldsymbol{x}$, as well as the proposed solution $\boldsymbol{x}'$ in $\tilde{\mathcal{A}}$, is that $\triangle_E(\boldsymbol{x}', \boldsymbol{x}) < 0$ if $\boldsymbol{x}' \prec \boldsymbol{x}$. Besides efficiency in the promotion of the storage of nondominated solutions, a further benefit of the energy measure in (4.9) is that it encourages the exploration of sparsely populated regions of the estimated Pareto front in $\mathcal{A}$, regardless of the portion of the true Pareto front that dominates the solutions $\boldsymbol{x}$ and $\boldsymbol{x}'$. This principle is illustrated in Figure 4.4, where it appears as though $\mu(\mathcal{P}_{\boldsymbol{x}'}) > \mu(\mathcal{P}_{\boldsymbol{x}})$, but it can be seen that, in fact, $|\tilde{\mathcal{A}}_{\boldsymbol{x}'}| = 1 < 3 = |\tilde{\mathcal{A}}_{\boldsymbol{x}}|$. This ensures that the search moves to a more unexplored region of the nondominated front.

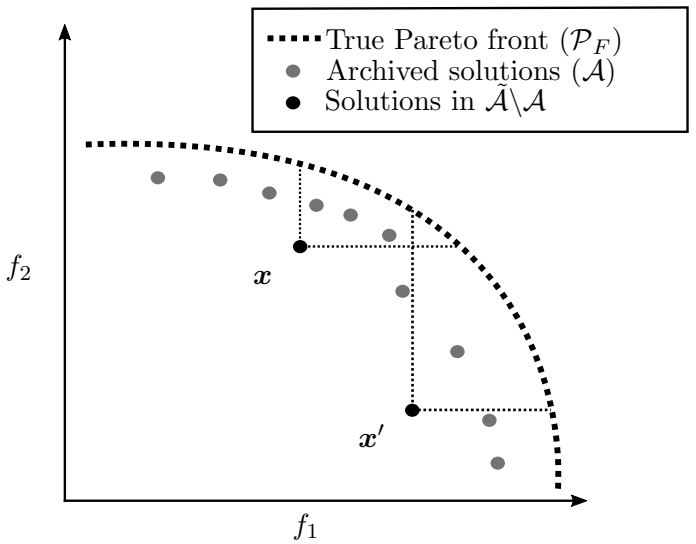

FIGURE 4.4: *The energy measure for a current solution and its neighbouring solution in a bi-objective maximisation problem with objective functions f_1 and f_2. Here $|\tilde{\mathcal{A}}_{\boldsymbol{x}'}| = 1 < 3 = |\tilde{\mathcal{A}}_{\boldsymbol{x}}|$.*

The function used to determine the probability of acceptance of a neighbouring solution $\boldsymbol{x}'$ is then given by

$$P(\boldsymbol{x}') = \min\left\{1, \exp\left(-\frac{\triangle_E(\boldsymbol{x}', \boldsymbol{x})}{T}\right)\right\}, \tag{4.10}$$

where T represents the current temperature of the search. Naturally, a neighbouring solution dominated by fewer elements of the current estimate of the Pareto front in $\mathcal{A}$ has a lower energy

and is consequently automatically accepted to be the new current solution, since, by definition, it represents an improving move in the search. If, however, there is a large positive energy difference between the current solution and the neighbouring solution, and the temperature is low, the probability of acceptance of the move is small. It is emphasized that this probability of acceptance does not depend on an *a priori* weighting of the objectives and will, as a result, remain unaffected by rescalings of the objectives. It follows that, if the move is accepted, the neighbouring solution becomes the current solution from which a new neighbouring solution will be generated. A pseudo-code description of the basic steps of the multiobjective SA algorithm of Smith *et al.* [38] is given in Algorithm 4.1.

Algorithm 4.1: Dominance-based multiobjective simulated annealing

Input : A multiobjective maximisation problem of the form (4.1)–(4.4), the maximum allowable number of iterations per epoch I_{max}, the minimum number of accepted moves A_{min} per epoch, the cooling function used to determine the cooling schedule, and a restriction on the maximum number C_{max} of epochs which may pass without the acceptance of any new solutions.

Output: A non-dominated set of solutions $\mathcal{P}_S$ in the decision space and the corresponding set of performance vectors $\mathcal{P}_F$ in objective space.

```
Generate an initial feasible solution x;
Initialise the archive A = {x};
Initialise the cooling schedule epoch c ← 1;
Initialise the number of iterations t ← 1;
Initialise the number of epochs without an accepted solution ξ ← 0;
while ξ ≤ C_max do
    A ← 0;
    while t ≤ t + L_c and A < A_min do
        Generate a neighbouring solution x' from the current solution x;
        Assess the energy difference △_E(x', x) according to (4.9);
        Generate a random number r ∈ (0, 1);
        if r < min{1, exp(−△_E(x', x) / T_c)} then
            x ← x';
            if |A_x| = 0 then
                A ← A ∪ {x};
                for y ∈ A do
                    if x ≺ y then
                        A ← A\{y};
                        A ← A + 1;
        t ← t + 1;
    c ← c + 1;
    Update the system temperature T_c;
    if A = 0 then
        ξ = ξ + 1;
P_F ≈ A;
```

4.4 Algorithmic Implementation

The *general* working of the multiobjective SA algorithm proposed by Smith *et al.* [38] was described in §4.3.2 above. A detailed description of the *specific* SA algorithmic implementation adopted in this project for the transmitter facility location problem is presented in this section. The supporting algorithms were all implemented by the author in Matlab [28], following the pseudocode outlined in this section. The SA algorithm was implemented according to the pseudocode outlined in Algorithm 4.1.

4.4.1 Algorithm Initialisation

The initialisation step of the SA algorithm consists of generating an initial feasible solution to the radio transmitter facility location problem, as well as the specification of an initial temperature. A random initial solution is generated using the procedure outlined in pseudocode form in Algorithm 4.2. The if-statement spanning Steps 5–8 ensures that the same transmitter location can never be selected twice.

Algorithm 4.2: Generating an initial feasible solution

Input : A data set containing the elevation data for the area under consideration as well as the number k of transmitters to be located.

Output: An initial feasible binary solution vector $\boldsymbol{x} = [x_1, \ldots, x_n]$ for which $\sum_{i=1}^{n} x_i = k$.

```
1 for i = 1 to n do
2     x_i ← 0
3 for i = 1 to k do
4     Generate a random integer s between 1 and n;
5     if x_s ≠ 1 then
6         x_s ← 1;
7     else
8         Go to Step 2
9 Return x;
```

Once the initial solution has been generated, the initial temperature T_0 may be determined using the *average increase method* described in detail in [42]. This method relies on an initial acceptance ratio χ_0, which is defined as the ratio of the number of accepted worsening moves to the number of attempted moves during a trial run of the algorithm, and on the average increase in energy $\bar{\triangle}_E{}^{(+)}$ of the accepted worsening moves. The value of $\bar{\triangle}_E{}^{(+)}$ may be estimated through the execution of a random walk over the solution space, using the initial solution as the starting point. Once $\bar{\triangle}_E{}^{(+)}$ has been determined, the initial temperature may be calculated from the relationship

$$\chi_0 = \exp\left(-\frac{\bar{\triangle}_E{}^{(+)}}{T_0}\right),$$

which may be rewritten as

$$T_0 = -\frac{\bar{\triangle}_E{}^{(+)}}{\ln(\chi_0)}. \tag{4.11}$$

Busetti [7] states that initially the temperature should be assigned a value such that approximately 80% of non-improving moves are accepted. This corresponds to the choice of $\chi_0 = 0.8$

in (4.11). A pseudocode description for the determination of the initial temperature T_0 is given in Algorithm 4.3.

The average inrease in energy $\bar{\triangle}_E^{(+)}$ of the objective function is calculated for both objectives $\Gamma_c^{(\alpha)}(\boldsymbol{x})$ and $\Gamma_\ell^{(P_t,\alpha,S_{min})}(\boldsymbol{x})$ separately in the for-loop spanning Steps 2–11 of Algorithm 4.3. In Step 12, T_0 is assigned the maximum value for the initial temperature thus obtained from the two objective functions. The maximum is taken, since a larger initial temperature is expected to encourage broader coverage of the Pareto-front as it results in a more random search initially.

Algorithm 4.3: Generating an initial temperature

Input : An initial feasible solution vector $\boldsymbol{x}$, the length w of the random walk, as well as a grid of elevation data, the quality of demand satisfaction matrix $\boldsymbol{C}^{(\alpha)}$ and the quality of signal strength matrix $\boldsymbol{Q}^{(P_t,\alpha,S_{min})}$.

Output: An initial temperature T_0.

1 Initialise $j \leftarrow 0, t \leftarrow 0$;
2 **for** *i = 1 to w* **do**
3 Generate a neighbouring solution $\boldsymbol{x}'$;
4 $\triangle_{E_{\Gamma_c}}(\boldsymbol{x},\boldsymbol{x}') \leftarrow \Gamma_c^{(\alpha)}(\boldsymbol{x}) - \Gamma_c^{(\alpha)}(\boldsymbol{x}')$;
5 $\triangle_{E_{\Gamma_\ell}}(\boldsymbol{x},\boldsymbol{x}') \leftarrow \Gamma_\ell^{(P_t,\alpha,S_{min})}(\boldsymbol{x}) - \Gamma_\ell^{(P_t,\alpha,S_{min})}(\boldsymbol{x}')$;
6 **if** $\triangle_{E_{\Gamma_c}}(\boldsymbol{x},\boldsymbol{x}') > 0$ **then**
7 $\text{Increases}_{\Gamma_c} \leftarrow \text{Increases}_{\Gamma_c} + \triangle_{E_{\Gamma_c}}(\boldsymbol{x},\boldsymbol{x}')$;
8 $j \leftarrow j + 1$;
9 **if** $\triangle_{E_{\Gamma_\ell}}(\boldsymbol{x},\boldsymbol{x}') > 0$ **then**
10 $\text{Increases}_{\Gamma_\ell} \leftarrow \text{Increases}_{\Gamma_\ell} + \triangle_{E_{\Gamma_\ell}}(\boldsymbol{x},\boldsymbol{x}')$;
11 $t \leftarrow t + 1$;
12 $T_0 \leftarrow \max\left[-\frac{\text{Increases}_{\Gamma_c}}{j\ln(\chi_0)}, -\frac{\text{Increases}_{\Gamma_\ell}}{t\ln(\chi_0)}\right]$;
13 Return T_0;

4.4.2 The Neighbourhood Move Operator

Since SA is a local search method, a procedure has to be formalised for generating a neighbouring solution. In this project, the neighbourhood of a current candidate solution $\boldsymbol{x}$ to (4.5)–(4.8), for the case where k transmitters are to be placed, consists of all those candidate solutions which may be obtained by exchanging any one of the transmitter locations with one of its eight neighbouring grid points and keeping the locations of the remaining $k-1$ transmitters unchanged. An element $\boldsymbol{x}'$ of this neighbourhood is selected according to a uniform distribution as the neighbouring solution. A pseudocode description of the algorithm used to generate neighbouring solutions is given in Algorithm 4.4.

The random integer i generated in Step 1 of Algorithm 4.4 is used to determine which of the k transmitter placement location positions will be perturbed. The random number p generated in Step 2 is used to determine which of the adjacent grid points will be chosen for inclusion in the neighbouring solution. The for-loop spanning Steps 4–8 is used to determine the positions $x_s \in \boldsymbol{x}$ at which the transmitters are located in the current solution $\boldsymbol{x}$. These points are stored in a temporary vector $\boldsymbol{s} = [s_1, \ldots, s_k]$. The if-statements spanning Steps 9–24 follow a procedure similar to that of sampling from a discrete distribution in order to determine which

of the adjacent points will be chosen as part of the neighbouring solution $\boldsymbol{x}'$. For this procedure, the numbering of the candidate sites is assumed to comply with the labelling convention in Figure 3.9. The second part of the and-clause of each of the if-statements fulfils the purpose of constraint handling as it ensures that no infeasible location values can be generated when generating a neighbouring solution $\boldsymbol{x}'$.

Algorithm 4.4: Generating a feasible neighbouring solution

Input : The dimensions of the $n \times m$ grid of possible transmitter locations, the number k of transmitters to be located as well as a current solution vector $\boldsymbol{x}$.

Output: A neighbouring feasible solution vector $\boldsymbol{x}'$.

```
1  Generate a random integer i between 1 and k;
2  Generate a random number p between 0 and 1;
3  Initialise q ← 1;
4  for j = 1 to n × m do
5      if x_j = 1 then
6          s_q = j;
7          q ← q + 1;
8      j ← j + 1;
9  if p ≤ 0.125 and s_i > m + 1 then
10     x'_{s_i−(m+1)} ← 1;
11 else if p ≤ 0.25 and s_i > m then
12     x'_{s_i−(m)} ← 1;
13 else if p ≤ 0.375 and s_i > m − 1 then
14     x'_{s_i−(m−1)} ← 1;
15 else if p ≤ 0.5 and s_i > 1 then
16     x'_{s_i−1} ← 1;
17 else if p ≤ 0.625 and s_i < n × m then
18     x'_{s_i+1} ← 1;
19 else if p ≤ 0.75 and s_i < (n × m) − (m − 1) then
20     x'_{s_i+(m−1)} ← 1;
21 else if p ≤ 0.875 and s_i < (n × m) − m then
22     x'_{s_i+m} ← 1;
23 else if p ≤ 1 and s_i < (n × m) − (m + 1) then
24     x'_{s_i+(m+1)} ← 1;
25 Return x';
```

4.4.3 The Cooling Schedule

The outer while-loop spanning Steps 6–23 of Algorithm 4.1 describes the gradual lowering of the temperature of the system. In order to define the cooling schedule, a decreasing temperature function has to be selected. The widely used geometric law of decrease is adopted in this project as the decreasing temperature function due to its simplicity and effectiveness over a wide range of problems [42].

According to the geometric law of decrease, the temperature update is given by

$$T_{c+1} = \varphi T_c, \tag{4.12}$$

where T_c is the system temperature during epoch c and $\varphi \in (0, 1)$ is a constant known as the *cooling parameter*. The value for φ originally proposed by Kirkpatrick *et al.* [23] was 0.95. In practice, however, the value for φ is typically chosen between 0.8 and 0.99 [42].

Several other decreasing temperature functions have also been proposed in the literature. The temperature can, for example, be adjusted in one of the following alternative ways [41]:

Linear cooling. In this trivial cooling schedule, the temperature is simply updated linearly, subtracting a pre-defined value from the current temperature at the end of every epoch.

Logarithmic cooling. In the logarithmic cooling schedule, the initial temperature is divided by the logarithm of the current epoch index value to obtain the temperature value for the current epoch. This schedule is often too slow to be applied in practice, but it sometimes results in convergence to a global optimum (in the case of single-objective optimisation) [41].

Very slow decrease cooling. In the very slow decrease cooling schedule, only one iteration is allowed before the temperature is adjusted according to a specified formula.

Nonmonotonic cooling. Typically, cooling schedules are monotone (*i.e.* the temperature is a non-increasing function of increasing iteration number). Nonmonotonic cooling schedules allow for the possibility of reheating at various points in time in order to encourage diversification of the search.

Adaptive cooling. All of the above cooling schedules may be classified as static in the sense that the complete cooling schedule is defined *a priori*. In an adaptive cooling schedule, however, the temperature decreasing rate is dynamic and depends on problem instance-specific information obtained during the search. An example of an adaptive cooling schedule is that proposed by Huang *et al.* [19] in which the rule for decreasing the temperature depends on the average objective function value achieved during consecutive epochs. Other examples of adaptive cooling schedules have also been proposed by Van Laarhoven and Aarts [45], and by Triki *et al.* [42].

4.4.4 Termination Criteria

The duration of an epoch, *i.e.* the number of iterations spent by the search at a specific temperature, is determined by a Markov chain. Busetti [7] states that the value of the length L_c of epoch c should ideally be problem-specific, rather than being a function of the index c of the epoch. It would make sense to require a minimum of A_{min} move acceptances during any temperature stage before the temperature is lowered, where A_{min} is a pre-specified parameter. As the temperature decreases, however, the acceptance probability of a move decreases, and, as a result, the number of expected moves required before accepting A_{min} is expected to increase without bound as the search progresses, irrespective of the value of A_{min}. As a result, a compromise is to terminate the search after a maximum number of moves I_{max} have been attempted or A_{min} moves have been accepted, whichever occurs first. According to the rule of thumb proposed by Dreo *et al.* [12], $I_{max} = 100N$ and $A_{min} = 12N$, where N is a measure of the number of degrees of freedom of the optimisation problem. These values are, however, not

used in this project — where suitable values for I_{max} and A_{min} have instead been determined through experimentation.

The SA algorithm terminates when the outer while-loop spanning Steps 6–23 in Algorithm 4.1 terminates. The criterion implemented in order to terminate the while-loop is when a specified number of epochs C_{max} have passed without the acceptance of a newly generated neighbouring solution $\boldsymbol{x}'$. Dreo *et al.* [12] proposed using a value of $C_{max} = 3$ as the stopping criterion since by the time that no moves have been accepted at three consecutive temperatures, the search may be considered to have ceased making significant progress.

4.5 Model Validation

In order to validate the mathematical model and the author's implementation of the method of multiobjective SA as described in §4.4, the nondominated solutions to the transmitter placement problem obtained by the method of SA for $k = 2$ and $k = 3$ transmitters are compared to the Pareto optimal solutions computed by brute force in Example 4.1 (*i.e.* compared to all $\binom{400}{2} = 79\,800$ and to all $\binom{400}{3} = 10\,586\,800$ location combinations, respectively). This comparison is performed using the hypervolume as performance evaluation criterion. While *et al.* [47] define the *hypervolume* associated with a set of trade-off solutions to a multiobjective optimisation problem as a measure of the size of the objective space that is dominated by those solutions collectively. In the bi-objective function space of the model (4.5)–(4.8), the hypervolume represents the area under the approximated Pareto front, measured from a fixed reference point. Hypervolume is a preferred measure of the quality of an approximated Pareto front since it attempts to capture the closeness of the approximate solutions to the optimal set, as well as, to a certain extent, the spread of solutions across the objective space [47]. In order to determine the hypervolume achieved by the SA algorithm, the *Hypervolume by Slicing Objectives* algorithm introduced by While *et al.* [47] is used.

Example 4.2 (**Determination of the hypervolume**). *Suppose that the hypervolumes associated with the nondominated sets generated by the SA algorithm have to be determined and compared to the hypervolumes associated with the true Pareto fronts of the instances of the bi-objecitve facility location model (4.5)–(4.8) determined in Example 4.1. The hypervolumes associated with these true Pareto fronts were calculated as* 0.1233 *and* 0.1486 *for the placement of* $k = 2$ *and* $k = 3$ *transmitters, respectively.*

Ten iterations of the SA algorithm were also performed for each of these problem instances. The hypervolumes associated with the resulting approximation sets are reported in Table 4.1, as percentages of the hypervolumes of the true Pareto fronts. The initial temperatures T_0*, the required computation times, as well as the number of epochs* c *achieved by the SA algorithm are also shown in the table. The SA algorithm was executed on the same computer as that used for the computations reported in Example 4.1.*

The search progression corresponding to iteration $i = 1$ *in Table 4.1 (a) may be seen in Figure 4.5 (a). As can be seen in the figure, there is an increasing trend in the coverage objective* f_1*, which finally stabilises around the value* 0.9*. The conflicting nature of the objectives is also clearly indicated in the figure. This may be seen from the fact that an increase in* f_1 *is typically accompanied by a decrease in* f_2*, which finally stabilises around the value* 0.55*. The exponential decrease of the temperature throughout the duration of the search is indicated by the straight line, measured on a logarithmic scale. The true Pareto fronts, as well as the attainment fronts generated during the ten runs of the SA algorithm are shown in Figures 4.5 (b) and (c) for the placement of* $k = 2$ *and* $k = 3$ *transmitters, respectively. The hypervolumes of these attainment*

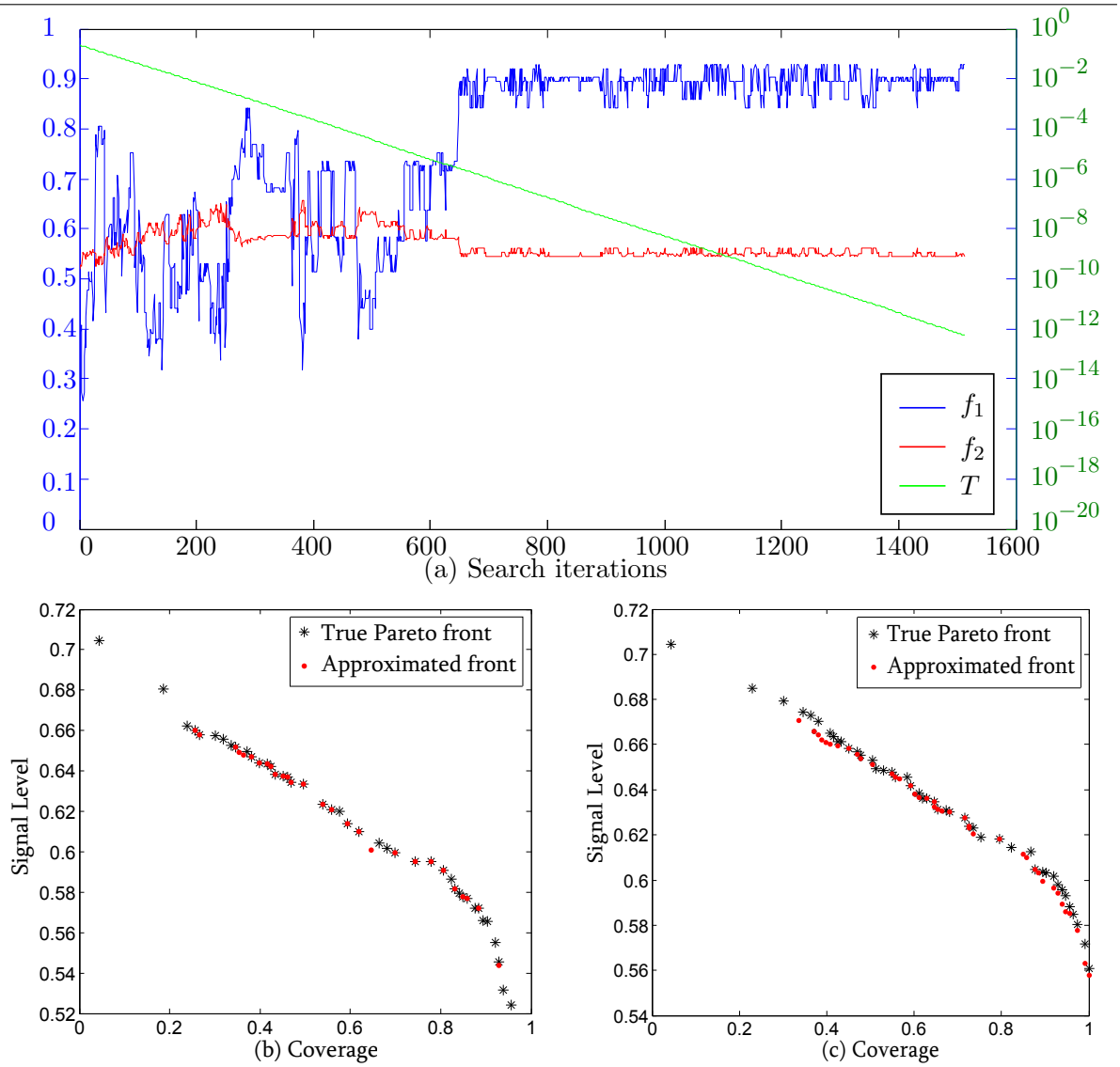

FIGURE 4.5: *(a) The search progression corresponding to iteration $i = 1$ in Table 4.1 (a), and the attainment fronts achieved by ten runs of the SA algorithm together with the true Pareto fronts for (b) $k = 2$ and (c) $k = 3$ transmitter placements.*

fronts are 97.40% *and* 95.62% *of the hypervolumes of the true Pareto fronts for the transmitter location problem instances with $k = 2$ and $k = 3$ transmitters, respectively. These percentages are collective quality measures associated with the entire nondominated sets of trade-off solutions and do not refer to the optimality gaps of any individual candidate solutions. The optimality gap for any single solution with respect to both objective functions is typically much less than* 3% *and* 5% *for the placement of $k = 2$ and $k = 3$ transmitters, respectively. The SA algorithm, in fact, uncovered a number of truely Pareto optimal solutions.* □

4.6 Chapter Summary

This chapter was devoted to the development of a bi-objective maximisation model which may be used to solve the radio transmitter facility location problem. The initial focus in §4.1 was on the explanation of some basic concepts pertaining to multiobjective optimisation. The focus

(a) The placement of $k = 2$ transmitters

i	T_0	H	c	Time	i	T_0	H	c	Time
1	0.2210	91.48	523	14.72	6	0.5790	92.13	391	8.71
2	0.1530	93.84	1456	38.56	7	0.6345	92.46	649	13.85
3	0.3966	91.16	1167	32.22	8	0.2062	90.43	402	12.05
4	0.3173	92.21	2171	55.14	9	1.1104	92.70	1112	29.26
5	0.2776	92.05	761	19.05	10	0.1782	92.21	481	12.64

(b) The placement of $k = 3$ transmitters

i	T_0	H	c	Time	i	T_0	H	c	Time
1	0.1813	89.03	878	44.97	6	0.1190	88.96	530	28.95
2	0.1373	92.40	659	31.83	7	1.1025	93.74	1757	99.69
3	0.1785	87.48	560	25.90	8	0.4600	88.62	546	26.81
4	0.2538	87.75	320	15.07	9	0.2181	91.45	426	19.09
5	0.4442	93.20	838	48.98	10	0.2727	92.46	594	27.28

TABLE 4.1: *The results of the ten iterations of the SA algorithm in which, $A_{min} = 3$, $A_{max} = 3$ and $I_{max} = 20$. For each iteration i, the initial temperature T_0 is given, the hypervolume H is given as a percentage of that of the true Pareto front, the required number c of search epochs is reported and the required computation time is specified in seconds.*

then shifted in §4.2 to the formulation of the mathematical model. In §4.3, the focus next shifted to the working of the method of SA. Initially the discussion centred around single-objective SA in order to provide the reader with a background as to how the technique functions. Thereafter, the dominance-based multiobjective SA algorithm, as proposed by Smith *et al.* [38], was described. Section 4.4 was devoted to the implementation of the dominance-based multiobjective SA algorithm. Detailed pseudocode descriptions of the supporting algorithms for the initialisation of the algorithm, as well as the generation of the neighbouring solutions, were provided. This was followed by a description of the cooling schedule and the termination criteria employed in this project. Finally, the chapter closed in §4.5 with a model validation, comparing the hypervolumes achieved by the SA algorithm to the hypervolumes of the true Pareto front calculated by brute force for instances of the problem where $k = 2$ and $k = 3$ transmitters were to be located.

CHAPTER 5

Decision Support System

Contents

This chapter is devoted to a description of the development and implementation of a DSS which combines the bi-criterion framework for the evaluation of a set of given transmitter locations developed in Chapter 3 and the bi-objective facility location model formulated in Chapter 4. The chapter opens in §5.1 with a detailed description of the design and implementation of the DSS user interface using the GUIDE package of Matlab [28] for the development of *graphical user interfaces* (GUI's). The focus then shifts in §5.2 to a discussion on how the evaluation framework of Chapter 3 and the mathematical model together with the SA approximate solution methodology of Chapter 4 were combined in order to create a user-friendly decision support tool. The chapter finally closes in §5.3 with a summary of the work included in this chapter.

5.1 User Interface Design

The primary design requirement for the GUI of the DSS developed during the course of this project was to enable the user to easily load the elevation and demand data pertaining to an instance of the transmitter location problem into the system, thereby facilitating access to the framework of Chapter 3 and the solution methodology developed in Chapter 4 to non-mathematically inclined users. These data may be loaded into the DSS by clicking the corresponding *Load Elevation Data* and *Load Demand Data* buttons, after which a windows explorer window, shown in Figure 5.1, appears which allows the user to browse for and select the correct files. Thereafter, the GUI allows the user to enter the network-specific parameters of the facility location problem instance. These parameters include the scalable parameter α for determining the required level of unobstruction of the first Fresnel ellipsoid, the base station and mobile antennae heights h_b and h_m, respectively, the frequency f at which the network will be transmitting, the transmitted power P_t' at the base stations, and the threshold minimum signal level S_{min}. By default, the values used in Examples 3.2–3.9 are loaded into the edit boxes for specification of these parameters at the top left of the main user interface, as shown in Figure 5.2. Once these values have been entered, the pre-optimisation processing phase may be initiated by clicking the corresponding *Execute Pre-Optimisation* button. Since this may take a few minutes, a message will be displayed to the user once the pre-optimisation phase has been completed.

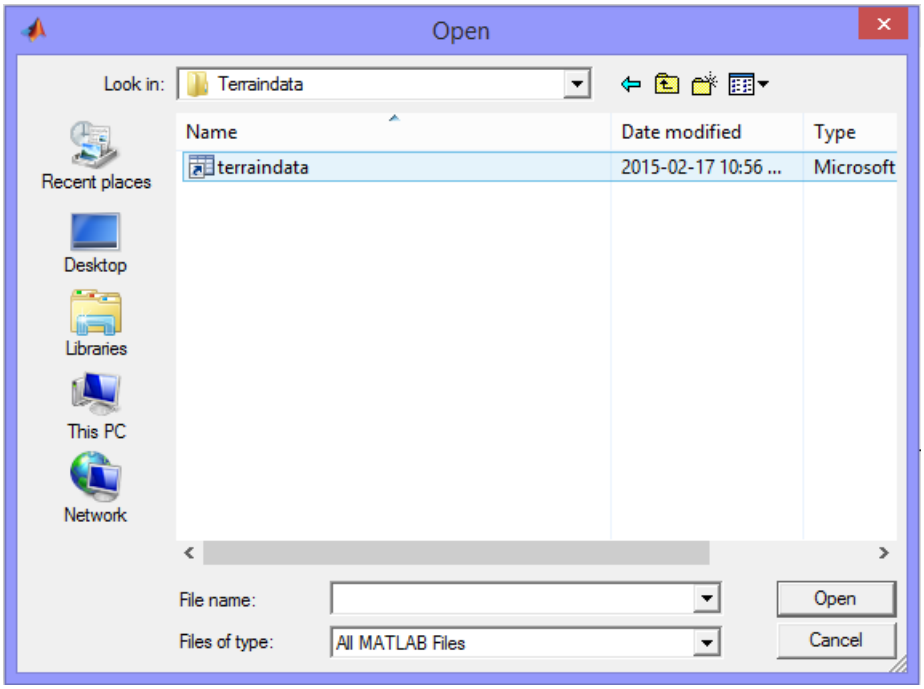

FIGURE 5.1: *The windows explorer browser window displayed to the user when selecting the elevation and demand data sets.*

Once the pre-optimisation phase is complete, the user may choose the number of transmitters k that are to be located and then initiate the optimisation phase by clicking the *Execute Optimisation* button. Once the optimisation phase has been completed, a message indicating the completion of the phase is again displayed to the user. The nondominated front corresponding to the Pareto optimal approximation set of transmitter locations is also displayed on the set of axes towards the top left side of the display, representing objective function space. The performance measures $\Gamma_c^{(\alpha)}(\boldsymbol{x})$ and $\Gamma_\ell^{(P_t,\alpha,S_{min})}(\boldsymbol{x})$ corresponding to this approximation set are displayed together with the associated set of transmitter grid locations in the table at the bottom of the screen.

The user may then enter any of these sets of transmitter locations into the text boxes labelled Location 1 to Location 10 towards the middle right of the screen and prompt the DSS to display the view shed and a heat map of the average signal level achieved by the set of transmitter locations. The view shed (coverage) plot is then displayed on the central set of axes, while the heat map of the average signal level achieved is displayed on the set of axes in the top right corner of the screen. A screenshot of the complete user interface showing the nondominated front, as well as the view shed plot and the corresponding average signal level heat map, is displayed in Figure 5.2.

5.2 Framework and Model Implementation

Both the bi-criterion pre-optimisation framework for evaluating the quality of a given set of transmitter locations of Chapter 3 and the SA algorithm of Chapter 4 for the approximate solution of the bi-objective mathematical model were implemented in Matlab R2012b [28]. The implementation of the pre-optimisation and the optimisation phases are elucidated in this section according to a top-down approach to diagramming data movement using *data flow diagrams*

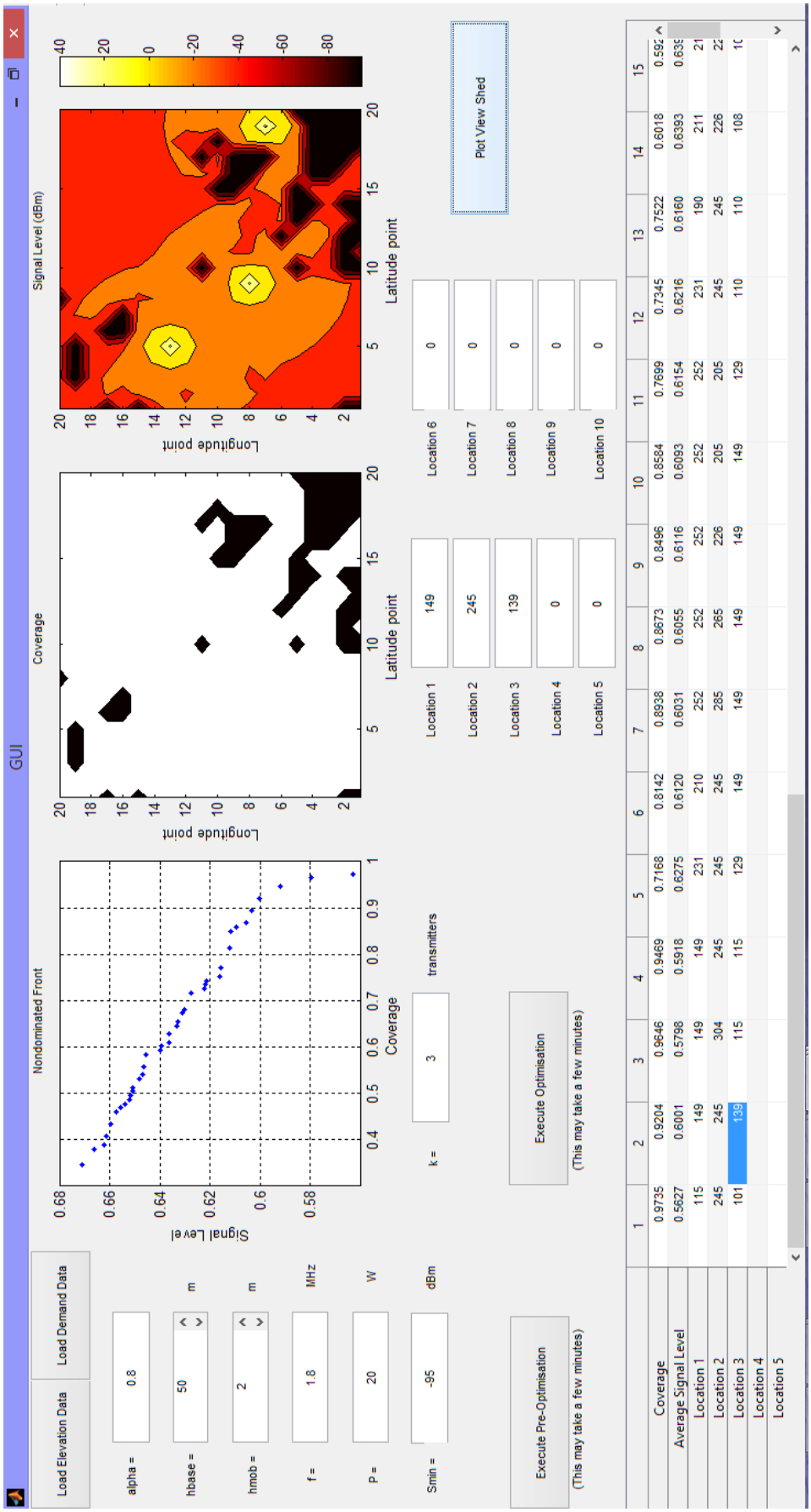

FIGURE 5.2: *The DSS user interface showing the nondominated front, the view shed plot and the average signal level heat map.*

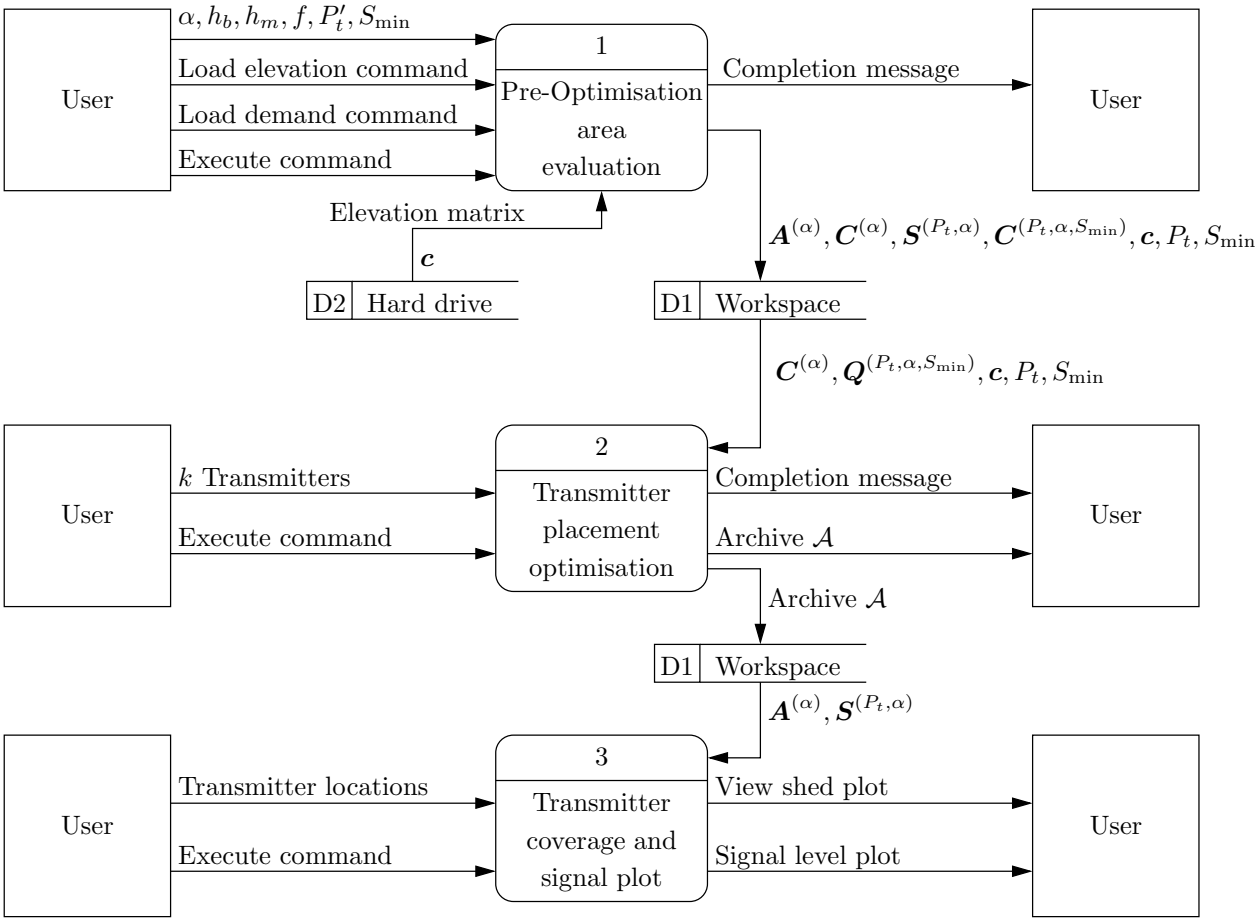

FIGURE 5.3: *The Diagram 0 of the DSS showing all user inputs and outputs for the respective sub processes.*

(DFDs), as described by Kendall and Kendall [21].

The DFD 0 shown in Figure 5.3 captures the basic user inputs, the general working of the system and the outputs of the system displayed to the user for each of the subsystems comprising the DSS. The working of Processes 1, 2 and 3 is explained in greater detail in the remainder of the section.

The pre-optimisation process (denoted Process 1 in Figure 5.3) is triggered by the user, by importing the elevation and demand data from a storage source. These data are then saved to the workspace. Thereafter, the user is prompted to enter the network-specific parameters of the facility location problem instance, as described in §5.1. Once this has been completed, the final stages of the pre-optimisation process consist of creating the potential coverage matrix $\boldsymbol{A}^{(\alpha)}$ defined in (3.3), the quality of demand satisfaction matrix $\boldsymbol{C}^{(\alpha)}$ defined in (3.4), the potential signal strength matrix $\boldsymbol{S}^{(P_t,\alpha)}$ defined in (3.7), and finally, the quality of signal strength matrix $\boldsymbol{Q}^{(P_t,\alpha,S_{min})}$ defined in (3.8). These matrices are calculated according to the procedures illustrated in Examples 3.1–3.6 and Example 3.8. Once these matrices have been computed, they are also saved to the workspace and a message indicating that the process has been completed is displayed to the user. The flows of the data in Process 1 described above are illustrated graphically in Figure 5.4.

Once the user has specified the number of transmission towers k which are to be located, the optimisation process (denoted Process 2 in Figure 5.3) is triggered by the user. This initiates

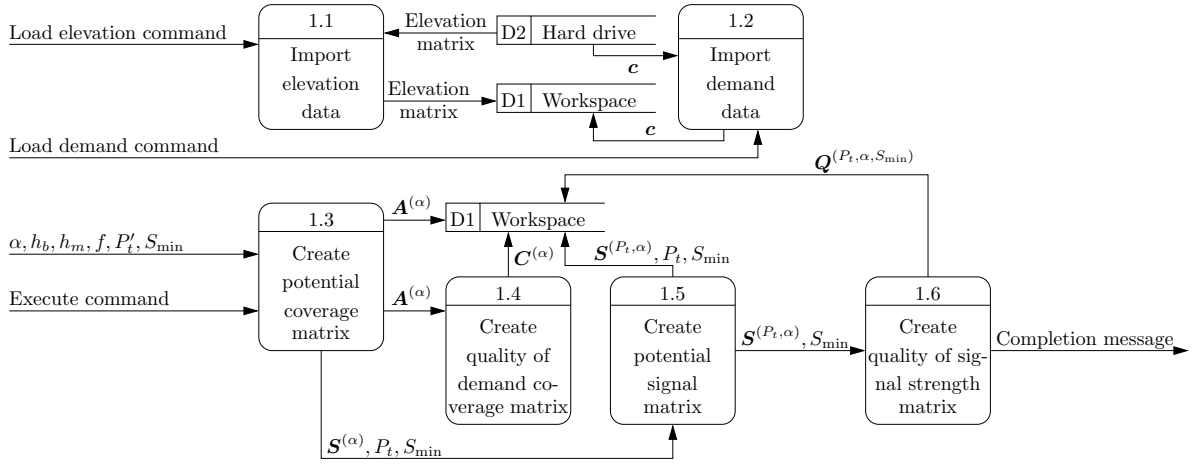

FIGURE 5.4: *The child diagram of Process* 1*, showing the data flows through the process, as well as the data entities created by the process, which are saved to the workspace.*

execution of the SA algorithm which follows the implementation described in §4.4, including the generation of an initial feasible solution according to Algorithm 4.2, the determination of the initial temperature according to Algorithm 4.3 and finally the completion of the SA search process as described in Algorithm 4.1. The generation of neighbouring solutions follows the process outlined in Algorithm 4.4. In order to determine the performance of a given set of transmitter locations, expressions (3.6) and (3.9) are used, as illustrated in Examples 3.7 and 3.9. The quality of demand satisfaction matrix $\boldsymbol{C}^{(\alpha)}$, the quality of signal strength matrix $\boldsymbol{Q}^{(P_t,\alpha,S_{min})}$, the demand importance values c_j, the transmitted power P_t and the threshold minimum signal level S_{min} which serve as inputs to the various algorithms are read from the workspace, and the nondominated front generated in objective function space, together with the corresponding transmitter locations in decision space, stored in the archive $\mathcal{A}$, are saved to the workspace. Finally, a plot of the nondominated front stored in $\mathcal{A}$ is generated using Matlab's built-in plot function and the archive is displayed to the user in table format. Once this process has been completed, the user is again notified. The flows of the data in Process 2 decribed above are illustrated graphically in Figure 5.5.

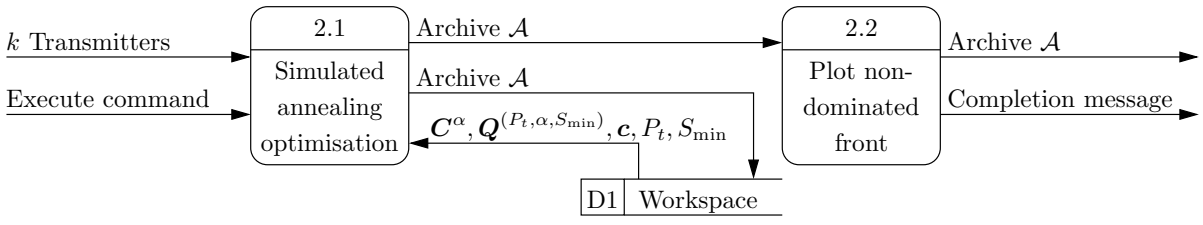

FIGURE 5.5: *The child diagram of Process* 2*, showing the data flows through the process, as well as the data entities created by the process, which are saved to the workspace.*

Finally, the user may enter the locations of a given set of transmitters (typically those of a solution forming a part of the nondominated front as displayed in table format at the bottom of the user interface screen) and prompt the DSS to display a view shed plot, as well as a heat map indicating the signal level throughout the coverage area during a post-optimisation processing phase (denoted by Process 3 in Figure 5.3). It is anticipated that this functionality may facilitate the subjective post-optimisation selection by a service planner of a set of transmitter locations for actual implementation. The potential coverage quality matrix $\boldsymbol{A}^{(\alpha)}$ and the potential signal strength matrix $\boldsymbol{S}^{(P_t,\alpha)}$ required for the generation of these plots are again read from

the workspace. For each of the demand points j, the coverage, as well as the maximum signal level provided there, is determined, again by taking the maxima across the columns for those rows representing the transmitter locations in $\boldsymbol{A}^{(\alpha)}$ and $\boldsymbol{S}^{(P_t,\alpha)}$. These values are then stored in interim matrices, which are plotted using Matlab's built-in contour plot function and displayed to the user. The flows of the data in Process 3 described above are illustrated graphically in Figure 5.6.

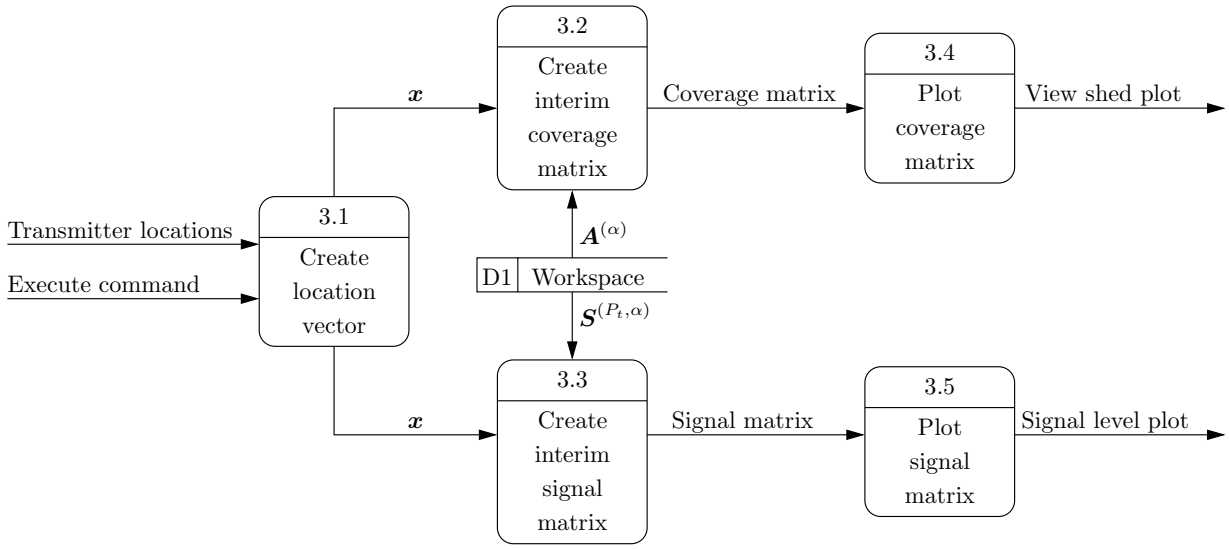

FIGURE 5.6: *The child diagram of Process* 3*, showing the data flows through the process, as well as the data entities created by the process, which are saved to the workspace.*

5.3 Chapter Summary

This chapter was devoted to a demonstration of the way in which the framework for evaluating the quality of a given set of transmitter placement locations (developed in Chapter 3) and the mathematical model together with the SA approximate solution technique (described in Chapter 4) were implemented by the author in a user-friendly DSS. The initial focus in §5.1 was on the design of the user interface, stating its intended purpose and describing the functionality of each of its buttons and text boxes. Thereafter, the focus shifted in §5.2 to a high-level description of the implementation of the DSS in Matlab according to standard DFDs in order to illustrate the manner in which data pass through the DSS.

CHAPTER 6

The Stellenbosch Area: A Case Study

Contents

In this chapter, a special case study is conducted with the aim of evaluating the DSS of Chapter 5 in the context of a realistic problem instance. The initial focus in §6.1 is on a discussion of the input data pertaining to the case study, which comprise terrain elevation and demand data for an area surrounding the town of Stellenbosch in the South African Western Cape. In §6.2, the DSS is used to generate nondominated sets of trade-off transmitter locations for varying numbers of transmitters. The results thus obtained are subsequently compared to the existing networks of two local mobile telecommunication network providers in §6.3, before the chapter closes in §6.4 with a summary of the work included in this chapter.

6.1 Input Data

The elevation data for an area surrounding the town of Stellenbosch in the Western Cape Province of South Africa, obtained from [30] and considered in the case study of this chapter, are shown in Figure 6.1. A contour plot representation of these data is given in Figure 6.2. The area consists of a 16 km $\times$ 16 km portion of land stretching from S33° 51′ 20″ to S34° 00′ 00″ and from E18° 45′ 48″ to E18° 56′ 12″. This area includes Stellenbosch, whose central coordinates are located at S33° 55′ 12″ and E18° 51′ 36″, as well as the outskirts of Cloetesville, Welgevonden, Idas Valley and Kleingeluk. Because of the unavailability of mobile telecommunication coverage importance data (due to their sensitive nature), these data are approximated by spatial census data, obtained from [39]. These census data are shown in Figure 6.3. The resolution of these surrogate coverage importance data are measured as the number of people living per square kilometre. As may be seen from the figure, the central part of Stellenbosch has a relatively high population density (in excess of 2 000 people per square kilometre), which fades away towards the Stellenbosch winelands. The use of spatial census data as surrogate coverage importance values follows the approach of Tutschku and Tran-Gia [44], who used discretised spatial land use data,

including population density, to approximate mobile communication network demand. For the purposes of this case study, however, the expected demand and resulting coverage importance value data are assumed to be directly proportional to the population density in the corresponding area.

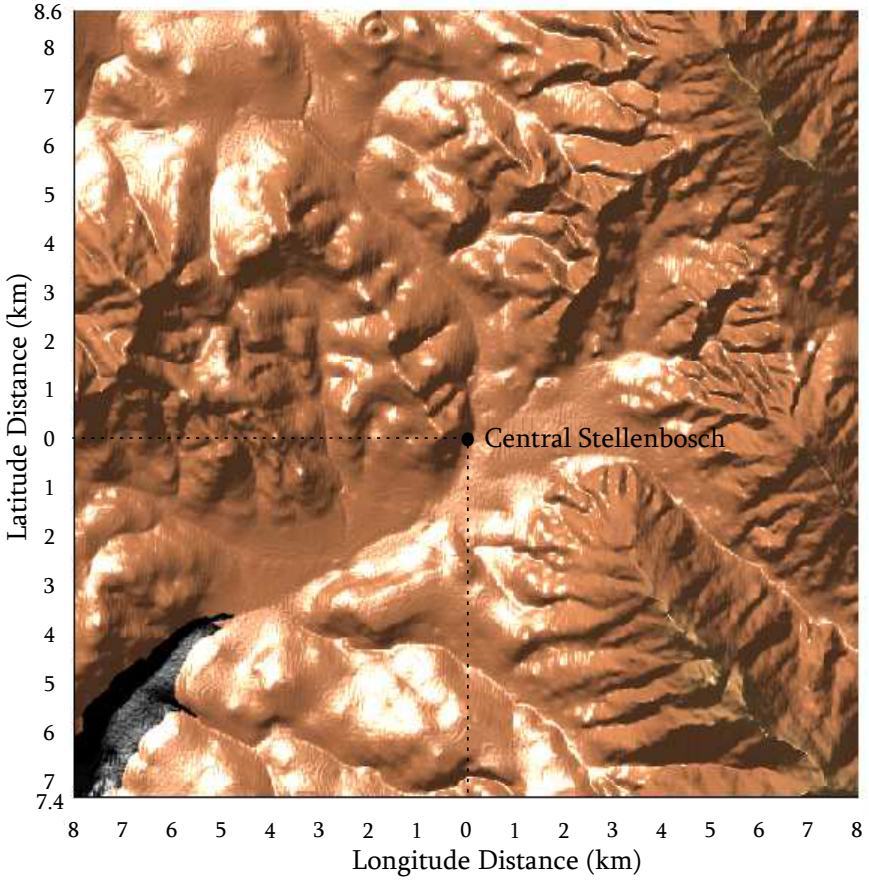

FIGURE 6.1: *Elevation data for a* 16 *km* × 16 *km portion of terrain surrounding the town of Stellenbosch.*

The resolution of the data considered in this case study is such that there is a distance of approximately 216 metres in the latitude direction between successive grid points and 180 metres in the longitude direction. This results in 6 750 candidate sites and demand points arranged in two 75×90 grids. Two 75×90 data matrices are therefore required as input to the DSS — one containing elevation data, and one containing census data.

6.2 Transmitter Placement Suggestions

The DSS of Chapter 5 is applied in this section to two instances of the radio transmitter facility location problem in the context of the area shown above. The difference between the two instances lies in the base station height. In the first part of the case study, a base station height of $h_b = 25$ metres above ground level is assumed, whereas the base station height is increased to $h_b = 50$ metres for the second part. These are typical transmission tower heights used in urban and semi-urban areas [33], although they typically do not provide the range achievable from 200 or 250 metre towers, which are typically set up in rural areas. The reason for this difference

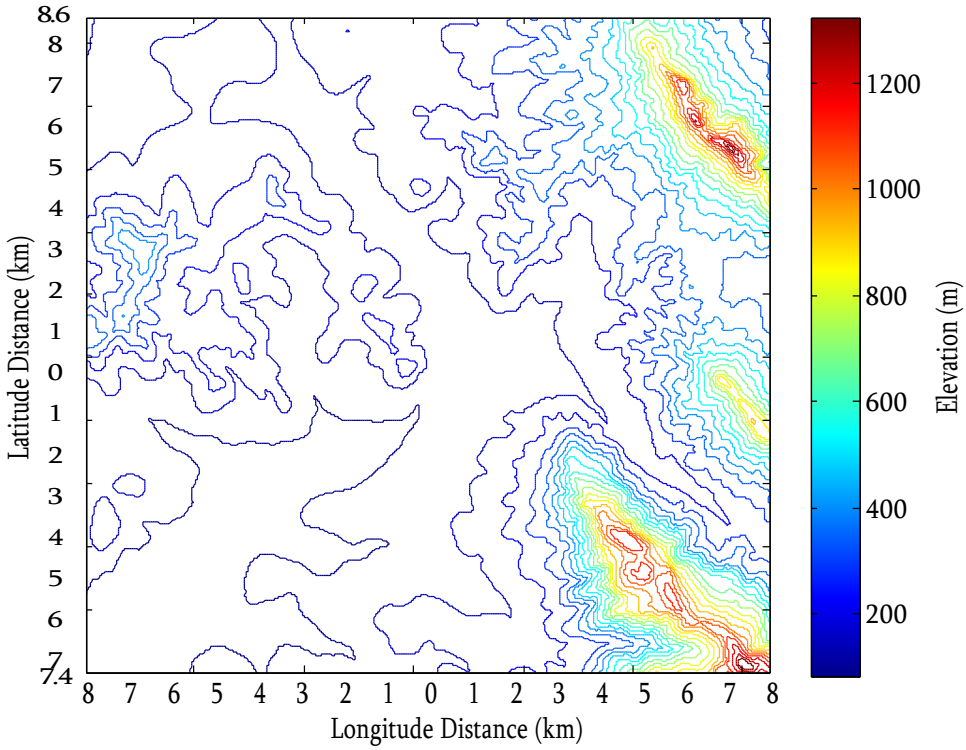

FIGURE 6.2: *A contour representation of the elevation data of Figure 6.1.*

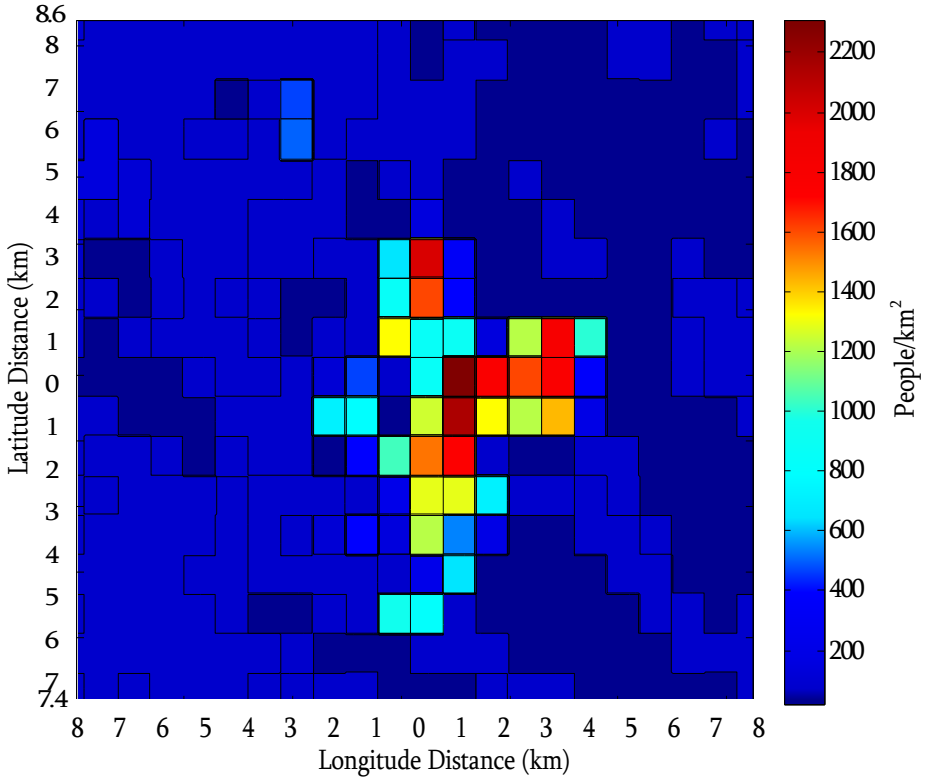

FIGURE 6.3: *The population density in and around Stellenbosch measured as the number of people per square kilometre.*

in height convention is that, although the range and resulting coverage area may be lower in urban areas, fewer complications are expected to result due to interference between the signals provided by different towers as a result of the presence of buildings and other infrastructure. Furthermore, the use of more transmitters to cover an urban area increases the network capacity in the area, which is favourable for densely populated areas [33].

After having loaded the terrain elevation and coverage importance data described in §6.1 into the DSS, the pre-optimisation area evaluation, consisting of a population of the potential coverage matrix $\boldsymbol{A}^{(\alpha)}$ in (3.3), the quality of demand satisfaction matrix $\boldsymbol{C}^{(\alpha)}$ in (3.4), the potential signal strength matrix $\boldsymbol{S}^{(P_t,\alpha)}$ in (3.7) and the quality of signal strength matrix $\boldsymbol{Q}^{(P_t,\alpha,S_{min})}$ in (3.8), may be completed. The computation times required for this pre-optimisation evaluation were 25 804 seconds and 26 111 seconds for the cases with $h_b = 25$ metres and $h_b = 50$ metres, respectively. The same computing hardware as described in Examples 4.1 and 4.2 was used. Thereafter, ten iterations of the SA algorithm were performed for each of the seven instances in which $k = 2$ to $k = 8$ transmitter placements are required. The SA parameter values $A_{min} = k+1$ and $I_{max} = 10(k+1)$ were assumed for this purpose. These values were determined by empirical experimentation, whereas the maximum number of epochs which may pass without acceptance of a neighbouring solution was kept constant at 3, as proposed by Dreo *et al.* [12]. The variability in the A_{min} and I_{max} values was incorporated in order to allow for longer, more in-depth searches as the complexity of the problem increases (*i.e.* as the value of k increases). In order to encourage SA exploration of the search space through slower cooling, the cooling parameter was selected as $\varphi = 0.99$. The attainment fronts achieved by the ten iterations of the SA algorithm for each of the seven transmission placement instances are shown in Figures 6.4 and 6.7 for the problem instances in which the base station heights are 25 metres and 50 metres, respectively. The average initial temperature $\overline{T}_0$, the hypervolume H, the average number of SA epochs $\bar{c}$ and the total computation time for all ten iterations of the SA algorithm are presented in Tables 6.1 and 6.2 for each of the problem instances, respectively. The reference point used in all the hypervolume calculations was $(0.3, 0.3)$.

The view shed (coverage) and signal level heat map plots for the points labelled A and D in Figure 6.4 are shown in Figures 6.5 and 6.6, respectively. In the view shed plots, the white areas again denote those areas covered by the set of transmitter placements, whereas the black areas denote those areas not covered. The signal level heat map plots are not only useful in the sense that they provide an indication of the expected signal level in an area, but they also show where the transmitters are located. These locations are indicated by the light areas (indicating a high signal level) surrounding each transmitter in the plot. The view shed plots and the signal level heat maps for the points B and C in Figure 6.4 are shown in Figures C.1 and C.2 in Appendix C, respectively. Keeping the terrain elevation data in mind, it may be observed that, when maximising the coverage $\Gamma_c^{(\alpha)}(\boldsymbol{x})$ achievable, the transmitters are typically placed at locations of high elevation above sea level, which are simultaneously not too far apart. This trend is evident in Figures 6.6 and C.2. When, however, more emphasis is placed on the objective of maximising the average signal level $\Gamma_\ell^{(P_t,\alpha,S_{min})}(\boldsymbol{x})$, the transmitters tend to be clustered in the high-demand region around central Stellenbosch. This trend is evident in Figures 6.5 and C.1.

The view shed and signal level heat map plots for the points B and C in Figure 6.4 are shown in Figures 6.8 and 6.9, respectively, while the view shed plots and the signal level heat maps for the points A and D in Figure 6.4 are shown in Figures C.3 and C.4 in Appendix C. The same trends in terms of transmitter placement spacing as identified for the case where $h_b = 25$ metres are still evident when $h_b = 50$ metres. For the configurations of transmitter placements plotted in Figures 6.9 and C.4, where high coverage values have been achieved, the transmitters are placed

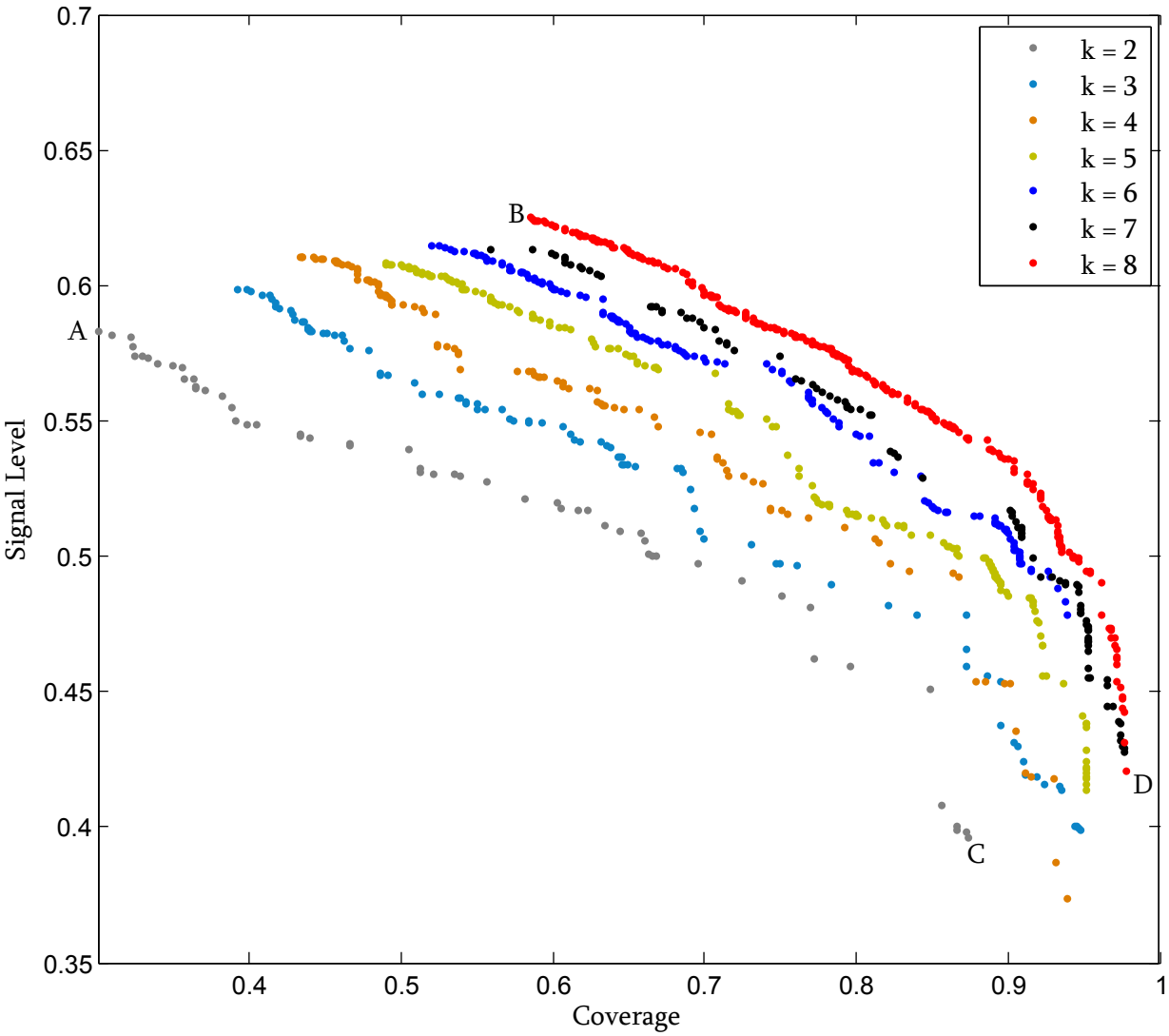

FIGURE 6.4: *The attainment fronts achieved by the ten iterations of the SA algorithm for each of the instances of $k = 2$ to $k = 8$ transmitter placements in the problem instance in which with $h_b = 25$ metres.*

k	$\bar{T}_0$	H	$\bar{c}$	Time
2	0.4383	0.1219	588.8	131.94
3	0.3488	0.1429	904.5	666.40
4	0.3916	0.1592	779.2	768.98
5	0.4765	0.1714	938.5	1 086.90
6	0.4362	0.1784	2 025.6	3 191.32
7	0.6304	0.1861	2 377.0	4 367.61
8	0.3287	0.1977	6 930.0	14 707.63

TABLE 6.1: *Results returned by the SA algorithm with $A_{min} = k + 1, I_{max} = 10(k + 1)$, $A_{max} = 3$ and $h_b = 25$ metres, where k denotes the number of transmitters placed. For each of the seven problem instances, the average initial temperature $\bar{T}_0$ is given, the hypervolume H is given, the average number of search epochs $\bar{c}$ is reported and the total computation time is specified in seconds.*

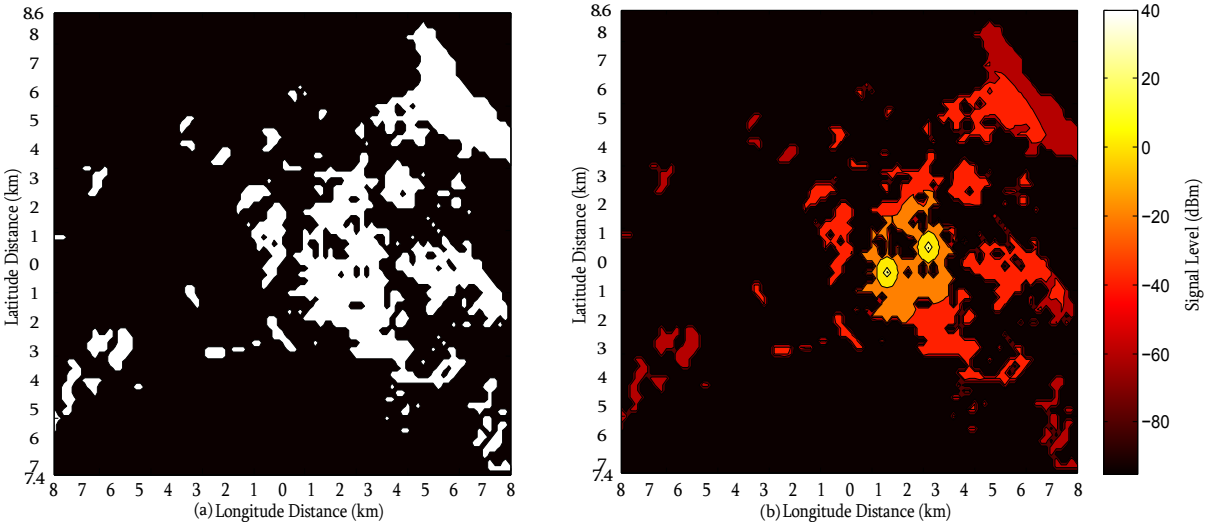

FIGURE 6.5: *View shed plot in (a) and signal level plot in (b) for the extreme point providing the maximum average signal level from $k = 2$ transmitters at a height of $h_b = 25$ metres, corresponding to point A in Figure 6.4.*

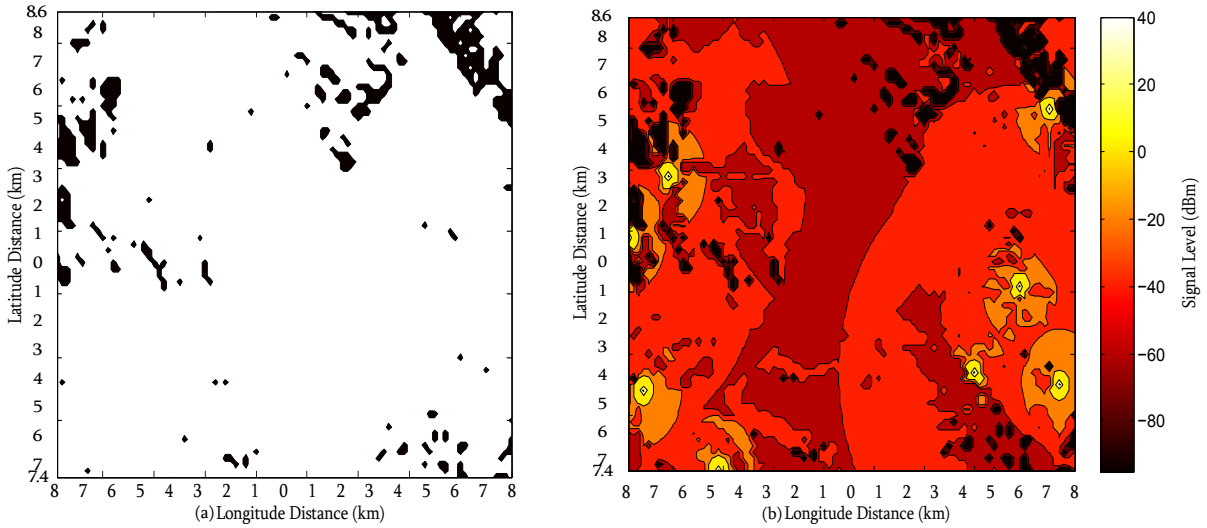

FIGURE 6.6: *View shed plot in (a) and signal level plot in (b) for the extreme point providing the maximum coverage from $k = 8$ transmitters at a height of $h_b = 25$ metres, corresponding to point D in Figure 6.4.*

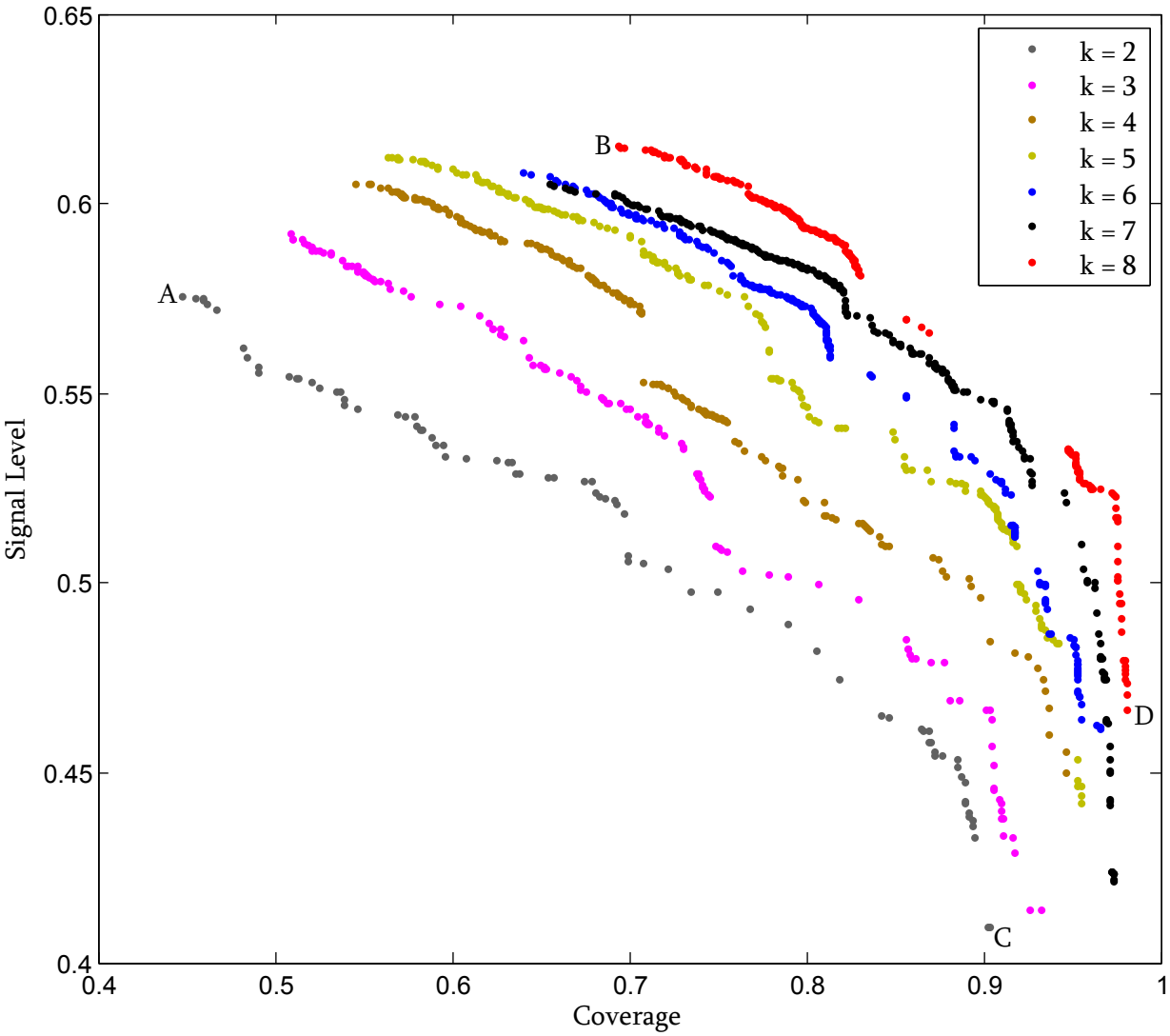

FIGURE 6.7: *The attainment fronts achieved by the ten iterations of the SA algorithm for each of the instances of $k = 2$ to $k = 8$ transmitter placements in the problem instance in which $h_b = 50$ metres.*

k	$\bar{T}_0$	H	$\bar{c}$	Time
2	0.4506	0.1376	821.6	223.77
3	0.6057	0.1569	875.1	419.54
4	0.5642	0.1732	969.6	892.99
5	0.5266	0.1852	1 856.8	1 905.53
6	0.5927	0.1893	1 194.6	1 370.48
7	0.5331	0.1934	2 627.5	4 556.51
8	0.3667	0.2016	3 158.5	11 199.17

TABLE 6.2: *Results returned by the SA algorithm with $A_{min} = k + 1, I_{max} = 10(k + 1)$, $A_{max} = 3$ and $h_b = 50$ metres, where k denotes the number of transmitters placed. For each of the seven problem instances, the average initial temperature $\bar{T}_0$ is given, the hypervolume H is given, the average number of search epochs $\bar{c}$ is reported and the total computation time is specified in seconds.*

not too far apart, typically in areas of high elevation above sea level, whereas in Figures 6.8 and C.3, where high average signal levels have been achieved (typically at the expense of total area coverage), the transmitters are again clustered around the high-demand region surrounding central Stellenbosch and its suburbs.

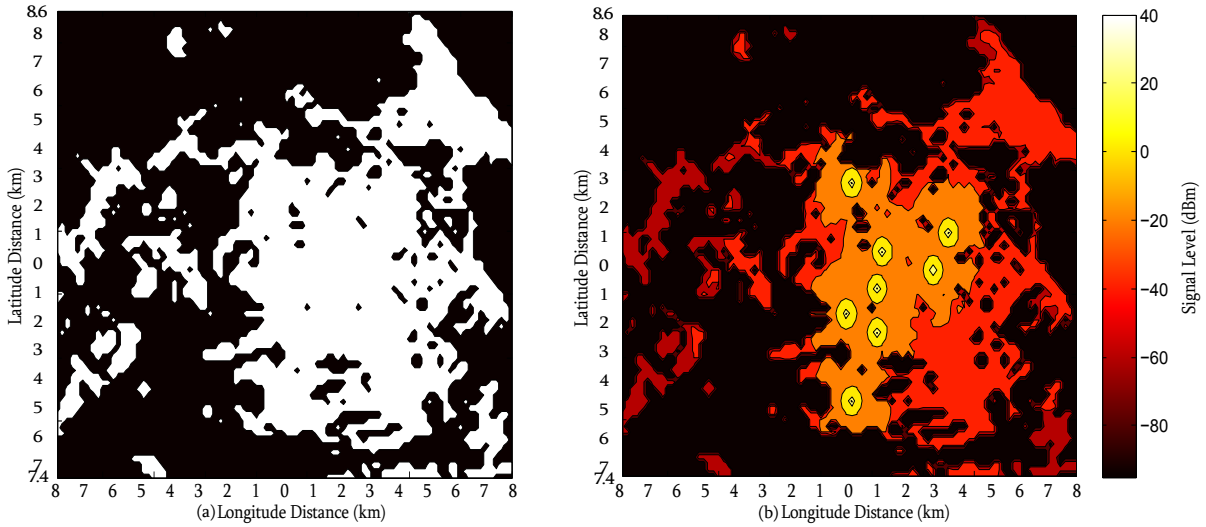

FIGURE 6.8: *View shed plot in (a) and signal level plot in (b) for the extreme point providing the maximum average signal level from $k = 2$ transmitters at a height of $h_b = 50$ metres, corresponding to point B in Figure 6.7.*

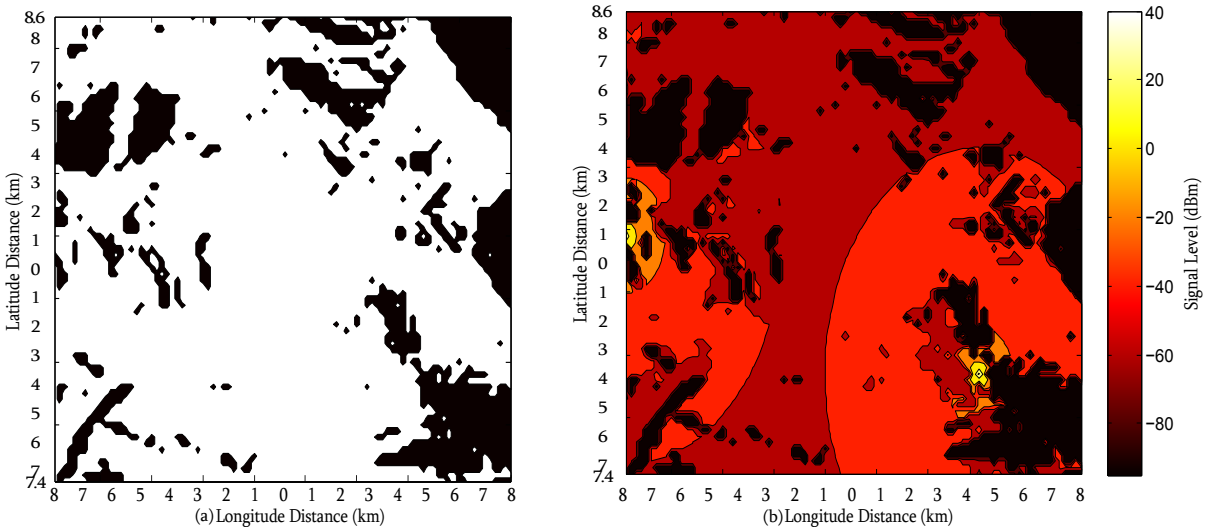

FIGURE 6.9: *View shed plot in (a) and signal level plot in (b) for the extreme point providing the maximum coverage from $k = 8$ transmitters at a height of $h_b = 50$ metres, corresponding to point C in Figure 6.7.*

When comparing the hypervolumes of the fronts achieved by the placement of $k = 2$ to $k = 8$ transmitters it may be observed, as expected, that there is an increasing trend in the hypervolume values as the number of transmitters increases. Furthermore, judging from the hypervolume calculations, a network with base station heights of $h_b = 50$ metres performs marginally better than a network with base station heights of $h_b = 25$ metres. This may be attributed to the fact that the higher base stations are able to provide coverage to a larger region.

6.3 Evaluation of Results Provided by the DSS

In order to assess the quality of the transmitter placement locations suggested by the DSS in the previous section, comparisons to the existing networks of two local mobile telecommunication network providers are conducted in this section. The locations and names of the base stations which form part of the existing transmission networks set up by these network providers were obtained from CellMapper [9], which is a crowd-sourced cellular tower and coverage mapping service. Data on the coverage and signal strength of the networks in various areas are contributed through the use of a mobile application. These data are then used to extract the details of individual antennae at the base stations, including their positions and other technical information.

6.3.1 Network Provider 1

The names, as well as the coordinates, of those transmitters forming part of the existing network established by network provider 1 are listed in Table 6.3.

Number	Base Station	Coordinates
1	BTS ID 2047	S33° 53′ 33″ E18° 49′ 47″
2	BTS ID 1006	S33° 54′ 23″ E18° 51′ 04″
3	BTS ID 6102	S33° 54′ 52″ E18° 51′ 19″
4	BTS ID 2324	S33° 55′ 51″ E18° 52′ 17″
5	BTS ID 2532	S33° 55′ 54″ E18° 51′ 48″
6	BTS ID 6095	S33° 56′ 09″ E18° 52′ 13″

TABLE 6.3: *The identification numbers and coordinates of the base stations which form part of network provider 1's transmission network.*

These locations were entered into the decision vector $\boldsymbol{x}$ and subsequently evaluated according to the coverage and average signal level criteria of the modelling framework of Chapter 3. Under the assumption that all antennae are located at a height of $h_b = 25$ metres above ground level, it was found that the transmitter locations in Table 6.3 achieve a coverage value $\Gamma_c^{(\alpha)}(\boldsymbol{x}) = 0.4356$ and an average signal level $\Gamma_\ell^{(P_t,\alpha,S_{min})}(\boldsymbol{x}) = 0.5976$. When the assumed base station antennae heights were increased to $h_b = 50$ metres, however, the values $\Gamma_c^{(\alpha)}(\boldsymbol{x}) = 0.5409$ and $\Gamma_\ell^{(P_t,\alpha,S_{min})}(\boldsymbol{x}) = 0.5897$ were obtained. These values are plotted in Figure 6.10 together with the associated attainment fronts for the situations where $h_b = 25$ metres and $h_b = 50$ metres for $k = 6$ transmitters, as calculated in §6.2. It should, however, be acknowledged that the performance measure values reported above for the existing networks only incorporate coverage provided by those transmitters actually located within the specific area considered in this case study. As a result, there may be areas, especially along the periphery of the study area shown in Figure 6.1, which do, in fact, receive coverage from base stations located just outside the area considered for transmitter placement in this case study.

Assuming base station antennae heights of $h_b = 50$ metres above ground level, the view shed plot and signal level heat map of the existing transmitter network, corresponding to the point A in Figure 6.10 are shown in Figures 6.11 (a) and (b), respectively. The view shed plots and signal level heat maps for the transmitter placements corresponding to the points B and C in Figure 6.10 are shown in Figures 6.12 and 6.13, respectively. As may be seen, the transmitter

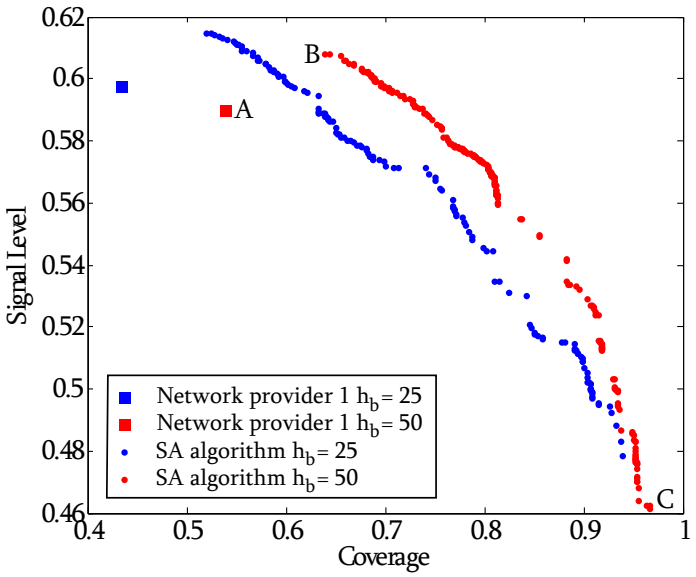

FIGURE 6.10: *Network provider 1's actual transmission network performance and the corresponding attainment fronts suggested by the DSS when placing $k = 6$ transmitters.*

configuration corresponding to the extreme point denoted by B in Figure 6.10 outperforms the existing network in both the coverage and the average signal level objectives, attaining performance values of $\Gamma_c^{(\alpha)}(\boldsymbol{x}) = 0.6408$ and $\Gamma_\ell^{(P_t,\alpha,S_{min})}(\boldsymbol{x}) = 0.6079$.

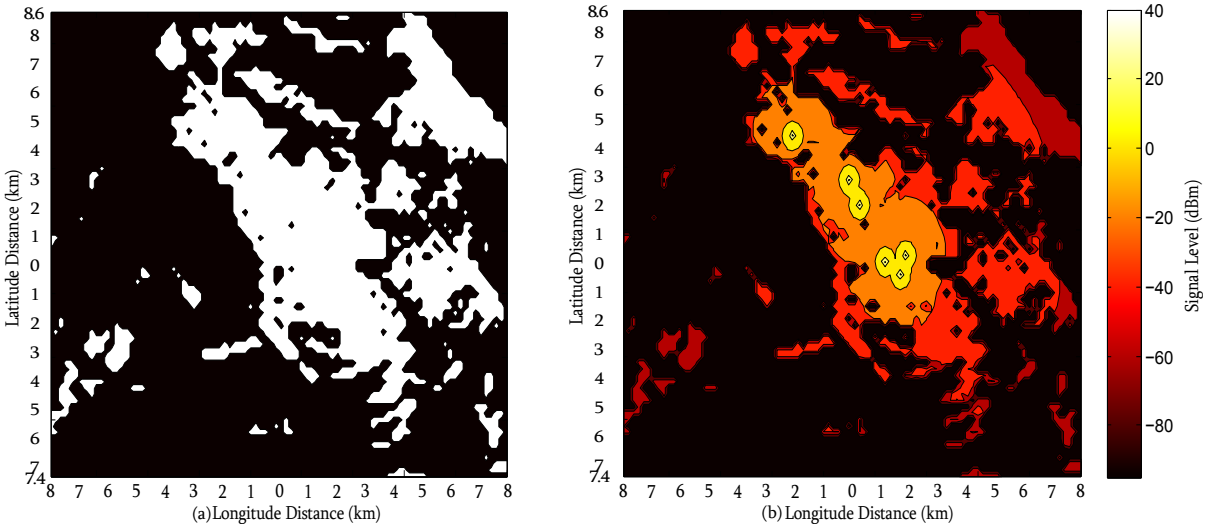

FIGURE 6.11: *View shed plot in (a) and signal level plot in (b) for the existing transmission network of network provider 1 with base station heights of $h_b = 50$ metres above ground level, corresponding to point A in Figure 6.10.*

The transmitter configuration corresponding to the extreme point C in Figure 6.10 outperforms the existing transmitter configuration in the coverage objective, attaining a value of $\Gamma_c^{(\alpha)}(\boldsymbol{x}) = 0.9665$. The existing network, however, outperforms this configuration in terms of the average signal level objective, for which a value of $\Gamma_\ell^{(P_t,\alpha,S_{min})}(\boldsymbol{x}) = 0.4614$ is achieved.

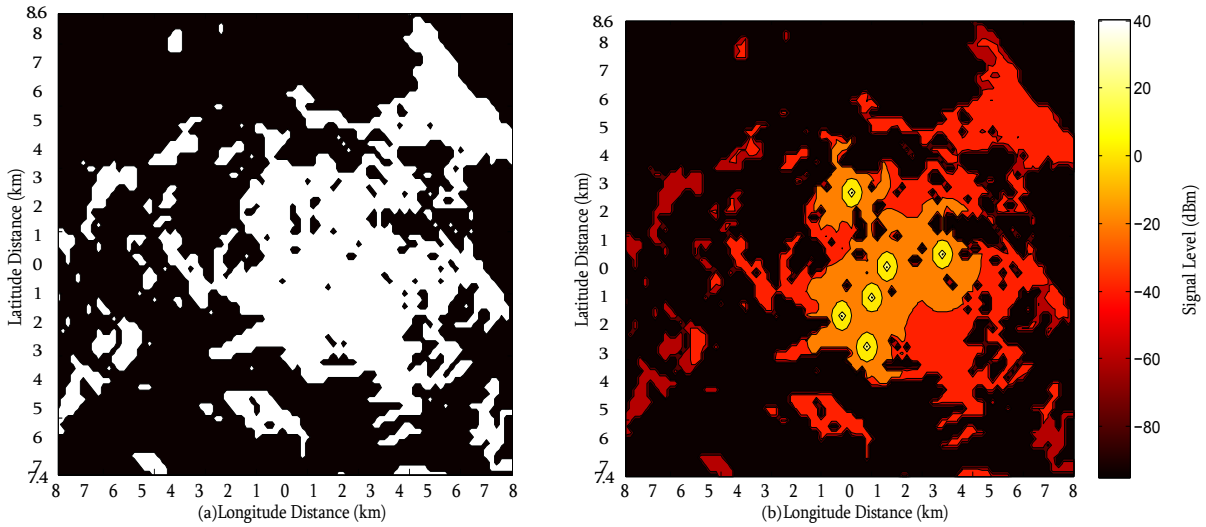

FIGURE 6.12: *View shed plot in (a) and signal level plot in (b) for the extreme point providing the maximum average signal level from $k = 6$ transmitters at a height of $h_b = 50$ metres above ground level, corresponding to point B in Figure 6.10.*

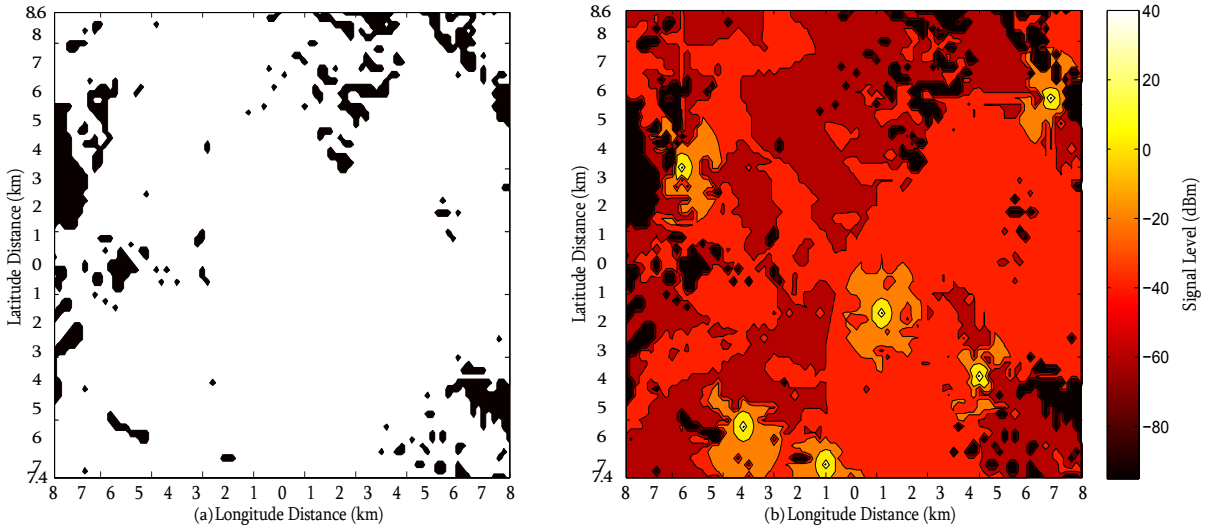

FIGURE 6.13: *View shed plot in (a) and signal level plot in (b) for the extreme point providing the maximum coverage from $k = 6$ transmitters at a height of $h_b = 50$ metres above ground level, corresponding to point C in Figure 6.10.*

6.3.2 Network Provider 2

The names, as well as the coordinates, of those transmitters forming part of the existing network established by network provider 2, are listed in Table 6.4.

These locations were again entered into the decision vector $\boldsymbol{x}$ and the performance measures outlined in Chapter 3 associated with the configuration in Table 6.4 were calculated for both the cases in which the base station antennae heights are assumed to be $h_b = 25$ metres and $h_b = 50$ metres above ground level, respectively. In the case where $h_b = 25$ metres, it was found that a coverage value of $\Gamma_c^{(\alpha)}(\boldsymbol{x}) = 0.3470$ and an average signal level of $\Gamma_\ell^{(P_t,\alpha,S_{min})}(\boldsymbol{x}) = 0.5390$ are achieved. An increase in the coverage percentage to $\Gamma_c^{(\alpha)}(\boldsymbol{x}) = 0.4750$ and a decrease of the average signal level to $\Gamma_\ell^{(P_t,\alpha,S_{min})}(\boldsymbol{x}) = 0.5386$ were recorded for the case where the base station

Number	Base Station	Coordinates
1	BTS ID 2776	S33° 55′ 54″ E18° 51′ 27″
2	BTS ID 1776	S33° 56′ 47″ E18° 51′ 04″
3	BTS ID 3417	S33° 58′ 35″ E18° 49′ 59″
4	BTS ID 1417	S33° 59′ 40″ E18° 50′ 30″

TABLE 6.4: *The identification numbers and coordinates of the base stations which form part of network provider 2's transmission network.*

antenna heights h_b were increased to 50 metres above ground level. These performance measures are plotted in Figure 6.14, together with the attainment fronts for $k = 4$ determined in §6.2. Again, it should be acknowledged that these performance measure values do not incorporate any coverage which may be provided by transmitters located outside the area shown in Figure 6.1, and that the actual values achieved may thus differ slightly from those reported.

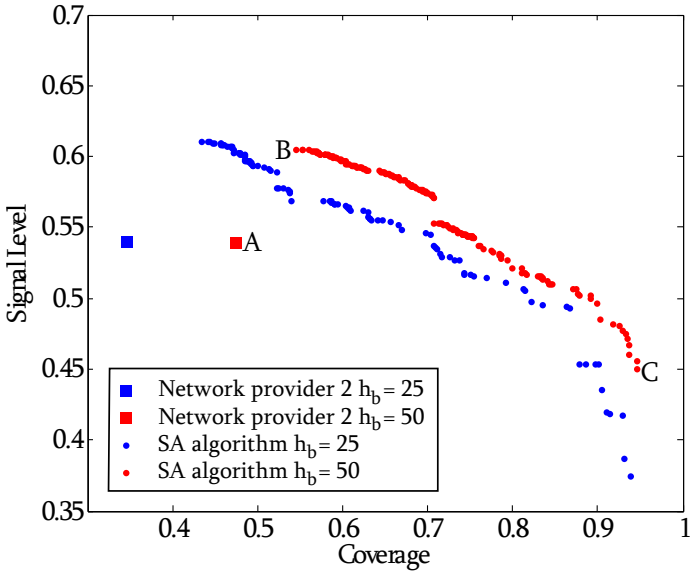

FIGURE 6.14: *Network provider 2's actual transmission network performance and the corresponding attainment fronts suggested by the DSS when placing $k = 4$ transmitters.*

The point A in Figure 6.14 corresponds to the existing transmitter configuration under the assumption that all antennae are fixed at base station heights of $h_b = 50$ metres above ground level. The view shed plot and signal level heat map of the existing transmitter network, assuming base station antennae heights of $h_b = 50$ metres above ground level are shown in Figures 6.15 (a) and (b), respectively. For the purpose of comparison, the extreme points B and C on the attainment front corresponding to a base station height of $h_b = 50$ metres above ground level were again chosen. The transmitter configuration corresponding to the point B achieved a coverage percentage of $\Gamma_c^{(\alpha)}(\boldsymbol{x}) = 0.5458$ and a normalised average signal level of $\Gamma_\ell^{(P_t,\alpha,S_{min})}(\boldsymbol{x}) = 0.6050$. As in the case of network provider 1 discussed above, this configuration outperforms the existing configuration for network provider 2 in terms of both the coverage and average signal level objectives as may be seen in Figure 6.14. The view shed plot and signal level heat map corresponding to the transmitter configuration of point B in Figure 6.14 are shown in Figures 6.16 (a) and (b), respectively.

Performance values of $\Gamma_c^{(\alpha)}(\boldsymbol{x}) = 0.9466$ and $\Gamma_\ell^{(P_t,\alpha,S_{min})}(\boldsymbol{x}) = 0.4499$ were achieved by the trans-

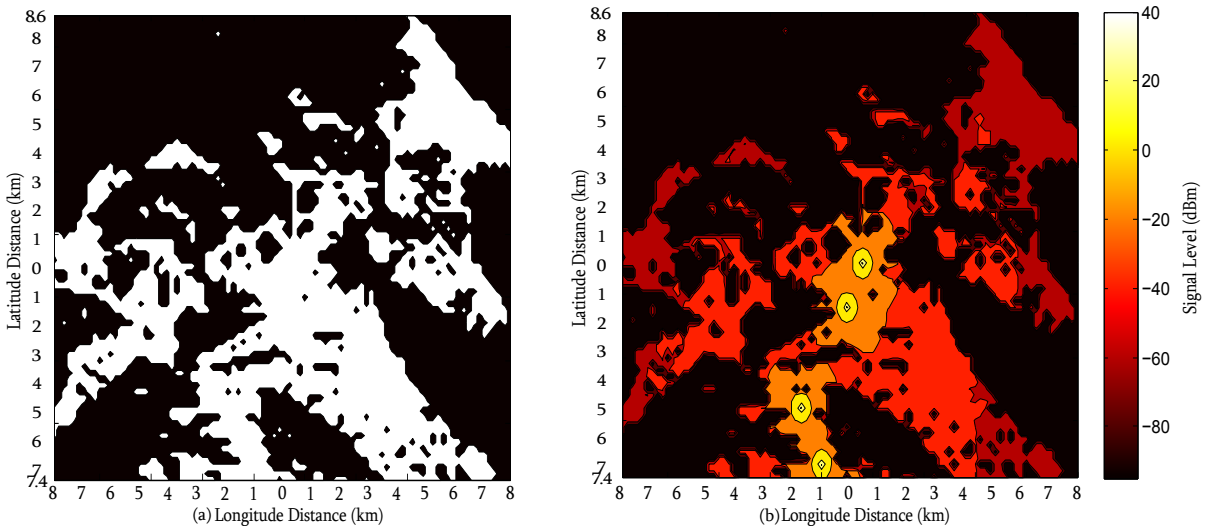

FIGURE 6.15: *View shed plot in (a) and signal level plot in (b) for the existing transmission network of network provider 2 with base station heights of $h_b = 50$ metres above ground level, corresponding to point A in Figure 6.14.*

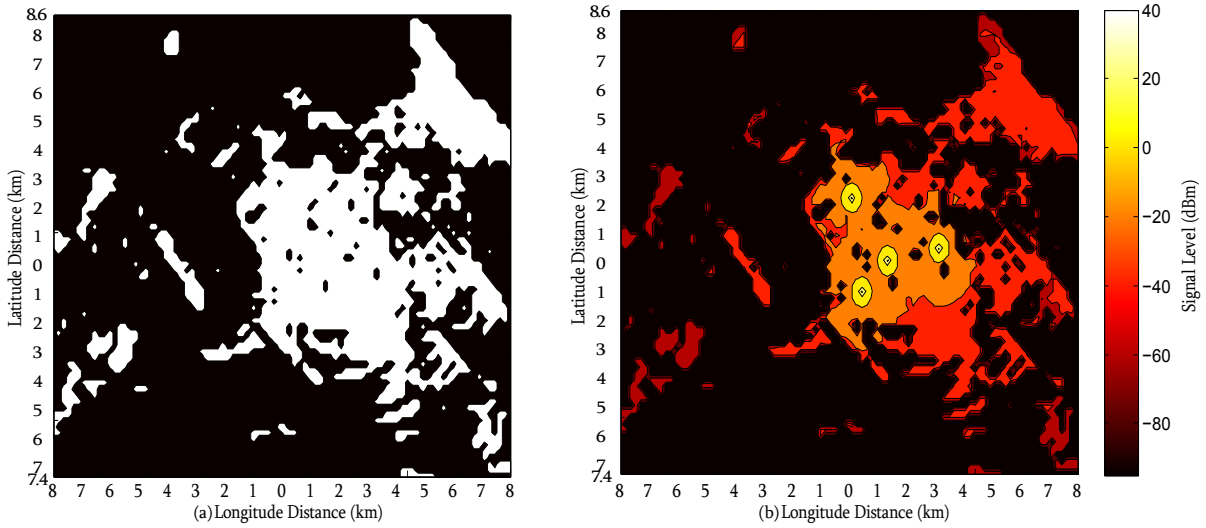

FIGURE 6.16: *View shed plot in (a) and signal level plot in (b) for the extreme point providing the maximum average signal level for $k = 4$ transmitters at a height of $h_b = 50$ metres above ground level, corresponding to point B in Figure 6.14.*

mitter configuration corresponding to point C in Figure 6.14. This transmitter configuration, whose view shed and signal level heat map are illustrated in Figure 6.17 (a) and (b), outperforms the existing network in the coverage objective, but is outperformed in the average signal level objective.

It should, at this point, finally be acknowledged that, although the transmitter configurations suggested by the DSS of Chapter 5 outperform the existing network configurations by a significant margin in both cases, this should not be seen as an absolute measure of network quality, since not all the performance measures adopted in the network planning process of the two network providers considered in this section are known to the author.

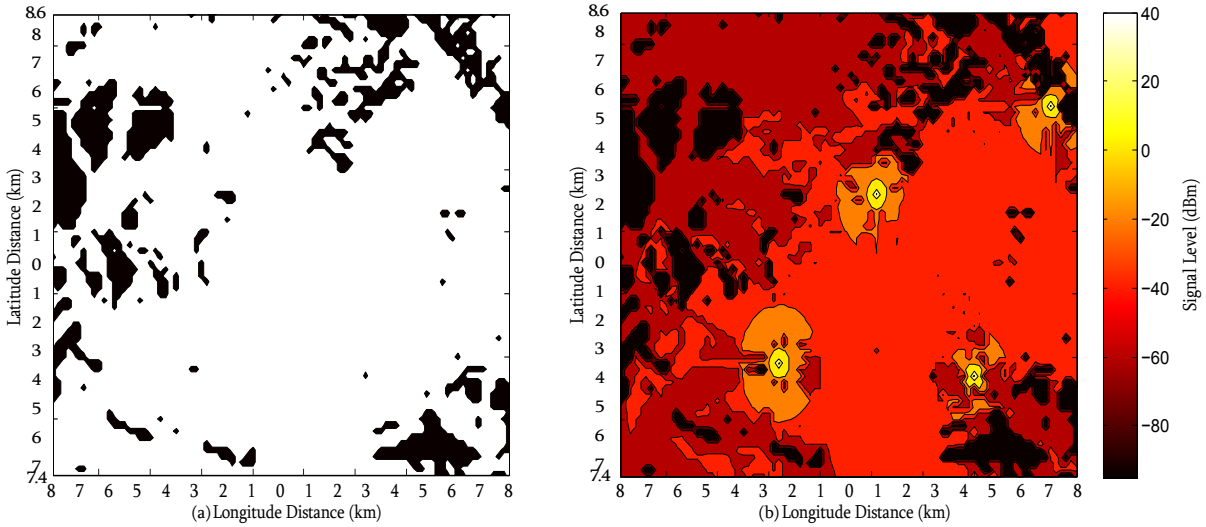

FIGURE 6.17: *View shed plot in (a) and signal level plot in (b) for the extreme point providing the maximum coverage for $k = 4$ transmitters at a height of $h_b = 50$ metres above ground level, corresponding to point C in Figure 6.14.*

6.4 Chapter Summary

A special case study was conducted in this chapter in order to showcase the ability of the DSS developed in Chapter 5 in respect of processing the data pertaining to a realistic problem instance and making high-quality trade-off suggestions for transmitter placements in pursuit of area coverage and average signal level maximisation. The initial focus in §6.1 was on a description of the input data used in this case study. Thereafter, the focus shifted in §6.2 to the alternative sets of transmitter placement locations suggested by the DSS. The transmission networks of two local mobile network providers were finally evaluated in §6.3 according to the coverage and average signal level criteria of the modelling framework of Chapter 3. These results were then compared to those of the DSS placement suggestions reported in §6.2. It was found that the configurations suggested by the DSS outperformed the existing networks of both network providers in terms of the coverage and average signal level objectives.

CHAPTER 7

Summary and Conclusions

Contents

In this project, a DSS was developed to aid decision makers in the process of locating transmission towers for mobile telecommunication applications. A prerequisite for the development of this system was the design of a framework for evaluating the effectiveness of a given set of transmitter locations. Using this framework, a bi-objective mathematical model was formulated with the goal of finding an acceptable trade-off between maximising the total area (and as a result demand) coverage and maximising the average signal level provided in the service area. Due to the complex nature of the problem, the method of multiobjective SA was adopted as an approximate solution methodology. The framework for the evaluation of a set of transmitter locations, the bi-objective mathematical model and the SA algorithm were then combined to create the above-mentioned DSS in a user-friendly fashion. This decision support system was finally applied to determine a set of transmitter placements in a special case study involving estimated demand and terrain elevation data from a town in South Africa's Western Cape region.

7.1 Project Summary

Apart from the introductory chapter, in which the project background, as well as the problem description, the project objectives and the proposed research methodology, was given, and this concluding chapter, this report comprises a further five chapters.

Chapter 2 contains a thorough review of various types of facility location models from the operations research literature, in fulfilment of Objective I of §1.3. This review includes the well-known covering problem, the centre problem, the median problem and the fixed-charge facility location problem, as well as common extensions which may be applied to these basic models so as to improve their level of realism when dealing with real-life situations. This was followed by an investigation of models which have specifically been designed for the placement of radio transmitters in mobile telecommunication networks. It was found that generally two main approaches have been followed in the literature to solve the radio transmitter facility location problem: either a continuous optimisation approach or a discrete optimisation approach. Various factors that have an influence on the effectiveness of radio transmission were discussed in order

to gain insight into the major factors that influence the quality of the transmission provided by the transmitters located in a mobile telecommunication network. It was found that the line of sight between a transmitter, the first Fresnel ellipsoid and radio signal propagation loss are the most important factors to be considered in the development of a decision support framework for the location of transmitters in a mobile telecommunication network. An investigation was finally conducted into the nature of the data required to generate an instance of the bi-objective optimisation problem described in §1.1.

Chapter 3 was devoted to the establishment of a bi-criterion framework for evaluating the effectiveness of a given set of placement locations for a network of radio transmitters, in fulfilment of Objective II. The initial focus in §3.1 was to determine the area over which, for a given *single* transmitter location, LOS between the transmitter and potential receiver demand points would exist. This LOS depends on a sufficiently unobstructed first Fresnel ellipsoid which has its foci at the transmitter and receiver. Then the focus shifted in §3.2 to a description of the signal propagation prediction model adopted to determine whether a potential receiver location would receive an adequate signal level should a *single* transmitter, in fact, be located at the given position. Finally, the chapter closed in §3.3 with a discussion on how the quality of a network of *multiple* transmitter placements may be measured. This quality was quantified by two unitless performance measures: the percentage of the demand that can be met by the set of transmitter placement locations and the normalised average signal level provided by the transmitters within the demand region.

A bi-objective maximisation model, which may be used to solve the radio transmitter facility location problem, was developed in Chapter 4, in fulfilment of Objective III. The initial focus in §4.1 was on the explanation of some basic concepts pertaining to multiobjective optimisation. The focus then shifted in §4.2 to the formulation of the mathematical model. Section 4.3 was devoted to a discussion on the working of the method of SA. Initially the discussion centred around single-objective SA in order to provide the reader with a background as to how the technique functions. Thereafter, the dominance-based multiobjective SA algorithm, as proposed by Smith *et al.* [38], was described in some detail. Section 4.4 contained a description of the implementation of the dominance-based multiobjective SA algorithm in the context of the problem considered in this project. Detailed pseudocode descriptions of the supporting algorithms for the initialisation of the algorithm and for the generation of the neighbouring solutions were provided. This was followed by a description of the cooling schedule adopted and the termination criteria employed in this project. Finally, the chapter closed in §4.5 with a model validation, comparing the hypervolumes achieved by the approximation sets returned by the SA algorithm to the hypervolumes of the true Pareto fronts calculated by brute force for small hypothetical instances of the radio transmitter facility location problem where $k = 2$ and $k = 3$ transmitters were to be located.

Chapter 5 was devoted to a demonstration of the way in which the framework for evaluating the quality of a given set of transmitter placement locations, developed in Chapter 3, as well as the mathematical model and SA approximate model solution technique, described in Chapter 4, was implemented in a user-friendly computerised DSS, in fulfilment of Objectives IV and V. The initial focus in §5.1 was on the design of the DSS user interface, stating its intended purpose and describing the functionality of each of its buttons and text boxes. Thereafter, the focus shifted in §5.2 to the DSS computer implementation in Matlab, which was described using DFDs to illustrate the manner in which the data pass through the DSS.

The focus in Chapter 6 was on a specific case study conducted to showcase the ability of the DSS of Chapter 5 to process data pertaining to a realistic problem and provide high-quality trade-off suggestions for transmitter placements in terms of the area coverage and average signal level, in

fulfilment of Objectives VII and VIII. The initial discussion in §6.1 centred around a description of the input data used in the case study. Thereafter, the focus shifted in §6.2 to the alternative sets of transmitter placement locations suggested by the DSS. Finally, the networks of two local network providers were evaluated in §6.3 according to the coverage and average signal level objectives of the modelling framework of Chapter 3. These results were then compared to the DSS placement suggestions reported in §6.2. It was found that the configurations suggested by the DSS outperformed the existing networks for both network providers in terms of both the coverage and average signal level objectives.

7.2 Critical Project Assessment

Although still widely used and applicable (especially in the Southern African context), it is acknowledged that 2G mobile telecommunication network technology, which was the focus of this project, is a dated technology that will be phased out over time. Due to the relative simplicity of the offline network planning approach usually adopted in the context of 2G networks, this type of network was nevertheless chosen for consideration in this project. The 2G network still forms the basis of most of the mobile networks currently in operation. The 2G infrastructure is used almost exclusively for voice traffic, in order to keep the 3G and 4G channels open so as to be able to provide the improved download speeds achievable by 3G and 4G technology. Due to the increased range of 2G network technology, compared to 3G and 4G network technology, the former networks are widely used in rural areas where large areas need to be covered. In these rural areas, the demand for high download speeds is typically not as large as in urban centres. This may be attributed to the lower income households typically associated with rural areas in Southern Africa, resulting in the use of more basic feature phones instead of the more costly, data intensive smartphones.

The author observed, in the literature studied, that there has not been a case of the transmitter facility location in which a truly multiobjective optimisation approach was adopted. In the case considered by Mathar and Niessen [27], for example, a weighted objective function was used instead, whereas Krzanowski and Raper [24] implemented a convex combination of objective functions in their solution approach. Since the objective functions involved in radio transmitter placement problems typically differ in units, however, and their values are thus difficult to compare directly, even when normalised, it was decided rather to adopt a bi-objective modelling approach in this project, which seems to be a novel approach in the context of 2G transmitter placement decisions.

The dominance-based multiobjective SA algorithm is well suited to solving the transmitter facility location problem considered in this project, as indicated by the quality of the solutions uncovered in Chapter 4. The high quality of the solutions is substantiated by the comparison of the hypervolumes enclosed by the attainment fronts returned by the SA algorithm and the true Pareto fronts for the small, hypothetical instances of the problem in which $k = 2$ and $k = 3$ transmitters have to be placed, as described in Example 4.2. This is further confirmed by the fact that for the existing radio transmission networks of the two local mobile providers investigated during the case study of Chapter 6, transmitter configurations were uncovered by the SA algorithm which outperform the existing networks by a significant margin in terms of both the coverage and average signal level objectives.

A paper by the author and the supervisor of this project, describing the above-mentioned modelling approach, was published in double-blind peer-reviewed proceedings of the 44th Annual Conference of the Operations Research Society of South Africa [34]. The author also presented

this paper orally at the conference at Hartebeespoort.

7.3 Suggestions for Future Work

A number of suggestions for possible future work have been identified during the course of this final year project. These suggestions are documented in this final section.

The neighbourhood move operator of the SA algorithm adopted in this project was defined in a very simplistic manner, which proved effective for the purposes of this project under the assumption that all of the discretised grid points serve equally well as candidate sites and as demand points. In reality this will, however, not necessarily be the case — only certain specified areas may typically be considered for transmitter placement. In this case, neighbourhoods would have to be defined differently (possibly by defining each candidate site's neighbourhood *a priori*) and further constraint handling techniques may have to be introduced into the SA solution approach in order to ensure the feasibility of the proposed solutions.

Furthermore, alternative cooling schedules may be considered for inclusion in the SA algorithm, possibly incorporating nonmonotonic or adaptive temperature functions in order to improve the search performance.

Since time is typically not a critical factor during the mobile telecommunication network planning phase, exact solution approaches, which may take longer than the method of SA to converge to feasible solutions, may be investigated. As stated in §4.3, this may involve using multiple iterations of the branch-and-bound method with an added constraint on one of the objective function values. Alternatively, Benders decomposition may be applied in order to enhance this exact solution approach.

As an alternative approximate solution approach, a comparison between the single-threaded SA algorithm implemented in this project and multi-threaded alternatives, such a genetic algorithm or a particle swarm optimisation algorithm, may be conducted in order to determine which algorithm yields the best trade-off between solution quality and computation time.

The DSS developed in this project may also be further validated by applying it to other case studies incorporating different terrain elevation data so as to test its flexibility in different contexts. In order to improve on the current DSS, post-optimisation decision support may also be included in terms of facilitating a choice of one of the solutions forming part of the nondominated front for implementation. A further improvement which may be incorporated into the current DSS is to develop the functionality required to be able to enter a set of transmitter locations which have already been placed, and then use the DSS to add transmitters to the network, in addition to the existing transmitter locations, in pursuit of the coverage and average signal level maximisation objectives.

Due to the multipath nature of radiowave propagation, interference in wireless environments between orthogonal signals can never be completely avoided. Amaldi *et al.* [3] define one measure of signal interference, called the *signal interference ratio* (SIR), as

$$SIR = SF\frac{P_{received}}{\sigma I_{in} + I_{out} + \eta},$$

where $P_{received}$ is the received signal strength at the demand point, σ is an orthogonality loss factor, I_{in} is the total interference caused by signals transmitted from the same base station (inter-cell interference), I_{out} represents the interference resulting from signals transmitted from other base stations (intra-cell interference), η is the thermal noise power and SF is a spreading

factor, which is defined as the ratio between the spread signal rate and the user rate. This latter factor essentially takes the locations of different users with respect to one another into account when determining the level of interference experienced. Ideally, the SIR should be kept as low as possible in order to improve the quality of service. Incorporating the minimisation of the SIR as a third placement objective may be considered as an extension to the work in this project.

As stated in §1.1, the transmitter facility location problem for 3G and 4G networks cannot be decomposed into the separate coverage planning and frequency allocation subproblems. Using the method for determining whether, LOS, nLOS or NLOS exists, together with the propagation loss calculations, as a basis, the online frequency allocation problem required for the planning of 3G and 4G networks may finally also be incorporated into the model. A different propagation loss function will, however, have to be incorporated for the 2 100 MHz and 2 300 MHz channels which are often used in 3G and 4G networks, since these values fall outside of the range of the COST 231-Hata-Model.

References

[1] Alizadeh M, 2009, *Facility location in supply chains*, pp. 473–505 in Farahani RZ & Hekmatfar M (Eds), *Facility location: Concepts, models, algorithms and case studies*, Physica-Verlag, Heidelberg.

[2] Amaldi E, Capone A & Malucelli F, 2008, *Radio planning and coverage optimization of 3G cellular networks*, Wireless Networks, **14(4)**, pp. 435–447.

[3] Amaldi E, Capone A, Malucelli F & Mannino C, 2006, *Optimization problems and models for planning cellular networks*, pp. 917–939 in Resende M & Pardalos PM (Eds), *Handbook of optimization in telecommunications*, Springer, New York (NY).

[4] Anonymous, 2014, *The mobile economy sub-saharan Africa 2014*, (Unpublished) Technical Report, Groupe Speciale Mobile Association.

[5] Bastani S & Kazemzadeh N, 2009, *Hierarchical location problems*, pp. 219–243 in Farahani RZ & Hekmatfar M (Eds), *Facility location: Concepts, models, algorithms and case studies*, Physica-Verlag, Heidelberg.

[6] Biazaran M & SeyediNehzad B, 2009, *Center problems*, pp. 193–219 in Farahani RZ & Hekmatfar M (Eds), *Facility location: Concepts, models, algorithms and case studies*, Physica-Verlag, Heidelberg.

[7] Busetti F, 2003, *Simulated annealing overview*, [Online], [Cited September 8th, 2015], Available from `http://www.cs.ubbcluj.ro/~csatol/mestint/pdfs/Busetti_Annealing Intro.pdf`.

[8] Caramia M & Dell'Olmo P, 2008, *Multi-objective management in freight logistics: Increasing capacity, service level and safety with optimization algorithms*, 1st Edition, Springer, London.

[9] CellMapper.net, 2015, *CellMapper*, [Online], [Cited October 12th, 2015], Available from `https://www.cellmapper.net/map`.

[10] Costa AM, 2005, *A survey on benders decomposition applied to fixed-charge network design problems*, Computers and Operations Research, **32(6)**, pp. 1429–1450.

[11] Daskin MS, 1995, *Network and discrete location models, algorithms, and applications*, 1st Edition, John Wiley & Sons, New York (NY).

[12] Dreo J, Petrowski A, Siarry P & Taillard E, 2006, *Metaheuristics for hard optimzation: Methods and case studies*, 1st Edition, Springer, Berlin.

[13] Fallah H, NaimiSadigh A & Aslanzadeh M, 2009, *Covering problems*, pp. 145–177 in Farahani RZ & Hekmatfar M (Eds), *Facility location: Concepts, models, algorithms and case studies*, Physica-Verlag, Heidelberg.

[14] Farahani RZ & Hekmatfar M (Eds), 2009, *Facility location concepts, models, algorithms and case studies*, 1st Edition, Physica-Verlag, Heidelberg.

[15] Feuerstein MJ, Blackard KL, Rappaport TS, Seidel SY & Xia HH, 1994, *Path loss, delay spread, and outage models as functions of antenna height for microcellular system design*, IEEE Transactions on Vehicular Technology, **43(3)**, pp. 487–498.

[16] Fleury BH & Leuthold PE, 1996, *Radiowave propagation in mobile communications: An overview of European research*, IEEE Communications Magazine, **34(2)**, pp. 70–81.

[17] Hata M, 1980, *Empirical formula for propagation loss in land mobile radio services*, IEEE Transactions on Vehicular Technology, **29(3)**, pp. 317–325.

[18] Hekmatfar M & SteadieSeifi M, 2009, *Multi-criteria location problems*, pp. 473–505 in Farahani RZ & Hekmatfar M (Eds), *Facility location: Concepts, models, algorithms and case studies*, Physica-Verlag, Heidelberg.

[19] Huang MD, Romeo F & Sangiovanni-Vinentelli AL, 1986, *An effective general cooling schedule for simulated annealing*, Proceedings of the IEEE International Conference on Computer-Aided Design, Santa Clara (CA), pp. 381–384.

[20] Iskander MF & Yun Z, 2002, *Propagation prediction models for wireless communication systems*, IEEE Transactions on Microwave Theory and Techniques, **50(3)**, pp. 662–673.

[21] Kendall KE & Kendall JE, 2014, *Systems analysis and design*, 9th Edition, Pearson, Essex.

[22] Kim YK & Prasad R, 2006, *4G roadmap and emerging communication technologies*, 1st Edition, Artech House, Boston (MA).

[23] Kirkpatrick S, Gelatt CD & Vecchi MP, 1983, *Optimization by simulated annealing*, Science, **220(4598)**, pp. 671–680.

[24] Krzanowski R & Raper J, 1999, *Hybrid genetic algorithm for transmitter location in wireless networks*, Computers, Environment and Urban Systems, **23(5)**, pp. 359–382.

[25] Kürner T, 1999, *COST Action 231 digital mobile radio towards future generation systems*, (Unpublished) Technical Report, European Cooperation in the Field of Scientific and Technical Research.

[26] L-com, 2012, *Line of sight and the Fresnel zone*, [Online], [Cited April 8th, 2015], Available from `http://www.l-com.com/content/Article.aspx?Type=N&ID=10162`.

[27] Mathar R & Niessen T, 2000, *Optimum positioning of base stations for cellular radio networks*, Wireless Networks, **6(6)**, pp. 421–428.

[28] Mathworks, 2012, *MATLAB version 7.14.0.739 (R2012a)*, The MathWorks Inc., Natick (MA).

[29] McKinney AL & Agarwal KK, 1992, *Development of the Bresenham line algorithm for a first course in computer science*, The Journal of Computing Sciences in Colleges, **8**, pp. 70–81.

[30] OpenTopography.org, 2015, *OpenTopograghy: A portal to high-resolution topography data and tools*, [Online], [Cited October 2nd, 2015], Available from `http://opentopo.sdsc.edu/gridsphere/gridsphere?cid=datasets`.

[31] Reed M, Jotishky N, Newman M, Mbongue T & Escofet G, 2013, *Africa telecoms outlook 2014: Maximising digital service opportunities*, (Unpublished) Technical Report, Informa.

[32] Schlünz EB, Bokov PM, Prinsloo RH & Van Vuuren JH, To appear, *A unified methodology for single- and multiobjective in-core fuel management optimisation based on augmented Chebyshev scalarisation and a harmony search algorithm*, Annals of Nuclear Energy.

[33] Schmidt-Dumont HH, 2015, Coordinator: Access network quality and support at *Mobile Telecommunications Limited (MTC)*, [Personal Communication], Contactable at `hschmidt@mtcmobile.com.na`.

[34] Schmidt-Dumont T & Van Vuuren JH, 2015, *Radio transmission tower placement in cellular telephone communication networks*, Proceedings of the 44th Annual Conference of the Operations Research Society of South Africa, Hartebeespoort, South Africa, pp. 91–101.

[35] Seidel SY & Rappaport TS, 1994, *Site-specific propagation prediction for wireless in-building personal communication system design*, IEEE Transactions on Vehicular Technology, **43(4)**, pp. 879–891.

[36] Sherali HD, Pendyala CM & Rappaport TS, 1996, *Optimal location of transmitters for micro-cellular radio communication system design*, IEEE Journal on Selected Areas in Communications, **14(4)**, pp. 662–673.

[37] Smith K, Everson RM & Fieldsend JE, 2004, *Dominance measures for multi-objective simulated annealing*, Proceedings of the 2004 Congress on Evolutionary Computation, pp. 23–30.

[38] Smith K, Everson RM, Fieldsend JE, Murphy C & Misra R, 2008, *Dominance-based multiobjective simulated annealing*, IEEE Transactions on Evolutionary Computation, **12(3)**, pp. 323–342.

[39] Socioeconomic Data and Applications Center (SEDAC), 2015, *Gridded population of the world (GPW)*, [Online], [Cited October 2nd, 2015], Available from `http://sedac.ciesin.columbia.edu/data/set/gpw-v3-population-count`.

[40] Suppapitnarm A, Seffen K, Parks G & Clarkson P, 2000, *A simulated annealing algorithm for multiobjective optimization*, Engineering Optimization, **33(1)**, pp. 59–85.

[41] Talbi EG, 2009, *Metaheuristics: From design to implementation*, 1st Edition, Wiley, Hoboken (NJ).

[42] Triki E, Collette Y & Siarry P, 2005, *A theoretical sudy on the behaiviour of simulated annealing leading to a new cooling schedule*, European Journal of Operational Research, **166**, pp. 77–92.

[43] Tutschku K, 1998, *Demand-based radio network planning of cellular mobile communication systems*, Proceedings of the 17th Annual Joint Conference of the IEEE Computer and Communications Societies, pp. 1054–1061.

[44] Tutschku K & Tran-Gia P, 1998, *Spatial traffic estimation and characterization for mobile communication network design*, IEEE Journal on Selected Areas in Communications, **16(5)**, pp. 804–811.

[45] Van Laarhoven PJM & Aarts EHL, 1987, *Simulated annealing: Theory and applications*, 1st Edition, Reidel, Dordrecht.

[46] Weisman CJ, 2002, *The essential guide to RF and wireless*, 2nd Edition, Pearson Education, Upper Saddle River (NJ).

[47] While L, Hingston P, Barone L & Huband S, 2006, *A faster algorithm for calculating hypervolume*, IEEE Transactions on Evolutionary Computation, **10(1)**, pp. 29–38.

[48] Winston WL, 2004, *Operations research: Applications and algorithms*, 4th Edition, Brooks/Cole, Belmont (CA).

APPENDIX A

Project Timeline

The project timeline is given in Figure A.1 in Gantt-chart form.

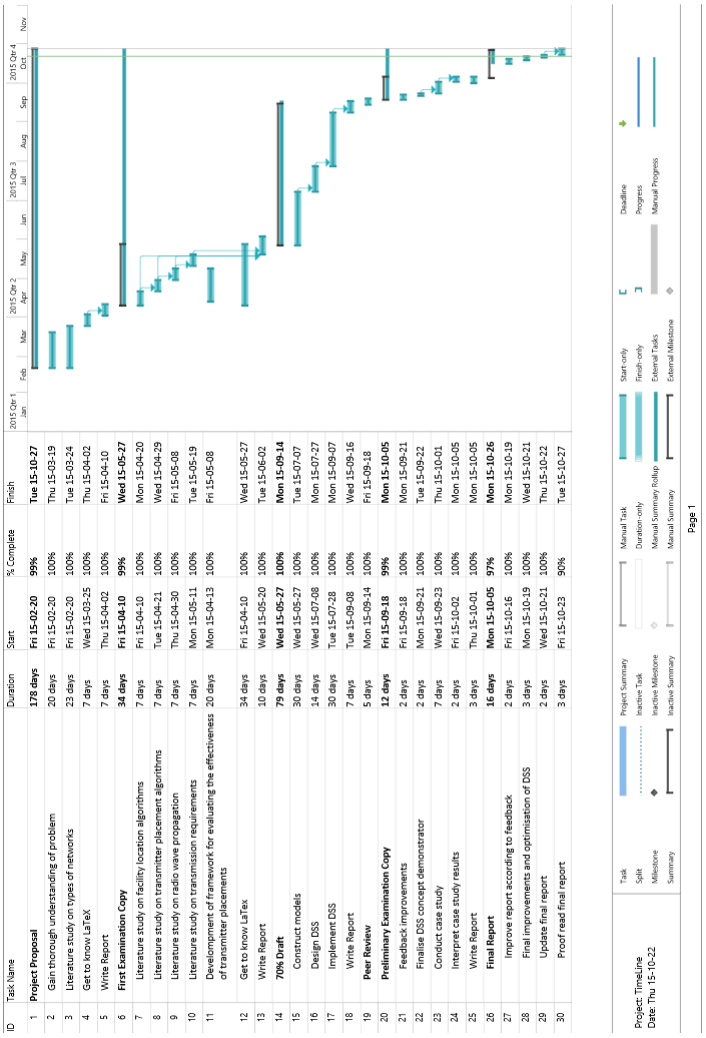

ID	Task Name	Duration	Start	% Complete	Finish
1	**Project Proposal**	**178 days**	**Fri 15-02-20**	**99%**	**Tue 15-10-27**
2	Gain thorough understanding of problem	20 days	Fri 15-02-20	100%	Thu 15-03-19
3	Literature study on types of networks	23 days	Fri 15-02-20	100%	Tue 15-03-24
4	Get to know LaTeX	7 days	Wed 15-03-25	100%	Thu 15-04-02
5	Write Report	7 days	Thu 15-04-02	100%	Fri 15-04-10
6	**First Examination Copy**	**34 days**	**Fri 15-04-10**	**99%**	**Wed 15-05-27**
7	Literature study on facility location algorithms	7 days	Fri 15-04-10	100%	Mon 15-04-20
8	Literature study on transmitter placement algorithms	7 days	Tue 15-04-21	100%	Wed 15-04-29
9	Literature study on radio wave propagation	7 days	Thu 15-04-30	100%	Fri 15-05-08
10	Literature study on transmission requirements	7 days	Mon 15-05-11	100%	Tue 15-05-19
11	Development of framework for evaluating the effectiveness of transmitter placements	20 days	Mon 15-04-13	100%	Fri 15-05-08
12	Get to know LaTex	34 days	Fri 15-04-10	100%	Wed 15-05-27
13	Write Report	10 days	Wed 15-05-20	100%	Tue 15-06-02
14	**70% Draft**	**79 days**	**Wed 15-05-27**	**100%**	**Mon 15-09-14**
15	Construct models	30 days	Wed 15-05-27	100%	Tue 15-07-07
16	Design DSS	14 days	Wed 15-07-08	100%	Mon 15-07-27
17	Implement DSS	30 days	Tue 15-07-28	100%	Mon 15-09-07
18	Write Report	7 days	Tue 15-09-08	100%	Wed 15-09-16
19	**Peer Review**	5 days	Mon 15-09-14	100%	Fri 15-09-18
20	**Preliminary Examination Copy**	**12 days**	**Fri 15-09-18**	**99%**	**Mon 15-10-05**
21	Feedback improvements	2 days	Fri 15-09-18	100%	Mon 15-09-21
22	Finalise DSS concept demonstrator	2 days	Mon 15-09-21	100%	Tue 15-09-22
23	Conduct case study	7 days	Wed 15-09-23	100%	Thu 15-10-01
24	Interpret case study results	2 days	Fri 15-10-02	100%	Mon 15-10-05
25	Write Report	3 days	Thu 15-10-01	100%	Mon 15-10-05
26	**Final Report**	**16 days**	**Mon 15-10-05**	**97%**	**Mon 15-10-26**
27	Improve report according to feedback	2 days	Fri 15-10-16	100%	Mon 15-10-19
28	Final improvements and optimisation of DSS	3 days	Mon 15-10-19	100%	Wed 15-10-21
29	Update final report	2 days	Wed 15-10-21	100%	Thu 15-10-22
30	Proof read final report	3 days	Fri 15-10-23	90%	Tue 15-10-27

FIGURE A.1: *Project timeline in Gantt-chart form.*

APPENDIX B

Personal Reflections

This appendix contains the author's personal reflections on his own development during the course of completing this project as well as how the work reported in this project may potentially be of benefit to society at large.

B.1 What the Author has Learnt

During the course of this project, the author was exposed to the concepts of nonlinear optimisation, multiobjective optimisation and approximate solution techniques for optimisation problems in the form of metaheuristics. None of these concepts are covered in the undergraduate curriculum of the bachelors degree in industrial engineering at Stellenbosch University. As a result, the author's academic knowledge horizon was considerably widened by gaining a thorough understanding of these concepts. On the more practical side, the author was also exposed to a range of technical aspects pertaining to radio signal transmission in mobile telecommunication networks. Apart from increased practical understanding in a highly relevant, modern industry, this exposure also improved the author's ability to assimilate technical engineering knowledge outside the realm of formal tuition. The different kinds of exposure referred to above were facilitated by an in-depth study of the literature related to the topic of this project and contact with experts in the telecommunication industry.

In terms of skills acquired, the author learnt how to conduct a research project over a sustained period of time, establishing a sound research methodology, from problem description through to a comprehensive study of the related literature and finally to the process of building a suitable mathematical model according to which the problem at hand could be solved effectively.

The author was also able to improve his communication skills significantly. This was achieved by learning how to present work effectively, both in written form and orally, by writing this project report and presenting the work contained therein clearly and concisely to an audience. The publication of a paper in national conference proceedings on the work in this project also exposed the author to the working of the academic peer-review process followed during publication. The exposure gained through the oral presentation of the work in this project at the 44th Annual Conference of the Operations Research Society of South Africa was of great value, both in terms of an expansion of the author's presentation planning and delivering skills and in terms of defending one's work before experts during question time.

Finally, effective time management was an essential part of the successful completion of this final year project. Balancing the considerable workload of ten final year modules with the work required over the course of this project required careful planning and strong self-discipline.

B.2 How this Final Year Project may Benefit Society

This final year project may potentially benefit society in that a user-friendly decision support tool was developed for the placement of radio transmitters in 2G cellular communication networks. This tool may be used by network providers who frequently have to make transmitter location decisions when expanding their networks. The aim of the tool was to enable network planning employees, who do not necessarily have strong mathematical backgrounds, to make near-optimal decisions when transmitter placements have to be made. Such high-quality transmitter placements may potentially lead to improved cellular telephone coverage as well as improved signal quality which, in turn, may result in an increase in competitiveness in the marketplace. The decision support tool was demonstrated informally to a subject matter expert who stated that it appeared to be a useful tool which could be implemented in industry.

APPENDIX C

Further Case Study Results

The view shed (coverage) and signal level heat map plots for the nondominated front extreme points labelled B and C in Figure 6.4, as returned by the SA algorithm for $k = 2$ to $k = 8$ transmitter placements at a height of $h_b = 25$ metres, are shown in Figures C.1 and C.2, respectively.

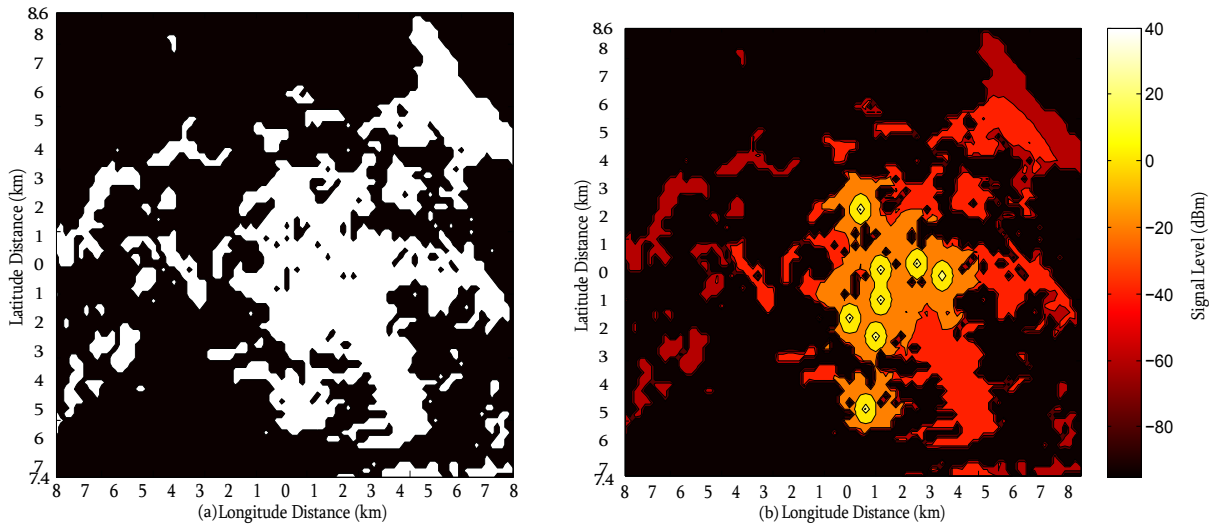

FIGURE C.1: *The view shed plot in (a) and signal level plot in (b) for the extreme point providing maximum average signal level from $k = 8$ transmitters at a height of $h_b = 25$ metres, denoted by B in Figure 6.4.*

The view shed (coverage) and signal level heat map plots for the nondominated front extreme points labelled A and D in Figure 6.7, as returned by the SA algorithm for $k = 2$ to $k = 8$ transmitter placements at a height of $h_b = 50$ metres, are shown in Figures C.3 and C.4, respectively.

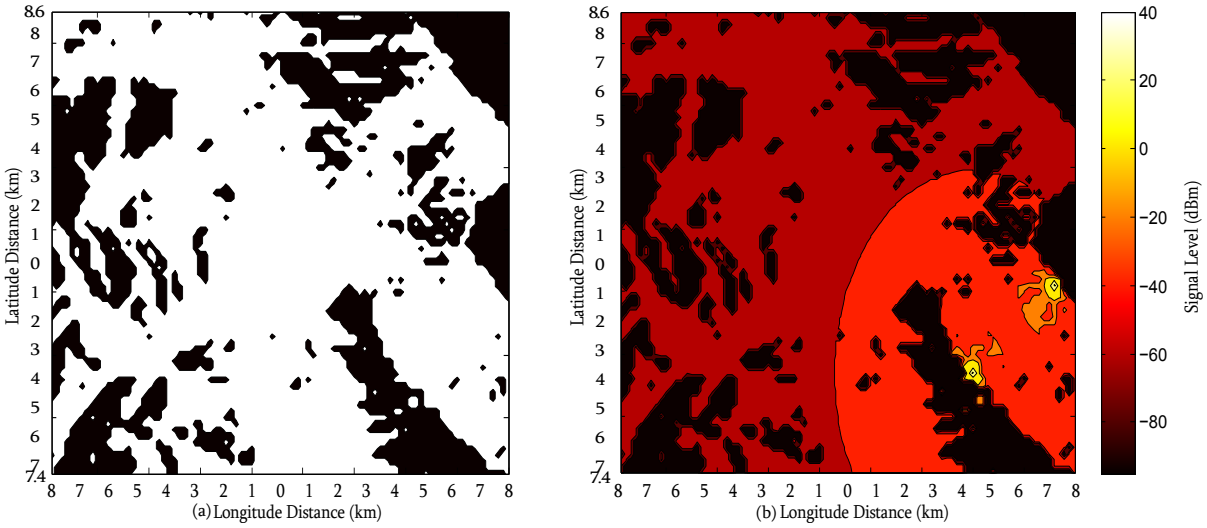

FIGURE C.2: *The view shed plot in (a) and signal level plot in (b) for the extreme point providing maximum coverage from $k = 2$ transmitters at a height of $h_b = 25$ metres, denoted by C in Figure 6.4.*

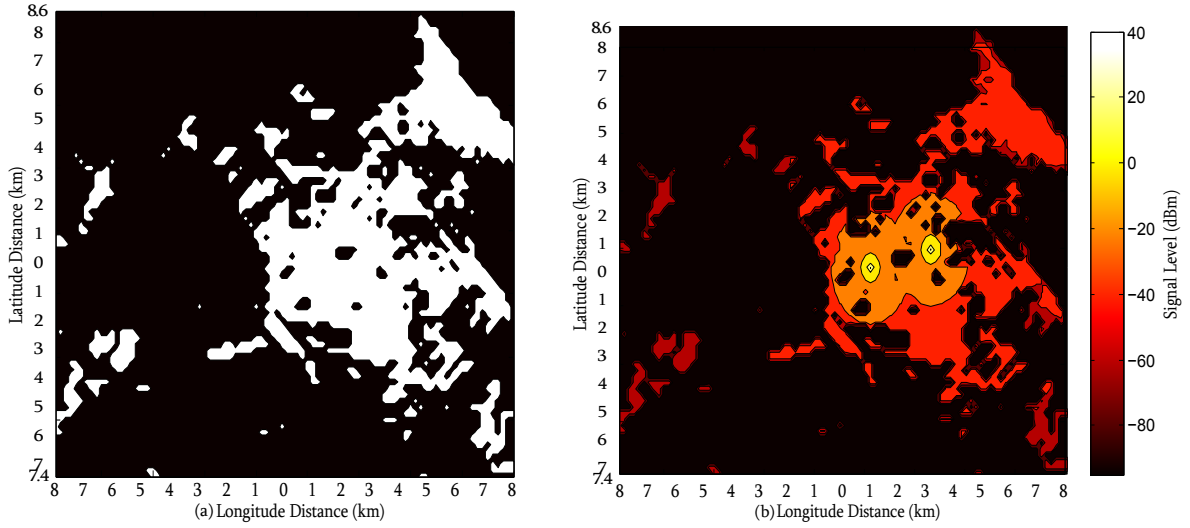

FIGURE C.3: *The view shed plot in (a) and signal level plot in (b) for the extreme point providing the maximum average signal level from $k = 2$ transmitters at a height of $h_b = 50$ metres, denoted by A in Figure 6.7.*

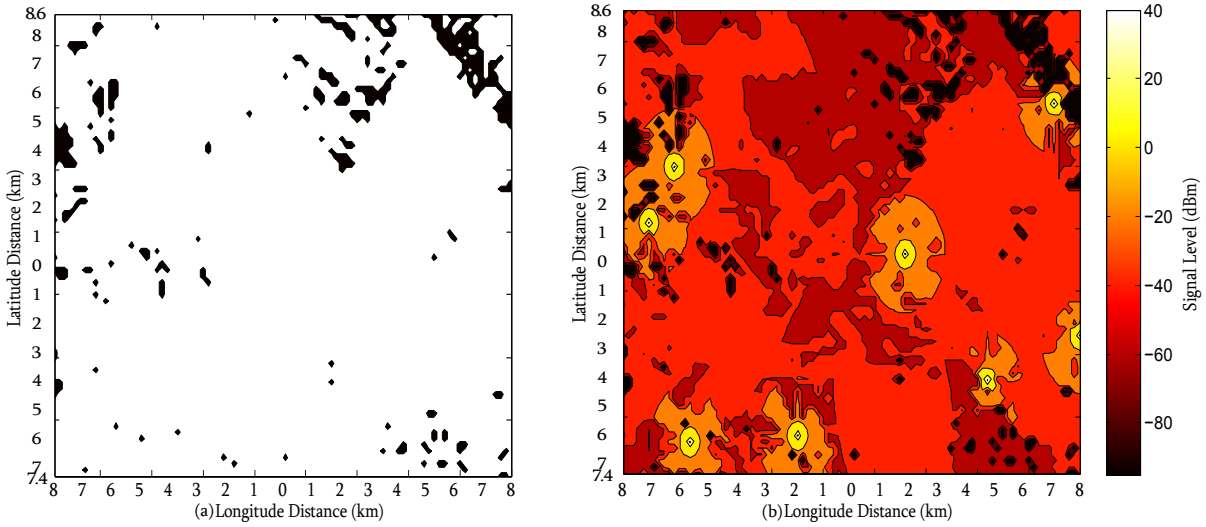

FIGURE C.4: *The view shed plot in (a) and signal level plot in (b) for the extreme point providing maximum coverage from $k = 8$ transmitters at a height of $h_b = 50$ metres, denoted by D in Figure 6.7.*